UNIVERSITY OF BIRMINGHAM

EXPERIMENTAL INVESTIGATION OF MOF ADSORPTION SYSTEM FOR ICE MAKING, FREEZE WATER DESALINATION AND COOLING APPLICATIONS

By

Hassan Jawdat Fadhiel Dakkama

A thesis submitted to the
University of Birmingham
For the degree of

Doctor of Philosophy

School of Engineering
Department of Mechanical Engineering
The University of Birmingham
September- 2017

ABSTRACT

This research describes the development of a novel Metal Organic Frameworks (MOF) based adsorption system to produce ice, cooling, ice slurry and potable water for multioutput applications like fish industry. MOF materials are new class of advanced adsorbent materials that have high surface area (up to 5500 m^2/g), high pore volume, highly tunable structural properties and uniform pore size leading to superior adsorption characteristics. CPO-27(Ni) is a nickel based coordination polymer with open metal sites of organic frameworks which has shown a relatively high water adsorption uptake (0.45g/g) compared to commercially available adsorbents (0.3g/g). This thesis investigates the use of CPO-27(Ni) with potable/saline water as working pair in an adsorption system for ice, cooling and potable water production. Also a novel vacuum based direct freezing technique has been developed using the evaporator of the adsorption ice making system with sea and potable water as the refrigerants. In this new technique, cooling is generated due to the evaporation of the refrigerant caused by the adsorption process to produce three outputs, namely, ice, ice slurry and cooling by lowering the freezing point of water using sea salt. The ice and ice slurry are produced from the potable and saline water in the evaporator during the adsorption-evaporation process, while the cooling process is produced by circulating the water/antifreeze to be cooled in the evaporator. Moreover, the usage of seawater as refrigerant offers producing fresh water as a fourth output from the condensation of the water vapour desorbed during the desorption process. Therefore, the proposed technology will provide four useful outputs compared to providing a maximum of two outputs as reported in the literature.

A single bed CPO-27(Ni) MOF adsorption system was developed using the above novel technique to investigate the system performance in terms of Specific Daily Ice Production (SDIP), Specific Daily Ice Slurry Production (SDSP), Specific daily Water Production (SDWP) and Coefficient of Performance (COP). The effects of fresh water specific volume in the

evaporator, cycle's number, switching time, adsorption/desorption time, salinity of saline water, desorption temperature, water/antifreeze temperature and condensation temperature on the performance of the adsorption system in terms of multi outputs were investigated. Results showed that the maximum ice production achieved was 8.2 ton/day/ton_ads at desorption, water/antifreeze and ambient temperatures of 95^0C, 1^0C and 24^0C, respectively.

A two bed adsorption ice making system was developed using the same novel technique to study continuous production of ice, ice slurry, cooling and fresh water. The effect of cycle's number, switching time, adsorption/desorption time, mass flow rate of the heating/cooling fluid through the adsorber beds and water/antifreeze temperature on the performance of the adsorption system in terms of the same outputs were investigated. Results showed that the optimum number of cycles, switching time, adsorption/ desorption time, salinity, mass flow rate of the heating/cooling fluid and evaporation temperature were found as up to 3 cycles, 3 min, 15 min and 35,000 ppm, 8 L/min and -1^0C, respectively.

Compared to published literature, the proposed technology showed significantly higher Specific Daily Ice Production (SDIP) of 3 times those reported in literature with additional outputs of ice slurry, cooling and distilled water. Also, the new technology offered four outputs compared to a maximum of two outputs reported in the literature using other techniques. Moreover, sea and potable water could be used as refrigerant in the adsorption ice making system compared to very limited work which used just water as refrigerant for ice making application. Using CPO-27(Ni) MOF material as an adsorbent in the adsorption system for application below 0 ^{0}C was firstly investigated.

DEDICATED

To

The Soul of My beloved Father

My Lovely Mother

My Beloved Brother and His Lovely Family

ACKNOWLEDGEMENT

I gratefully acknowledge the funding towards my Ph.D. study from **The Higher Committee for Education Development in IRAQ (HCED)**. I truly appreciate the efforts of all staff in the HCED for their continuous support and prompt response to any request from me.

I owe my deepest gratitude to my supervisors **Dr. Raya Al-Dadah** for her patient guidance and constant feedback during the four years that I spent to do my Ph.D. study. Without her support and invaluable efforts, this thesis would hardly have been completed.

A very special thank you to **Dr. Saad M. Mahmoud** for his supervision and feedback so I appreciate his invaluable advice and he always being so supportive of my work. I am also indebted to Dr. Ahmed Elsayed for his cooperation to do publication together during my Ph.D. years.

I would like to thank Mr. Simon Rowan for helping me to build my test facilities. I appreciate his talent for machining many parts required in the test facilities. I appreciate him for providing me with any requirements during my work in the workshop. I also would like to thank Mr. Carl Hingley and Mr. Peter Thornton for their kind advice and help during my work in the workshop.

I would like to thank my colleague Mr. Peter Youssef as we work together to build the both test facilities and it was not easy to achieve this work through this time without his support. I also would like to thank Ms. Eman Elsayed for providing me with some information. Special mention goes to all of my colleagues who I know during my postgraduate years.

My deep and sincere gratitude to my family for their continuous unparalleled love. They selflessly encouraged me to explore new directions in life and seek my destiny so thank you very much.

It is a pleasure to thank my friends, especially Dr. Faris Elia, Wisam Al-Shohani, Ammar Zakar, Jamal Balushi and Dr. Mustapha Alkhafaaf for their friendship and for the wonderful times we shared and for always making me feel so welcome.

Respectfully,
Hassan J. F. Dakkama

TABLE OF CONTENTS

LIST OF FIGURES

LIST OF TABLES

LIST OF PUBLICATIONS

Journal Publications

[1] Dakkama HJ, Elsayed A, Al-Dadah RK, Mahmoud SM, Youssef P. Integrated evaporator–condenser cascaded adsorption system for low temperature cooling using different working pairs. Applied Energy. 2017 Jan 1;185:2117-26**.** DOI: 10.1016/j.apenergy.2016.01.132. (Impact Factor: 7.182).

[2] Dakkama HJ, Youssef PG, Al-Dadah RK, Mahmoud S. Adsorption ice making and water desalination system using metal organic frameworks/water pair. Energy Conversion and Management. 2017 Jun 15;142:53-61. DOI: 10.1016/j.enconman.2017.03.036. (Impact Factor: 5.589)

[3] Youssef PG, Dakkama H, Mahmoud SM, AL-Dadah RK. Experimental investigation of adsorption water desalination/cooling system using CPO-27Ni MOF. Desalination. 2017 Feb 17;404:192-9. DOI: 10.1016/j.desal.2016.11.008. (Impact Factor: 5.527).

[4] Elsayed AM, Askalany AA, Shea AD, Dakkama HJ, Mahmoud S, Al-Dadah R, Kaialy W. A state of the art of required techniques for employing activated carbon in renewable energy powered adsorption applications. Renewable and Sustainable Energy Reviews. 2017 Nov 30;79:503-19. DOI: 10.1016/j.rser.2017.05.172. (Impact Factor: 8.050)

Book Chapter Publication

[1] Elsayed AM, Dakkama HJ, Mahmoud S, Al-Dadah R, Kaialy W. Sustainable Cooling Research Using Activated Carbon Adsorbents and Their Environmental Impact. InApplied Environmental Materials Science for Sustainability 2017 Jan 1 (pp. 186-221). IGI Global**.** DOI: 10.4018/978-1-5225-1971-3.ch009.

Conferences Publications

[1] Dakkama HJ, Elsayed A, Al-Dadah RK, Mahmoud SM, Youssef P. Investigation of cascading adsorption refrigeration system with integrated evaporator-condenser heat exchanger using different working pairs. International Conference on Applied Energy (ICAE). Energy Procedia. 2015 Aug 1;75:1496-501. Abu Dhabi. DOI: 10.1016/j.egypro.2015.07.285.

[2] Dakkama HJ, Elsayed A, Al-Dadah RK, Mahmoud SM. Enhancement of Cascaded Adsorption Ice-Making System Using Mass and Integrated Heat Recovery. Sustainable Thermal Energy Management Network (SusTEM). 2015 Oct 20 (pp. 215-223) .

[3] Dakkama HJ, Youssef PG, Al-Dadah RK, Mahmoud S, Al-Shohani WA. Adsorption ice making and freeze water desalination using Metal Organic Framework materials. In Students on Applied Engineering (ICSAE), International Conference for 2016 Oct 20 (pp. 54-58). IEEE. DOI: 10.1109/ICSAE.2016.7810160.

[4] Youssef PG, Al-Dadah RK, Mahmoud SM, Dakkama HJ, Elsayed A. Effect of evaporator and condenser temperatures on the performance of adsorption desalination cooling cycle. International Conference on Applied Energy (ICAE). Energy Procedia. 2015 Aug 1;75:1464-9, Abu Dhabi. DOI: 10.1016/j.egypro.2015.07.263.

CHAPTER 1

Introduction

1.1 Introduction

There is a growing demand for fresh water and cooling in many developing countries where access to electricity is limited [1]. The International Institution of Refrigeration (IIR) has reported that about 15% of the entire electrical power consumption in commercial buildings and households in the world is used for refrigeration and air conditioning applications [2]. Furthermore, the World Health Organization (WHO) has reported that 884 million people have no access to fresh water and more than 2.4 billion have a limited access [2]. Desalination technologies have been used to produce potable water, however currently used desalination technologies suffer from being energy intensive with electricity being the dominant energy source needed. For example reverse osmosis (RO) is commonly used with more than 60% among all traditional desalination plants which normally consumes about 4 kW h of electrical energy to produce 1 m^3 of fresh water [2], therefore, such significant energy consumption leads to the depletion of fossil fuel resources, increasing the emissions of carbon dioxide and thus increasing the global warming effect.

Adsorption heat pump systems utilise waste heat from automobile exhaust gas, geothermal and solar energy to produce cooling effect without harmful environmental impact. Also, adsorption systems could utilize working fluids that are natural with no ozone depletion potential and extremely low global warming effect like water, ammonia and ethanol. Therefore, they have low global warming potential and zero ozone depletion potential [3].

Although absorption-cooling systems based on liquid absorbents have become commercially available in the last few decades, they suffer from corrosion, toxicity and the potential crystallisation of the working fluids. In contrast, adsorption cooling systems using solid adsorbents offer a number of advantages including the lower electrical energy consumption (no refrigerant circulating pump), low temperature heat sources, and increased operation reliability due to reduced number of moving parts.

1.2 Environmental concerns of adsorption cooling

Eighty percent of the greenhouse gas (GHG) emissions in Europe comes from the energy sector [4] where the extensive use of electrically driven cooling system is leading to capacity straining power demand peaks in the summer and increasing of greenhouse gas emissions-either through leakage of refrigerants or use of non-sustainable energy sources. Thus, improved building concepts targeting reduction of cooling loads by passive and innovative measures, and the use of alternative technologies in providing the required cooling and heating demands of buildings, are of interest [5].

Refrigerants such as R134a, R-141b and R507a that have been still used with mechanical vapour compression cooling systems were found to have a high global warming potential (GWP), also n-butane, propane, methanol, ethanol, diethyl ether and hydrogen are highly flammable gases, while ammonia is a highly toxic refrigerant. Water is a refrigerant that have high latent heat of vaporization, thermally stable, safe and environment friendly properties but it has not been recommended to use for cooling application below 0˚C due to freezing point of water. Also developing air conditioning and refrigeration systems that are driven by renewable energy resources such as solar and geothermal energy can reduce environmental impact. Solar cooling has the potential of significantly reducing the

electricity consumption, contributes to fossil fuels saving and electrical peak load reduction and furthermore, contributes in a positive way with the urban microclimate through absorbing the solar irradiation on the roofs, reducing the carbon emissions and using environmental friendly refrigerants [6].

Adsorption cooling provides innovative technology with almost no GHG emissions. Nevertheless, further research is still necessary not only to improve the performance of the adsorption working pairs in order to build compact, energy efficient, reliable, and long-life adsorption chillers, but also to develop adsorption pairs that have low or no adverse impact on the environment.

Adsorption cooling technology in automobile air conditioners provides another application where the use of heat from the exhaust gas or the cooling loop can reduce the fuel consumption [7].

1.3 Applications of ice making systems

Adsorption ice making is a promising technology that can utilise waste heat to produce ice for many applications due to its ability to exploit low temperature heat sources and the use of environment friendly refrigerants [8]. Consequently many researchers have investigated the use of adsorption systems for ice making application like storing fruit, vegetables, fish, medicines and vaccines for domestic and industrial sectors especially in many remote areas where there is no access to electricity [8, 9]. In those places, solar energy, waste energy produced by burning unwanted crops or biomass could be used to drive the adsorption ice making systems. In China, for example, there is a vital challenge to produce the ice as the cost of electricity generation is the major restriction for producing ice using the conventional mechanical vapour compression refrigeration system.

1.4 Enhancement of adsorption ice making systems: a state of the art

Significant research has been carried out on adsorption ice making systems to enhance their performance. Methods of enhancing adsorption ice making systems include (1) developing adsorbent materials with high adsorption uptake [10], (2) developing effective adsorption cycle configurations with heat and mass recovery [11], (3) developing compact adsorber beds and (4) increasing the number of outputs to enable wide range of applications.

Increasing the number of outputs of the adsorption ice making system enhances the system performance and increases its application in many industries that have several demands like food chain, fishing boats which require food cooling, air conditioning and potable water. For example; Lychnos et al (2014) integrated the adsorption refrigeration system with the vapour compression refrigeration cycle to increase the outputs of the system for ice making and air-conditioning applications. They exploited the exhausted heat form the mechanical compressor (ranging from 90 °C to 250 °C) to drive the thermal adsorber bed thus enhancing the performance of the system (COP ranged from 0.24 to 0.76) and increasing the potential application of the system by enabling evaporation at temperature ranging from -5 °C to 20 °C [12].

Some research work investigated means of increasing the specific daily ice production (SDIP). For example; Wang et al (2000) [13] achieved the maximum value of SDIP (2.6 ton/day/ton of adsorbent) by using spiral plate adsorber bed based adsorption ice making system with COP of 0.13 at evaporation and desorption temperatures of -15°C and 100°C.

The above described works showed that the increase of outputs from adsorption ice making system leads to exploiting the same system for more than one application and

enhancing the performance of the adsorption system. So far most research work is dedicated to improve adsorption ice making system as a single output; some research is available for combining ice making with other applications like air conditioning (cooling or heating) but very limited published work on producing more than two outputs from adsorption ice making systems. However, no work has been investigated to increase the potential of the system for achieving more than two outputs. Consequently, a comprehensive investigation is needed to find a new method to increase the outputs and improve the performance of the adsorption ice making system.

Commonly used adsorbents in adsorption ice making systems were activated carbon, composite adsorbents based on activated carbon and zeolite. Activated carbon has high uptake with refrigerants like methanol or ammonia but these refrigerants have low thermal properties compared to water. Zeolite has low uptake with water despite the high latent heat of vaporization of water. Metal Organic Framework (MOF) materials are new advanced adsorbent materials with high water adsorption uptake. However, no work has been reported to use MOF material as adsorbent for adsorption ice making application. Furthermore, using adsorption ice making systems for more than two outputs has not been reported.

1.5 Aim and objectives

The main aim of this study is to improve the cooling performance and ice production of adsorption systems by increasing the system outputs, namely, ice, ice slurry, cooling and desalinated water using Metal Organic Framework material (MOF) as an adsorbent material with potable and saline water as refrigerants through the following objectives:

1. Comprehensive review of adsorption refrigeration systems including (i) application and number of useful outputs, (ii) adsorption ice making system working pairs, bed design and Specific Daily Ice Production (SDIP) of adsorption ice making systems, (iii) various techniques used in freeze desalination systems, (iv) adsorption desalination systems including working pairs and Specific Daily Water Production (SDWP).
2. Develop a new evaporator concept based on vacuum-direct freezing to increase the outputs of the adsorption ice making system by using potable water and saline water as refrigerants.
3. Develop a single bed adsorption system to utilize the developed vacuum-direct freezing evaporator for producing ice, ice slurry, cooling and desalinated water using CPO-27 (Ni) MOF and potable/saline water as a working pair.
4. Develop a double bed adsorption system using the same technique for producing the same outputs of the single bed system however with an advantage of continuous cooling process to further enhance the performance.
5. Analyse and compare the performance of the single and double bed system based on the multi output and investigating the effect of various parameters to highlight the overall system performance compared to these reported in the literature review.

1.6 Contribution to new knowledge

The contributions to knowledge achieved in this research project are as follows:

- MOF based adsorption system with sea water as the refrigerant can be used for ice making where CPO-27Ni MOF with superior water adsorption characteristics has been used.

- A novel approach of using the adsorption process to generate the vacuum required in the evaporator for vacuum-direct freezing process which enabled evaporating at temperatures below zero. This approach is superior to conventional vacuum generating technology using mechanical electrically driven vacuum pumps since this adsorption system is heat activated.
- Using the above showed that it is feasible to produce four outputs namely, ice, ice slurry, cooling and desalinated water compared to two outputs either ice making and cooling or ice making and heating reported in the literature.

1.7 Thesis outline

This thesis consists of five chapters. Chapter one introduces the research topic and describes the aims and objectives and thesis outlines.

Chapter two reviews the theoretical and experimental research work on adsorption refrigeration system by highlighting the demand and outputs. A comprehensive review on adsorption ice making and adsorption desalination systems are included to highlight the SDIP, SDWP, working pairs, outcomes and shortages.

Chapter three describes all components of modified single bed adsorption system developed for multiple outputs. Moreover, the performance of the system in terms of multi outputs is experimentally investigated at different operating conditions.

Chapter four describes all components of double bed adsorption system for multi outputs and investigates the system performance at various operating conditions. A compression between the performance of the two bed and single bed adsorption system for multioutput was also given in this chapter.

Chapter five lists the major findings from the experimental study of single and double bed systems. The recommendations for future work are also suggested for improving the developed system performance further.

CHAPTER 2

Literature Review

2.1 Introduction

Adsorption refrigeration and desalination systems utilising (i) waste heat from power generation system, automotive engines and, industrial processes and (ii) renewable thermal energy from solar and geothermal sources have low global warming and zero ozone depletion potential. This chapter provides a comprehensive review of adsorption refrigeration and desalination systems including the outputs potential of these systems, working pairs of ice making systems, different configurations of adsorber bed designs, techniques to improve the production of ice and a brief review of desalination systems. All the above stated points are comprehensively reviewed to highlight the method used to increase the output of adsorption refrigeration/desalination systems and find an optimum working pair for enhancing the performance of such system.

2.2 Adsorption refrigeration system

2.2.1 Overview

The first work on a solid sorption refrigeration phenomenon was reported by Faraday in 1848 using silver chloride and ammonia as a working pair [14]. In the 1920s, Plank et al. experimentally proposed a commercial adsorption refrigerator utilizing activated carbon and methanol as a working pair. In the same period, Hulse proposed an adsorption refrigeration system working at evaporation temperature of 12 °C for food preservation using silica gel and sulphur dioxide as a working pair. From the early years of the thirties

century, a new generation of refrigeration system was developed known as a vapour compression cycles using chlorofluorocarbon (CFCs) and Hydrofluorocarbon (HFCs) refrigerants and its performance was considerably developed compared to the adsorption refrigeration system. Therefore the demand on the refrigeration systems was met dominantly by vapour compression system and there was an insignificant interest in adsorption refrigeration systems. As a result of Montreal and Kyoto Protocols, which legislated ban on substances that have ozone layer depletion like CFCs, HFCs and global warming due to high energy consumption with associated CO2 emissions, the demand on green refrigeration technology have increased [15]. The concern over the ozone depletion and greenhouse gas emission has been agreed in 1970s up to the current day [16].

Globally, there is a significant amount of waste heat emitted from power plants operating at an efficiency ranging from 30% to 50% [17-19]; a significant amount of this waste heat has a temperature below 100 °C as shown in Figure 2-1 [20, 21]. Adsorption and absorption refrigeration technologies are the most recommended technologies to exploit this waste heat to produce cooling; thus reducing fossil fuel consumption and CO_2 emissions. Despite the performance of absorption refrigeration systems (0.47 [22]) being higher than that of the adsorption systems (0.069 [23]) at same evaporation and driven temperature, they do have some drawbacks, such us: contamination, crystallization and corrosion [24-26]. Adsorption cooling technology offers many advantages compared to absorption and vapour compression system in terms of stability, lower vibration, quiet operation, low initial cost and the use of environment friendly working pairs [14, 27], but suffers from low COP values.

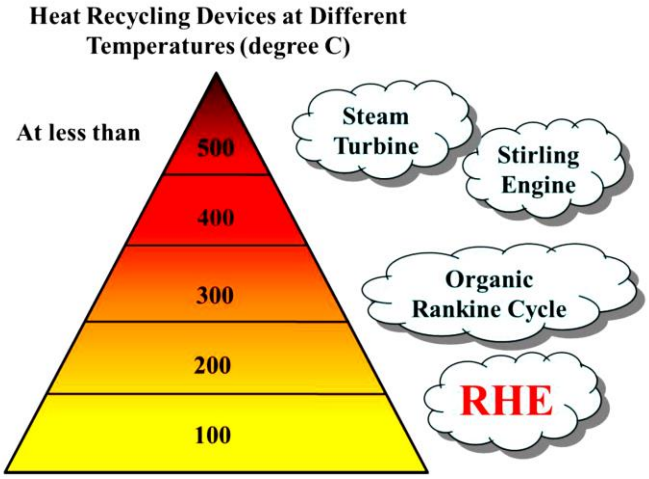

Figure 2-1 Availability of waste heat at wide range of temperature [20]

The development of adsorption refrigeration systems was firstly conducted regarding the performance of different working pairs including the characterisations of the adsorbents and refrigerants; therefore, the majority of researches were carried out by specialists in the chemistry and physics field. Furthermore, several researchers investigated the adsorption refrigeration system to be exploited in real applications like air conditioning [28], cooling [29] and ice making [30]. The combination between the experimental and theoretical results was also investigated using thermodynamics and chemical approaches [14].

2.2.2 Applications of adsorption refrigeration system

Globally, the demand on refrigeration systems has been increasing due to various industrial and residential applications including production of ice, cooling, freezing and air conditioning. Cooling is a commonly used method to store medicine, vaccine and food (meat, vegetables, milk, fruit and any product) to extend the interval of their validity [31] and [32]. Two stage adsorption cycle was used at evaporation temperatures of -15℃ and 5℃ for food storage purpose (fish, meat, vegetables) [33]. An adsorption solar refrigerator was constructed and tested to preserve vaccine for application in rural areas where there is

no electricity [34] and [29]. Another way to utilize the refrigeration system is ice making which can be used in many applications like domestic usage and preservation of food, medicine and vaccine especially in remote and rural regions where there is no access to electricity [34] and [35], and to preserve sea food on fishing boats [35]. The demand on air conditioning systems has also increased in developed and industrial countries especially in the warm regions of the world [32]. The refrigeration systems are also used in chemical engineering processes [31] and [36].

2.2.3 Potential outputs of adsorption refrigeration system

This section highlights the common outputs of adsorption refrigeration systems to determine the potential of increasing the outputs of such system, thus increasing their efficiencies and range of applications.

2.2.3.1 Single output

There are many studies on using adsorption refrigeration systems for one output only like cooling, ice making or air-conditioning. In these studies, different working pairs, system configurations and operating conditions were investigated as follows:

2.2.3.1.2 Ice making

The majority of the experimentally studied adsorption ice making systems are solar driven to produce ice as a single output to be used for different purposes and in rural areas where there is no electricity [1, 8, 13, 23, 34, 37-60]. Some research work was carried to investigate experimentally adsorption ice making system driven by IC engines waste heat for storing fish on boats [35]. However limited research work was carried out to investigate theoretically ice making adsorption systems driven by solar energy [61] and [9]. The

evaporation and desorption temperature were investigated at various values ranging from 0℃ to-27.5℃ and 78℃ to 300℃ as shown in Table 2.1.

(ii) Air conditioning

An adsorption air-conditioner was built using activated carbon and ammonia as a working pair with COP of 0.22 at evaporation and desorption temperatures of 20℃ and 90℃, respectively [28]. An air conditioning process was experimentally achieved using activated carbon- methanol based adsorption heat pump system with COP of 0.4 at evaporation and desorption temperatures of 6.7 and 89℃, respectively [13]. A novel adsorption refrigeration system was investigated for air conditioning purpose using silica gel/water as a working pair with COP of 0.41 at evaporation and desorption temperatures of 15 and 57℃, respectively [62].

(iii) Cooling > 0 ˚C

Using evaporator temperature higher than 0℃, there are many researches on the adsorption cooling system to be used for cold storage of food, vaccine or medical products. A solar adsorption cooling system was constructed for storing agricultural goods at temperature of about 2 to 4C with COP of 0.3 at desorption temperature of 85℃ [63]. A double stage adsorption chiller was theoretically studied to evaluate the optimum performance (COP of 0.2) of the system for cooling at evaporation temperature of 14℃ and desorption temperature of 80℃ [26]. An intermittent solar adsorption cooling was built and tested showing COP of 0.123 at desorption temperature of 87 ˚C for preserving vaccine at temperature of 2˚C [29].

(iv) Cooling < 0℃

Some researchers investigated adsorption systems for low temperature cooling (< 0℃). A cascaded adsorption cooling system with integrated evaporator-condenser was theoretically investigated using ATO/ethanol + AC-35/methanol to produce cooling at -10℃ using low desorption temperature of 70℃ with COP of 0.029 [64]. A dual stage adsorption refrigeration system was investigated using two types of working pairs to produce cooling at a temperature of -10 ˚C with COP of 0.85 using high desorption temperature of 275℃ [65].

2.2.3.2 Double outputs

Many works on adsorption refrigeration systems have been used to produce two beneficial effects, as follows:

(i) Ice making and air-conditioning

A hybrid adsorption – vapour compression refrigeration system was investigated for ice making and air conditioning application with COP ranging from 0.24 to 0.76 at evaporation temperature from -5˚C to 20˚C, the system was driven using thermal energy at temperature ranging from 90 ˚C to 250 ˚C and electricity [12].

(ii) Ice making and heating

An adsorption ice making system with a heat storage system was constructed using evacuated tube type solar collector [23, 66]or flat plate solar collector [67]. The two outputs were used for industrial or residential applications. A hybrid solar adsorption system was built to investigate the potential of producing cooling and heating for domestic

use showing COP and heating efficiency of 0.11 and 0.45 at evaporation and desorption temperatures of -0.5 and 50 ˚C, respectively [68].

(iii) Cooling (>0˚C) and desalination

The performance of a double stage four bed adsorption system was theoretically investigated for cooling and water desalination using silica gel/water and AQSOA-Z02/water as working pairs. SDWP of 15 ton/day/ton of adsorbent was achieved form both stages at desorption and evaporation temperatures of 80˚C and 10 ˚C , respectively [2]. Four-bed adsorption desalination system was theoretically and experimentally investigated using silica gel and water as a working pair to produce cooling (COP of 0.55) and fresh water at evaporation and desorption temperatures of 10 ˚C and 85 ˚C, respectively

(v) Cooling and freezing

An adsorption refrigeration system was built and investigated for cooling at 5℃ and freezing at -15℃ for food storage showing COP ranging from 0.13 to 0.28 at desorption temperature ranging from 70 to 90 ˚C [33].

(vi) Cooling (< 0˚C) and heat pump

An adsorption system was built for heat pumping to provide the heat required for multi hydride- thermal-wave and cooling at -10 ˚C application with COP of 0.8, using metal hydride and hydrogen as a working pair at desorption temperature of 220 ˚C [69].

(vii) Freezing and power generation

A cascaded adsorption freezer was combined with Organic Rankine Cycle (ORC) as a hybrid system to investigate the potential of producing electricity and freezing outputs [31].

2.2.4 Adsorption ice making system

Based on the significant demand for ice, there is a significant research regarding adsorption ice making systems [66]. This section provides detailed literature review of adsorption ice making systems including applications, working pairs, configurations and performance in terms of SDIP and COP.

2.2.4.1 Working pairs

The most essential component of the adsorption ice making system is the working pair which highly affects the performance of the adsorption ice making system in term of SDIP and COP [70]. There are many published research work on adsorption ice making systems using different working pairs.

2.2.4.1.1 Refrigerants

To achieve effective and environment friendly ice making system, the working fluid (refrigerant) should have good thermal properties including high specific latent heat of evaporation and high thermal conductivity. The refrigerant should also be environment friendly with no ozone depletion and low global warming potential [70]. In adsorption ice making applications, a number of refrigerant have been reported in the literature as follows:

(i) Methanol

The majority of literature on adsorption ice making systems used methanol as a refrigerant with about 65% of all listed researches in Table 2.1. It could be used with activated carbon, silica gel and zeolite. The advantages and disadvantages of methanol are:

- ***Advantages***

  a) Environmentally friendly refrigerant with zero ozone depletion and global warming[39].

  b) It has a moderate latent heat of vaporization (1182kJ/kg at -10°C) [41].

  c) It can be adsorbed by activated carbon [71]. Its molecules has an effective diameter of 4Å, thus it could be adsorbed by microporous activated carbon with 20 Å pores [41]

  d) It is stable at desorption temperatures lower than 120 °C without the risk of flammability [72].

  e) It has a high uptake with activated carbon about two times higher than silica gel-water at the same operating conditions [71].

  f) It evaporates at low temperature <0°C as the freezing point is -20°C [3] thus it is suitable for ice making application [41].

  g) It operates at vacuum condition thus has the advantage of good health and safety as in case of leakage problem, the methanol stay inside the system [39].

- Disadvantages

  a) It is flammable refrigerant and harmful to skin and eyes [53] thus it is very important to use an alarm sensor in the system as the requirement of health and safety [64]. But it is less dangerous and has no compatibility issue compared to ammonia [73].

  b) At desorption temperature >100℃, methanol is not compatible with copper due to corrosion[70].

c) The manufacturing process of the adsorption machine for vacuum operation is relatively complicated.

(ii) Ammonia

Ammonia has been investigated as a refrigerant in adsorption systems for ice making application but at a lower rate of about 22% of all listed references in Table 2.1. Ammonia was commonly used with activated carbon and metal chlorides, with the following advantages and disadvantages,

- Advantages
    a) It is natural and environmentally friendly refrigerant [73]
    b) It could be used for ice making application as the freezing point is about -83℃ [3].
    c) Its latent heat of vaporization is up to 1294.6 kJ/kg at -10°C [55].
    d) It operates at pressure higher than the atmospheric pressure thus the potential of air infiltration is very unlikely. Furthermore, the manufacturing process of a system with positive operating pressure is less demanding than that of a system operating with pressure below the ambient [8].
    e) Based on high operating pressure of its vapour, the mass transfer can be effectively achieved at low cycle times [73].
    f) Its thermodynamic properties with the commonly used adsorbents are stable up to the desorption temperature of 200℃ [73].
    g) The adsorption ice making system has a short cycle time compared to methanol and water as refrigerants [3].

h) It could be used with low temperature heat energy (<200) like solar and waste heat resources [27].

- Disadvantages
    a) It is toxic and not recommended to use in residential or office buildings [73].
    b) At desorption temperature >100℃, ammonia is not compatible with copper metal due to corrosion [70].

(iii) Water

Limited literature on adsorption ice making systems were focused where water was used as refrigerant with 7.8% of all listed papers in Table 2.1. Water has been used with zeolite or silica gel and has the following advantages and disadvantages.

- Advantages
    a) It has the highest value of latent heat of vaporization (2258 kJ/kg at 0℃) among the commonly used refrigerants, which is about two times as large as the value of ammonia. This means that the refrigeration effect and coefficient of performance are relatively higher than those of methanol and ammonia based system for cooling application > 0℃ [3].
    b) It is cheap, available and ecologically friendly [44].
    c) It is thermally stable [3].

- Disadvantages
    a) Due to its high freezing point (0 ^{o}C), most of the literature indicated that water cannot be used as a refrigerant for ice making applications [41, 63, 70].

(iv) Other refrigerants

There are other refrigerants that have been studied for adsorption ice making system like ethanol, acetone and hydrogen (about 2% of the all listed work in Table 2.1). They were used at various evaporation temperatures which are blow the freezing point of water.

2.2.4.1.2 Adsorbents

Adsorbent material is very important component in the adsorption ice making system as it circulates the refrigerant throughout the system using the adsorption and desorption processes which are activated by cooling and heating of the material respectively. There are many types of adsorbent materials that have been used in the adsorption ice making as described below:

(i) Activated carbon

Activated carbon is a commonly used adsorbent material in adsorption ice making systems with about 78.2% of the listed papers in Table 2.1. It has been used with numerous refrigerants to produce cooling below 0℃ [74-77]. Activated carbon has some advantages in terms of having a large surface area and relatively low cost. There were various types of activated carbon materials which have been described in previous works [78].

Activated carbon was used with ammonia [34], ethanol [53] and methanol [79] as they have the same chemical structures (non-polar or slightly polar structure). Moreover, activate carbon could be driven using low desorption temperature (<100℃) and its heat of desorption

is relatively lower than that of other adsorbent materials [78]. The activated carbon type Maxsorb III has superior adsorption uptake of ethanol but has a slow kinetics so it is only recommended in the long cycle's times.

Activated carbon mixed with calcium chloride ($CaCl_2$) has also been studied as a compound adsorbent in the adsorption ice making system. The rate of using the compound activated carbon was about 9% of the all listed literatures in Table 2.1.

(ii) Zeolite

Zeolite is a mineral material and polar adsorbent which was used in adsorption ice making systems with about 11% of the all reported work in Table 2.1. Zeolite is compatible with refrigerants like water and methanol, cheap and environment friendly material [44, 70]. There are some obstacles to using zeolite as an adsorbent in adsorption ice making systems. Zeolite has very slow response to changes in temperature during the adsorption process with water vapour. The refrigerant crystalizes at evaporator temperature below 0℃ which leads to reduction in the performance of the system [41]. Zeolite requires a high temperature heat source (150 to 250℃) to desorb the water vapour [44].

(iii) Other adsorbents

There were other adsorbents that have been investigated in adsorption ice making systems like silica gel as a physical adsorbent which is a polar adsorbent [70] and could be regenerated at desorption temperature below <100℃. Water has been used as a refrigerant with silica gel [44]. Chemical adsorbents have also been also used as sorbents like Chloride strontium [23], binary salt [60], metal hydride, binary salt system BaCl2+BaBr2, Manganese Chloride/Barium Chloride($MnCl_2$/$NiCl_2$). The usage of each of these

adsorbents hasn't not exceeded two percent of the all listed work in Table 2.1. Silica gel is commonly used in the adsorption refrigeration system but for cooling >0℃ [80]. Figure 2-2 shows all adsorbents and refrigerants which were investigated by researchers for adsorption ice making applications.

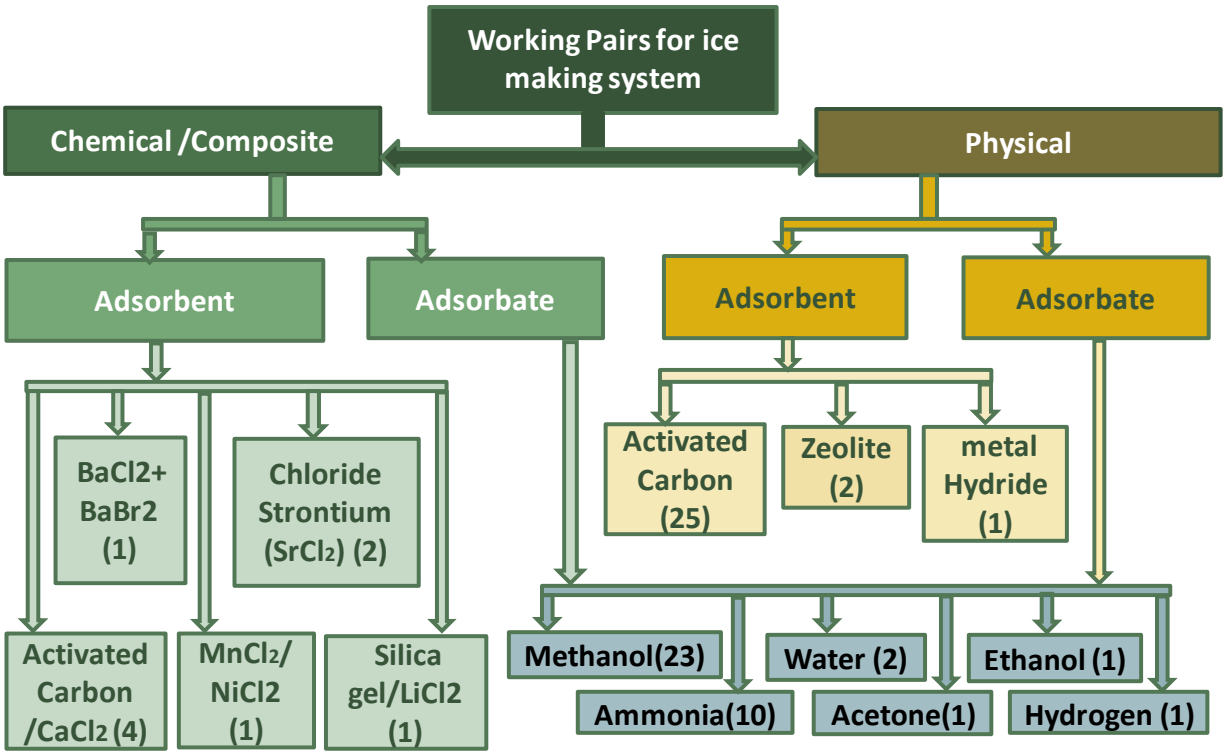

Figure 2-2 Classification of adsorbents and refrigerant based adsorption ice making system

(iv) New adsorbents; Metal Organic Framework materials

Recently, new adsorbents have been investigated for many applications; however they haven't been tested for adsorption ice making application. Metal Organic Frameworks (MOFs) are new type of solid sorbent materials, which have high pore volume, high surface area (up to 5500 m^2/g), uniform pore size and robustly tuneable structural properties. The MOF materials have been tested for gas storage [10], gas separation [81], sensors catalysis [82], water adsorption applications [83], thermal energy storage [24, 84],water desalination

[85] and automotive air conditioning [86]. For low temperature cooling, MOF material was investigated with ethanol as refrigerant [21]. Many MOF materials based adsorption cooling system have been investigated by Rezk et al. [83] with water as refrigerant. MIL-100(Fe) (Fe-BTC) and HKUST-1 were reported to have high water uptake (0.324 kg_w/kg_{ads}) compared to silica gel due to large porosity and surface area [83]. However, Henninger et al. (2010) [87] reported that the water uptake of HKUST-1 decreased after 30 cycles. Ehrenmann et al.(2011) [88] reported that the MIL-100(Cr) has high uptake with water ($1.43kg_w/kg_{ads}$) as shown in Figure 2-3, however, it is limited with application at high evaporation temperature [88] and currently just available in lab-scale [10]. Jeremias et al. (2014) reported the high uptake of aluminium fumarate MOF with water of 0.53 $kg_w/kg_{ads\ as}$ shown in Figure 2-3 [89]. Al-Dadah and her researches have experimentally and numerically investigated CPO-27(Ni) with water for adsorption desalination application [85] and thermal storage application [84]. They highlighted that CPO-27(Ni) has advantages in terms of Specific Daily Water Production (SDWP) at low evaporation temperature of 5˚C due to its low relative pressure and high water uptake (0.47 kg_w/kg_{ads}) (see Figure 2-3 and Figure 2-4) compared to other MOFs or common adsorbents [10, 82]. Elsayed et al. [84] investigated the effect of isotherm temperature on the water uptake of CPO-27(Ni) material. The CPO-27(Ni) showed a stable performance in terms of constant uptake at various temperatures of 25 ˚C, 35 ˚C and 55 ˚C as shown in Figure 2-5. Shi et al. [86] investigated the hydrothermal stability of CPO-27(Ni) material at 25˚C where it is clear that the material has a constant uptake over fifty successive adsorption/desorption cycles as shown in Figure 2-6. The pressure, temperature and water uptake (P-T-x) diagram of CPO-27(Ni) at evaporation temperature as low as 5˚C was only investigated by Elsayed

et al [90] to show the effect of evaporator temperature on the cycle performance for water desalination.

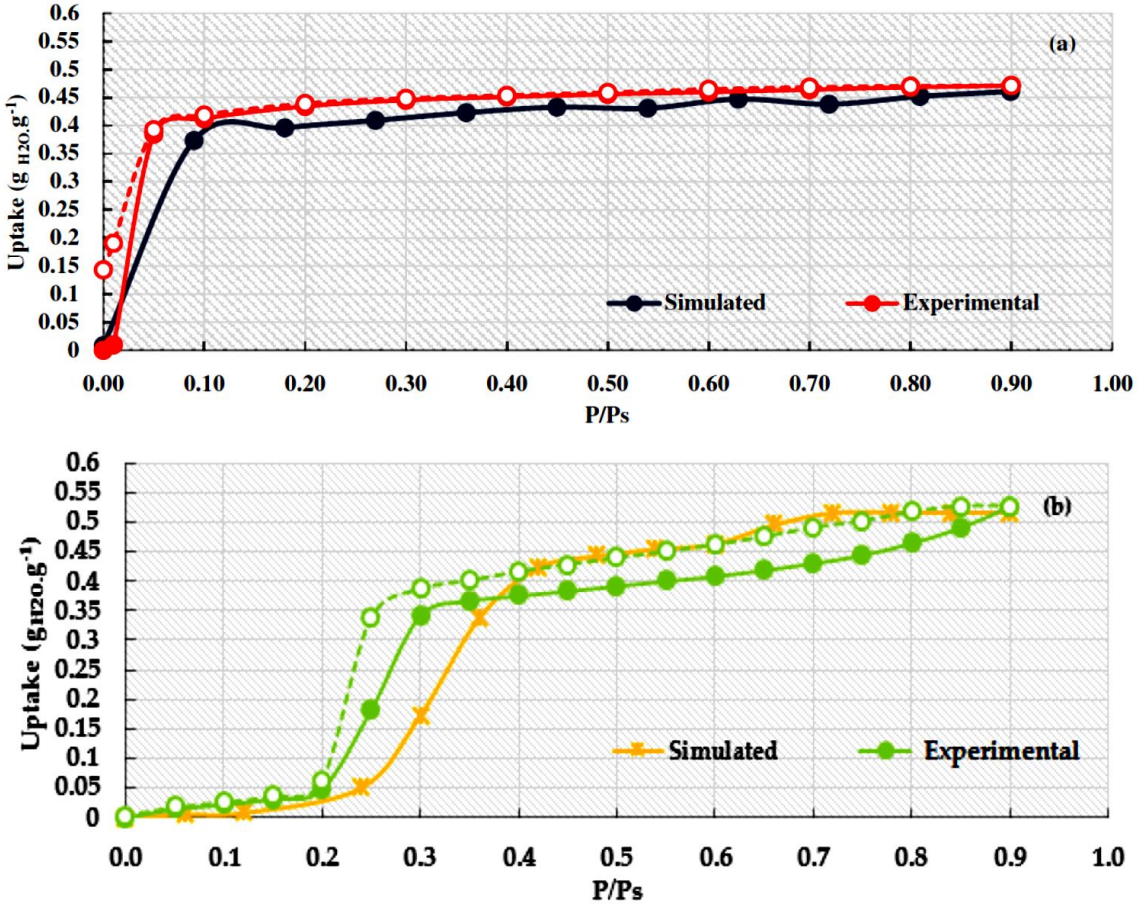

Figure 2-3 Water adsorption isotherm of (a) CPO-27(Ni) (b) aluminium fumarate and [10]

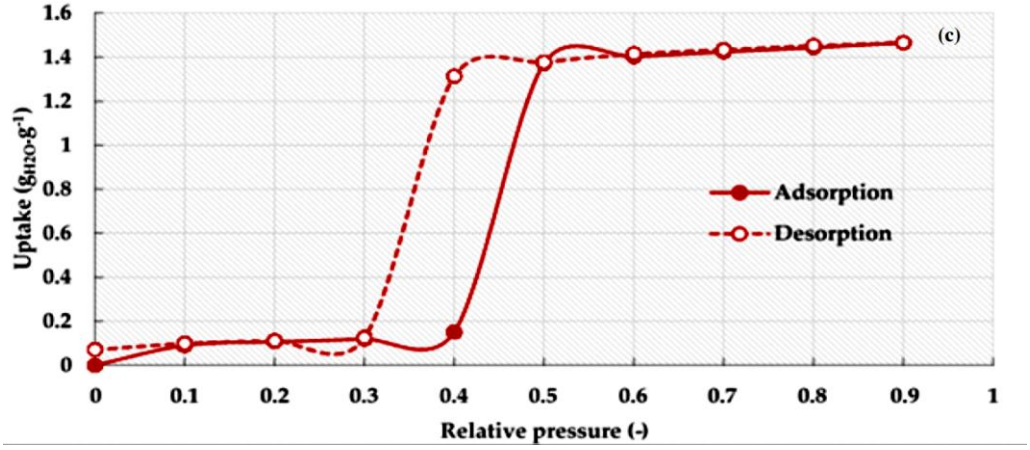

Figure 2-3 Water adsorption isotherm of (c) MIL-101(Cr) at 25 ˚C [10]

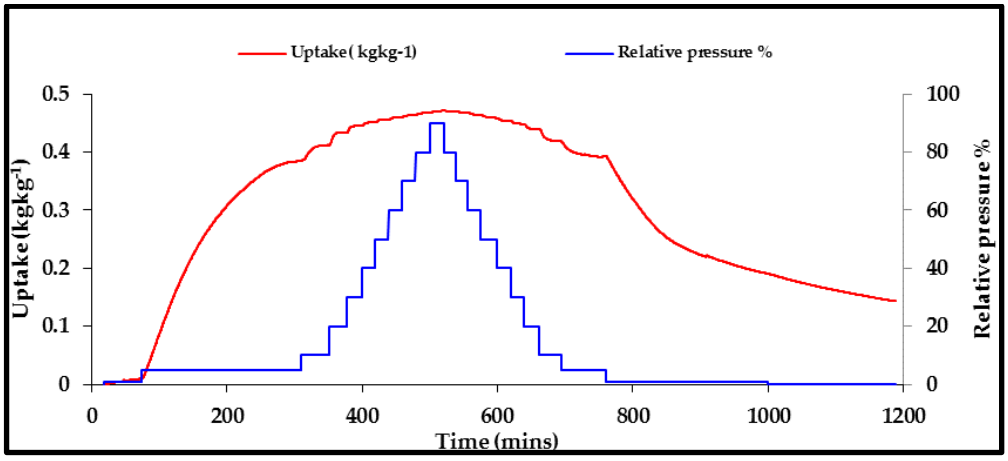

Figure 2-4 Adsorption kinetic of CPO-27(Ni) at 25˚C [86]

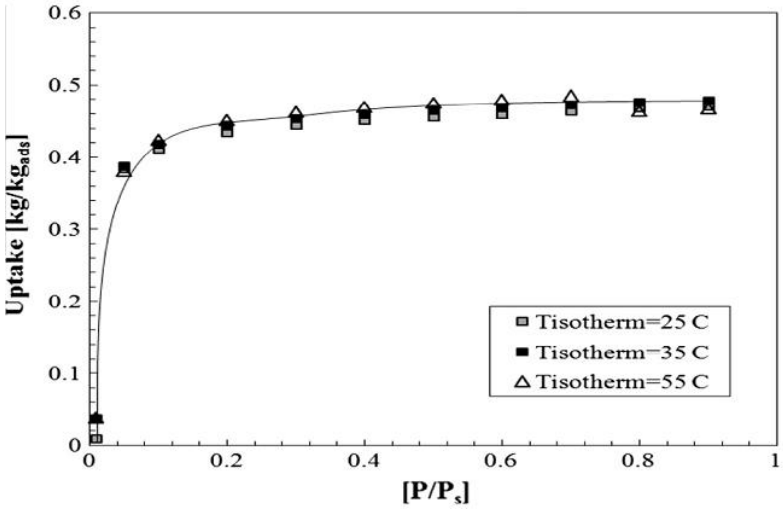

Figure 2-5 Water adsorption isotherms of CPO-27(Ni) MOF material at variant temperatures (25˚C, 35˚C and 55˚C) [84]

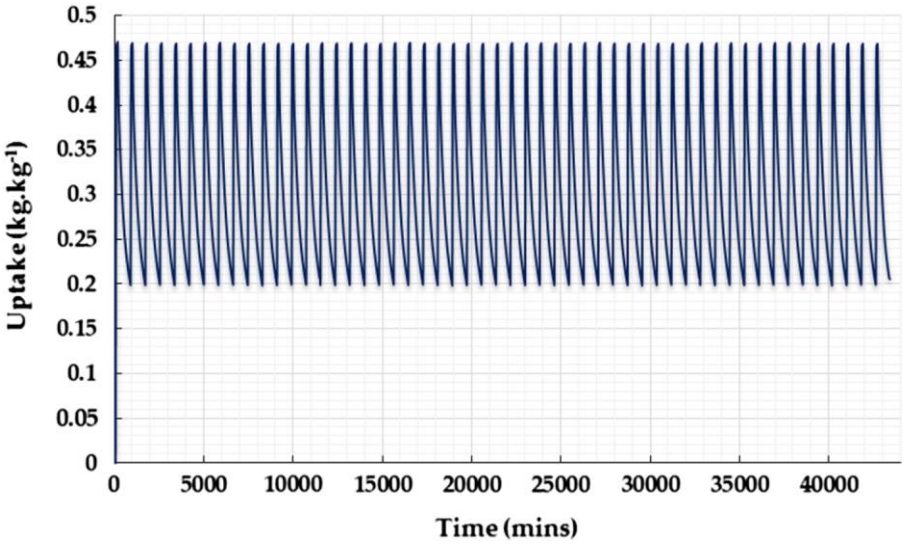

Figure 2-6 performance cyclic analysis of CPO-27(Ni) at 25˚C [86]

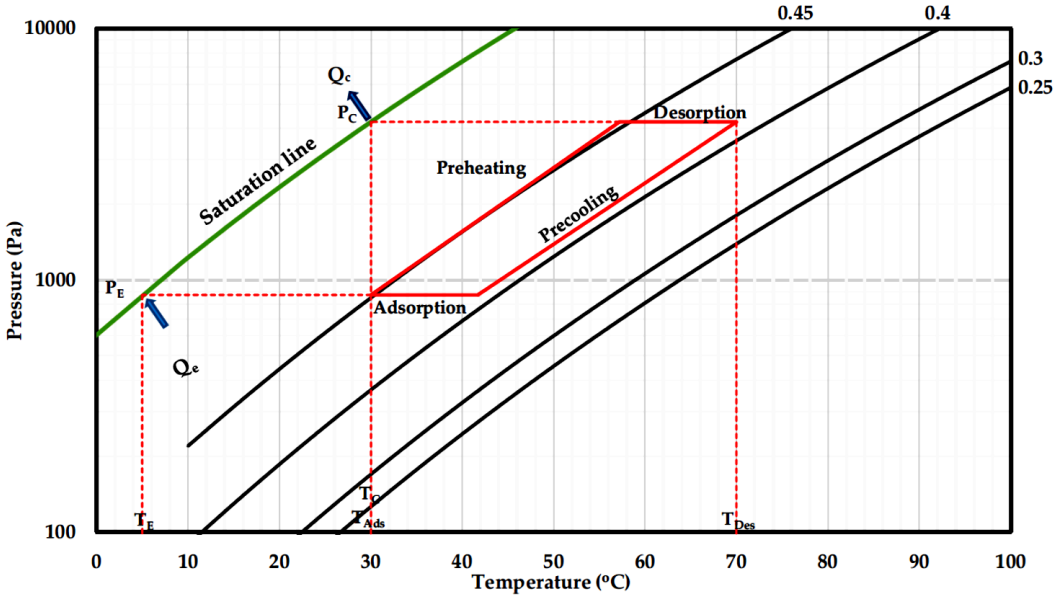

Figure 2-7 P-T-x diagram of CPO-27(Ni) at Adsorption, condenser, evaporator and desorption temperatures of 30 ˚C, 30 ˚C, 5 ˚C and 70 ˚C, respectively) [90]

2.2.4.2 Specific Daily Ice Production (SDIP)

Wide range of research activities were experimentally and theoretically carried out for the development of adsorption ice making systems. Table 2.1 summarises the performance of such systems in terms of the achieved SDIP, number of outputs, working pair, the heat source, and system performance. The majority of researchers used activated carbon as

adsorbent with methanol or ammonia as refrigerants as discussed in section 2.2.4.1 This is due to the potential of such working pairs to achieve cooling at the temperature required for ice making where the freezing point of such refrigerants are lower than that of water.

The table shows that the achieved values of specific daily ice production (SDIP) range from 0.03 to 2.6 ton/day/ton_ads (or kg/day/kg_ads). The maximum value (2.6 ton/day/ton_ads) was practically achieved by an adsorption refrigerator constructed by Wang R.Z. et al 2001 [13] using activated carbon and methanol as a working pair. The ice production was increased with the use of a spiral plate heat exchanger as adsorber bed [13]. SDIP of 1.66 ton/day/ton_ads was experimentally achieved using compound adsorbent Calcium chloride/Active Carbon ($CaCl_2$/ AC) /Ammonia as a working pair with COP of 0.15. The system was integrated with a parabolic trough solar collector to supply the required thermal energy for adsorption ice making and heat storage systems [8]. The third highest value of SDIP (0.83ton/day/ton_ads) was theoretically achieved by simulating a solar adsorption ice maker using silica gel/lithium chloride as a novel composite adsorbent with methanol as refrigerant [61]. An optimisation of solar adsorption ice maker was theoretically investigated to produce ice using AC NORIT RX3-Extra and methanol as a working pair showing SDIP of 0.93 ton/day/ton_ads [38]. The next highest value was up to 0.747 ton/day/ton_ads, which was theoretically obtained by simulating solar adsorption ice making system as a single output [39]. Up to now (see Table 2.1), only few studies have used zeolite-water as working pair for ice making applications using high desorption temperatures up to 180˚C to achieve SDIP ranging from 0.09 to 0.3125 ton/day/ton_ads and COP ranging from 0.08 to 0.8.

2.2.4.3 Input power and adsorption bed design

The thermal energy required by adsorption ice making systems was commonly based on solar energy with more than 60% of the all listed papers in Table 2.1. The solar energy was collected using various configurations of solar collector which are summarized in Figure 2-8. The other sources of thermal energy were either a waste heat from diesel engine or electrical heaters for study purpose.

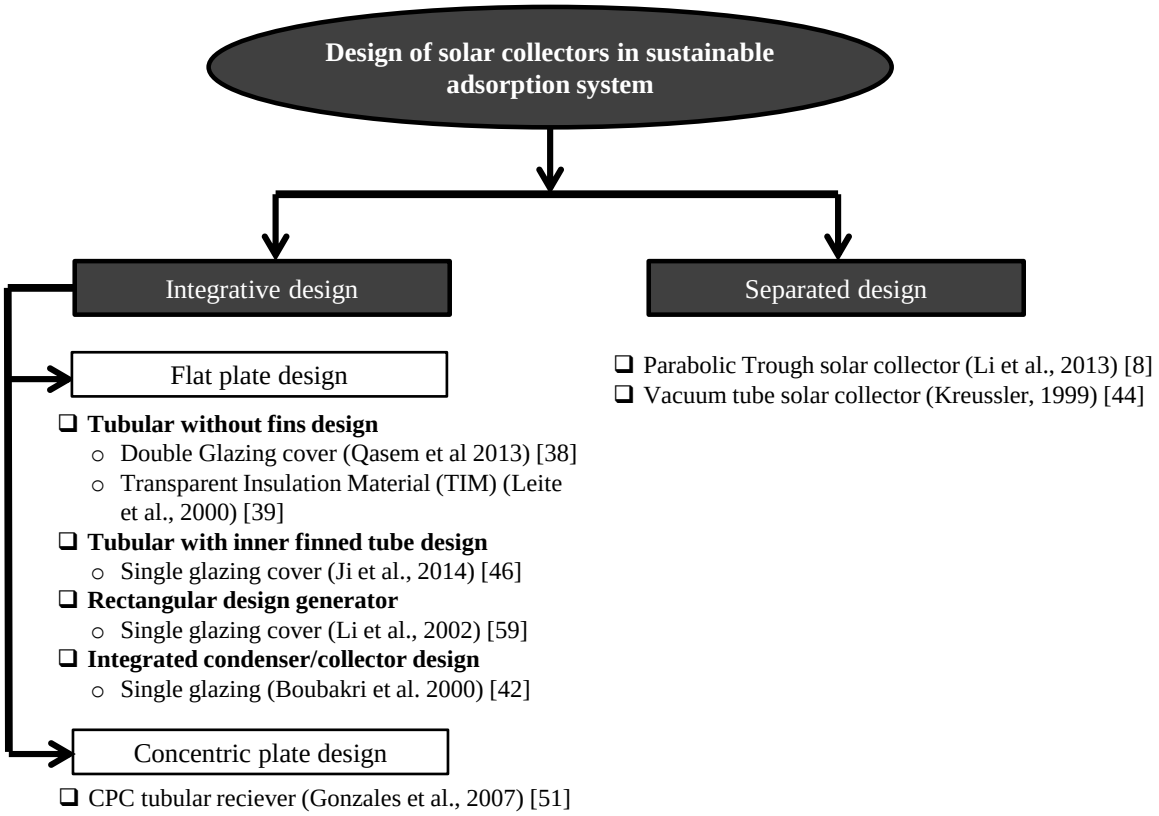

Figure 2-8 Type of solar collectors based adsorption ice making systems

Several adsorber bed designs have been used in adsorption ice making systems. Ji et al. (2014) [46] developed a new configuration of solar collector-bed consisting of a large diameter of inner finned aluminium tube as shown in Figure 2-9, packed with activated carbon as the adsorbent material where the solar radiation was absorbed by the outer surface of collector-adsorber tubes [46].

Figure 2-9 Configuration of the inner finned tube [46]

Gonzalez et al. (2007) produced a collector- bed design as shown in Figure 2-10. Compound parabolic concentrators (CPC) were used to focus the solar radiation on the adsorber bed in which the adsorbent material was packed. The adsorber beds were constructed as tubular collectors to receive the concentrated radiation from CPC [51].

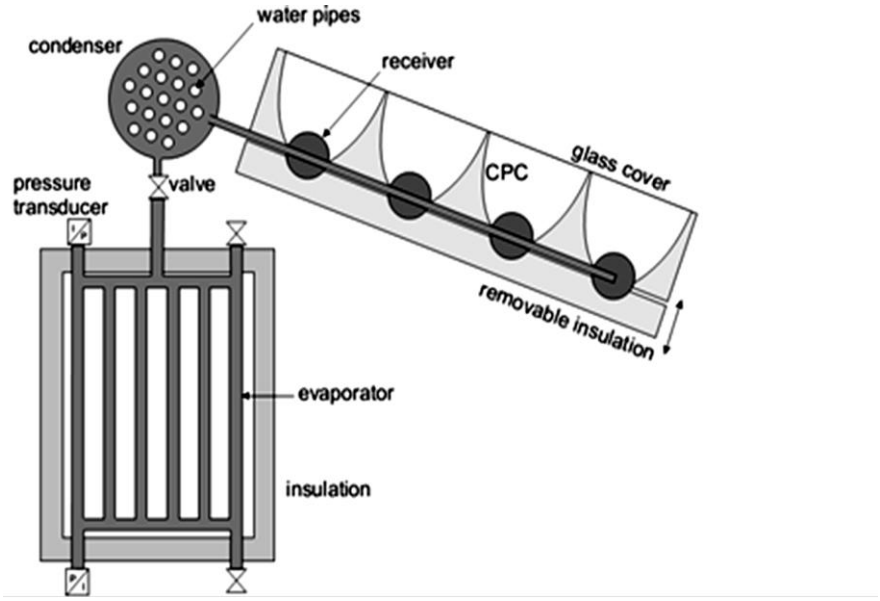

Figure 2-10 Schematic diagram of the whole unit by Gonzalez et al., 2007 [51]

The solar collector was integrated with adsorber bed to improve the heat transfer process in the collector-bed but fabricated with a different design as shown in Figure 2-11. The heat transfer process was also increased by adding many fins into the same unit, see Figure 2-11. The solar radiation was absorbed quickly by the top surface of this unit and transferred to

the adsorbent material. Li et al. (2002) used two units of such bed with a surface area of 0.75 m^2 for each one. Each flat-plate collector was loaded by 22 kg of activated carbon. After the black dye was coated on the top surface of the unit, the greenhouse effect was applied by adding glass cover at the top of flat-plate collector [79].

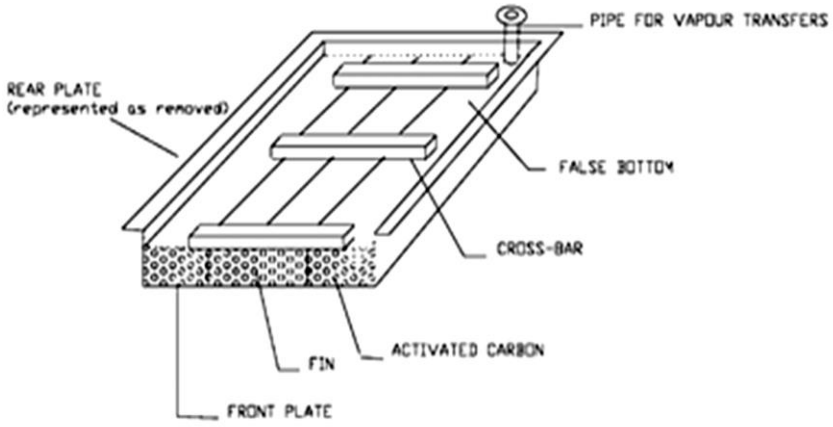

Figure 2-11 Schematic of the adsorbent bed [79]

Qi (2005) studied a hybrid system solar adsorption ice making system where the inner finned tubes were applied inside the adsorber unit, Figure 2-12. The adsorber here was not integrated with the solar collector, but, the hot water from the solar collector was pumped through the adsorber bed during the desorption process. The SDIP of 0.527 was achieved at evaporation temperature of -15 ˚C [23].

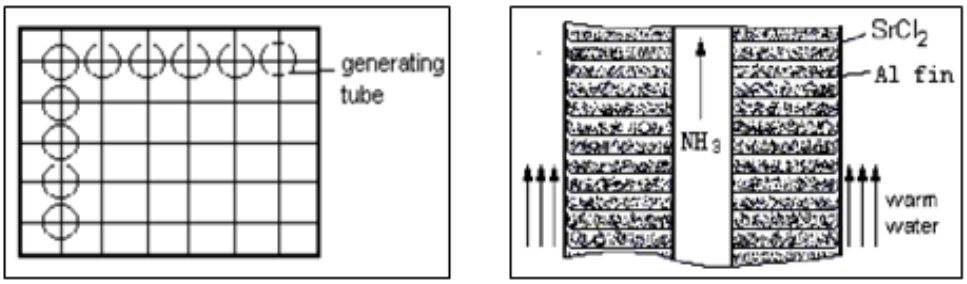

Figure 2-12 (a) Schematic of bed; (b) side section view of bed tube [23]

In order to reduce the size of the adsorption system, the adsorber was divided into units with smaller size. Li et al. (2013) built an adsorption icemaker with four adsorber units (shells) where each adsorber has the diameter of 159mm, see Figure 2-13. Seven finned tubes were installed into each shell, where the total mass of adsorbent packed in the 28 finned tubes was 30 kg. The SDIP of 1.66 ton/day/ton of adsorbent was achieved [8]. Similarly Wang et al. (2006) adopted the same approach using two units as shown in Figure 2-14. However, they included vapour channels to increase the mass transfer process and stainless steel mesh inside and outside the finned tube where the first one was to increase the heat transfer area and the second one was to seal the adsorbent grains [57]. Oliveira et al. (2006) used a similar bed configuration in which 145 grams of adsorbent material was packed inside the tubes as shown in Figure 2-15 to study the adsorption cycle for producing ice using low temperature heat source (-27.3 to -16 ˚C) [55]. Tamainot-Telto et al. (1999) developed another adsorber bed configuration for ice production application (at evaporation temperature ranging from -20 to 0 ˚C) as shown in Figure 2-16. The bed was made of aluminium alloy and consists of three passes to circulate different fluids. An inner shell with 25mm was located at the centre and two vessels with larger diameters were placed around the first one. There were many fins on the outer surface of the inner shell where adsorbent discs were placed [52].

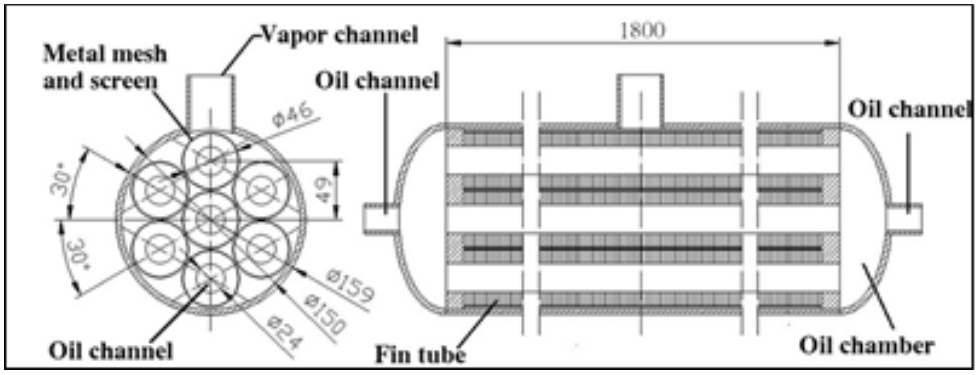

Figure 2-13 Adsorber bed unit by Li et al, 2013 [8].

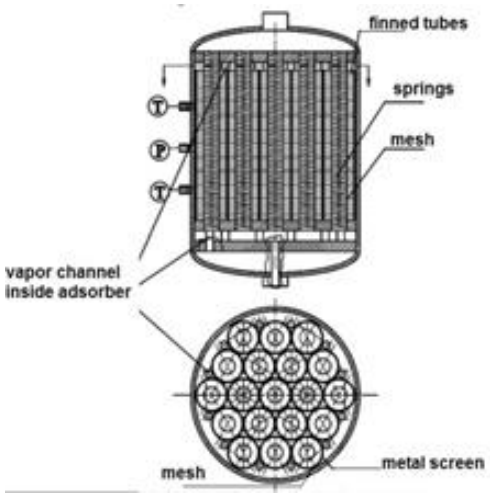

Figure 2-14 Adsorber bed unit by (Wang et al., 2006) [57]

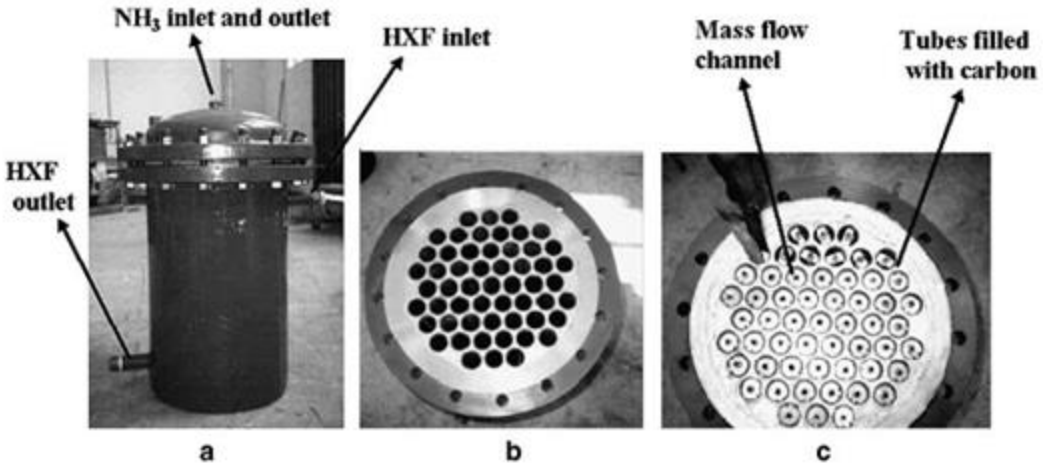

Figure 2-15 (a) Adsorber; (b) top view of the tubes; (c) tubes filled with adsorbent by (Oliveira et al., 2006) [55]

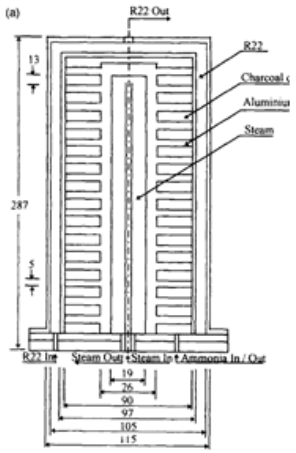

Figure 2-16 Sketch of adsorber bed unit (Tamainot-Telto et al, 1997) [52]

2.2.4.4 Techniques for enhancing adsorption ice making system

Many techniques have been experimentally or theoretically investigated to either increase the output or improve the performance of the adsorption ice making system. To increase the number of outputs of the solar adsorption ice making system, solar heating system was integrated with a hot water storage to provide the heat required for the adsorption ice making system and hot water for domestic/industrial applications as a dual effect [23] and [66]. An improvement on the performance of a hybrid adsorption-vapour compression system was investigated to increase the output of the system to include both ice making and air conditioning outputs [12].

Theoretical research have been carried out by optimizing many factors like the effect of double glazing, using thin metal in adsorber bed with selective coating, tilt angle, adsorption time [38], transparent insulation material [39], contact thermal resistance, adsorbent thermal conductivity, adsorbent packing density, environmental parameters and heat transfer fins [59] on the performance of the solar adsorption ice making system. For example, some researchers have integrated the adsorber bed with the solar collector to decrease the heat losses and improve the performance of the adsorption ice making system with COP of 0.147 [79] and 0.5 [41]. A novel solar adsorption refrigeration system was theoretically [47] and practically [67] investigated using new composite adsorbents materials to improve the performance of adsorption ice making system with COP of 0.33 [61] and 0.39 [27].

Another ways to improve the performance of the adsorption ice making system have been conducted by using different configuration of adsorber beds like spiral plate heat exchangers (COP of 0.13) [13], finned tubes (COP of 0.122) [46], flat-plate collector (COP

of 0.12) [58] a vacuum tube solar collector [44], a multi tubular configuration [40], a compound parabolic solar concentrators with tubular heat exchanger [51] or plate heat exchanger (COP of 0.7) [9]. An integration of the condenser with the solar adsorber bed was practically studied to improve the performance of system (COP of 0.36) [42]. A mobile adsorber was used to improve the performance of solar adsorption ice maker [45].

Some researchers have practically investigated the effect of intermittent heat input on performance of the adsorption ice making system (COP of 0.4) [35]. The potential of using transparent insulation material (COP of 0.33) [34] and consolidated composite adsorbent (COP of 0.35) [56] and [60] were practically investigated to improve the performance of solar adsorption ice making system. Capillary tube bundle was practically developed to improve the performance in the adsorption ice making system by investigating single, two stage and multi-hydride-thermal-wave system [69]. The effect of mass recovery (COP of 0.1) [55] and desorption time (COP of 0.0322) [91] were practically investigated to improve the performance of adsorption ice making system. An adsorption refrigeration system was constructed for ice making using heat pipe technique to enhance the heat recovery between the adsorbers beds with COP of 0.39 at evaporation and desorption temperatures of -20 ˚C and 114 ˚C, respectively [27].

Despite the significant efforts made by researchers regarding enhancing the performance of adsorption ice making systems, so far the highest SDIP achieved is 2.6 ton/day/ton of adsorbent [13] and the highest COP achieved is 0.8 [49]. Increasing the number of outputs for the adsorption ice making system can also enhancing the potential of employing adsorption ice making system for wide range of application which require more than one output.

Table 2.1 Lists of adsorption ice making systems

Ref.	Working pair	Outputs	SDP [ton/day/ton_ads]	$m_{adsorbent}/m_{refrigerant}$ [kg/kg]	COP [-]	T_{evap} [°C]	T_{des} [°C]	Notes	Heat source
[79]	AC/ methanol	1	**0.16-0.227**	44 / 3.23	0.452	-1	90-100	Flat plate solar collector-adrorber	Solar (quartz lamps)
[38]	AC NORIT RX3-Extra/ methanol	1	**0.357-0.93**	14/4.3	0.42	-4	108	Optimizing many factor	solar
[8]	(CaCl2/AC)/ Ammonia	1	**1.66**	30/_	0.15	-5	105	Heat storage	solar
[39]	AC / methanol	1	**0.35-0.5**	20/_	0.24	-0.9	115	Solar collector covered by Transparent Insulation Material	solar
[13]	AC/ methanol	1	**2.6**	12/_	0.13	-15	100	spiral plate heat exchangers as absorbers	Electrical heater
[41]	AC / methanol	1	**0.235-0.3**	17/_	0.12	-6	78	_	solar
[66]	AC / methanol	2	**0.46**	22/3.3	0.38	-2.5	98	evacuated tube solar collector	solar
[35]	AC /methanol	1	**0.118**	112/_	0.086	-11	110	Intermittent heat source	Waste heat
[48]	AC/ Methanol	1	**0.23-0.26**	130/20	0.43	-3	N/A	_	solar
[47]	AC (MD6070)-methanol	1	**0.6417-0.747**	N/A	0.6	-3	N/A	Continuously operating	solar
[42]	AC/ Methanol	1	**0.26-0.35**	20/_	0.12		N/A	_	solar
[61]	lithium chloride in silica gel pores-methanol	1	**0.83**	36/_	0.33	-6	N/A	Using a novel composite adsorbent	Solar
[34]	AC–Ammonia	1	**0.235**	16.99	0.25	0	N/A	_	solar

				/1.38					
[23]	$SrCl_2$ – ammonia	2	**0.527**	22/15	0.069	-15	93	evacuated tube solar collector	solar
[68]	AC / methanol	2	**0.2-0.3**	20/_	0.11	-0.5	N/A	Flat plate collector	solar
[43]	AC/ Methanol	1	**0.37-0.473**	19/0.4	0.15	N/A	N/A	No valve system	solar
[46]	AC/methanol	1	**0.224**	29/	0.122	-2	93	Finned tube solar collector	solar
[44]	Zeolite / water	1	**0.3125**	16 / 4	0.08	0	180	vacuum tube solar collector-adsorber	solar
[49]	Zeolite/Water	1	**0.09**	75.5 /_	0.8	-2.8	121	_	solar
[45]	Zeolite /water	1	**N/A**	4.2/_	0.25	N/A	200-300	Mobile adsorber	Solar
[40]	AC-Methanol	1	**0.285**	21 / 6	0.1	−3.3	94	multi-tubular adsorber- solar collector	Solar
[28]	AC-ammonia	1	**N/A**	20 / _	0.45	-5	80 to 200	_	N/A
[51]	AC(CNR115) – methanol	1	**N/A**	7.6 / (1.6 - 0.349)	0.078 to 0.096	-7.2	116	Compound parabolic concentrators - tubular adsorber	Solar
[52]	AC monolithic - ammonia	1	**N/A**	0.8 / _	0.12	-20 to 0	105	aluminium and monolithic carbon discs	Boiler
[27]	AC-CaCl2 / water or acetone	2	**N/A**	N/A	0.39 0.12	-20	114	New adsorbent AC -CaCl2 and heat pipe	waste heat and solar
[69]	Metal hydride–hydrogen	2	**N/A**	N/A	0.4	-10	N/A	Capillary tube bundle reaction beds	N/A
[53]	AC–methanol AC–ethanol	1	**N/A**	N/A	0.1 0.03	-8 2-4	N/A	_	Solar
[54]	$SrCl_2$–NH_3	2	**N/A**	N/A	0.3	-10	N/A	N/A	N/A

	$MnCl_2/NiCl_2–NH_3$				0.4	-25			
[55]	AC-Ammonia	1	**N/A**	N/A	0.1	-27.3 -16	115 85	Shell and tube (adsorber inside tube)	Heater
[70]	Zeolite 13x–methanol	1	**N/A**	N/A	N/A	-10	N/A	Container in copper collector 0.5m2	lump
[56]	expanded graphite+ CaCl2 or composite or consolidated composite adsorbent/ammonia	1	**N/A**		0.44	-10	150	N/A	Waste heat
[57]	- consolidated composite AC-methanol - consolidated AC–methanol	1	**N/A**	4.7 /_	0.38 0.125	-10.31	N/A	shell and tube type	Diesel engine
[58]	AC–methanol	1	**N/A**	N/A	0.1-0.12	N/A	N/A	simple flat-plate collector	solar
[59]	AC–methanol	1	**N/A**	N/A	N/A	0 to -10	N/A	Solar plate collector	solar
[12]	AC- ammonia	2	**N/A**	N/A	0.2	-5	120-250	heat and mass recovery	heat and/or electricity
[60]	binary salt BaCl2+BaBr2 /ammonia	1	**N/A**	N/A	N/A	N/A	100	N/A	N/A
[92]	AC Maxsorb III/ methanol	1	**N/A**	N/A	0.68	-5	N/A	N/A	N/A
[65]	Zeolite-water AC-methanol	1	**N/A**	N/A	0.65	-10	275 120	N/A	N/A
[67]	AC / methanol	2	**0.19**	61 / _	0.44	N/A	N/A	N/A	Solar
[1]	AC- ammonia	1	**N/A**	N/A	N/A	N/A	N/A	two-bed (evacuated tube collectors) and four-bed regenerative system	N/A

[11]	calcium chloride and activated carbon- ammonia	1	**N/A**	3.6 / –	0.27	-15	113.7	finned tubes adsorber with compound mass-heat recovery	solar
[30]	Activated carbon/ methanol	1	**0.26**	32 /_	0.139	-8.6	95	Aluminium alloy finned tubes- evacuated solar collector	solar
[91]	Activated carbon- methanol	1	**0.237**	32 / 7.62	0.037 - 0.050	-2	94	Aluminium alloy finned tubes- evacuated solar collector	solar

2.2.5 Freezing systems

Numerous industrial processes require huge cooling duties for short time within the day resulting in operating the cooling system part load which leads to increasing power consumption and CO2 emissions. Ice slurry is used in many applications like refrigeration systems, thermal energy storage in industrial food processing (cheese) [93] and freeze desalination at different temperatures ranging from -5 to -35 ^{0}C. Ice slurry is produced using mechanical vapour compression refrigeration system with the refrigerants used are either organic or non-organic refrigerants [10] like 1,1-Dichloro-1-fluoroethane (R141b) [94]. The thermal energy storage has an advantage of reducing the size of the refrigeration machine, reserving cooling effect, reduce electrical consumption and low energy cost compared to conventional refrigeration system.

2.3 Desalination systems

There is a growing demand for fresh water in many developing countries [1], the World Health Organization (WHO) has reported that 884 million people have no access to fresh

water and more than 2.4 billion have a limited access [2]. In order to produce a potable/fresh water from a desalination plant, general procedures are required to be followed as shown in Figure 2-17 from a pre-treatment up to final-treatment. Globally, there are many techniques for water desalination, which have been developed to produce a potable water from sea water including Reverse Osmosis (RO), multi stage flash distillation (MSF) and multi effect distillation [95] (see Figure 2-18) with the RO being the most efficient technique in terms of energy consumption but suffer from contamination issue due to the residual of chloride, bromide and boron, high maintenance cost and limited validity of membrane life [2]. In addition, the only outcome of such technologies is fresh water and no cooling can be achieved [96]. The aforementioned techniques use electricity to operate the hydraulic pump in the RO system or a compressor in the vapour compression cycle and MSF system (see Table 2.2). In order to reduce the demand on the fossil fuels which are used to generate the required electricity and reduce Carbon dioxide (CO2) emissions, heat driven adsorption desalination systems offer significant advantages for water desalination [97, 98].

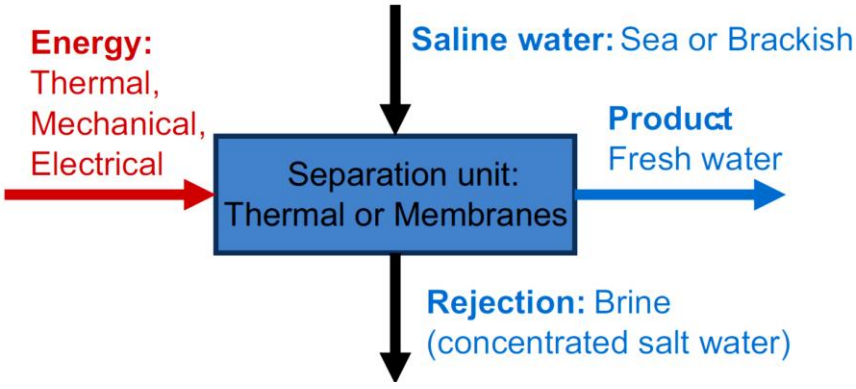

Figure 2-17 Scheme of a desalination plant [96]

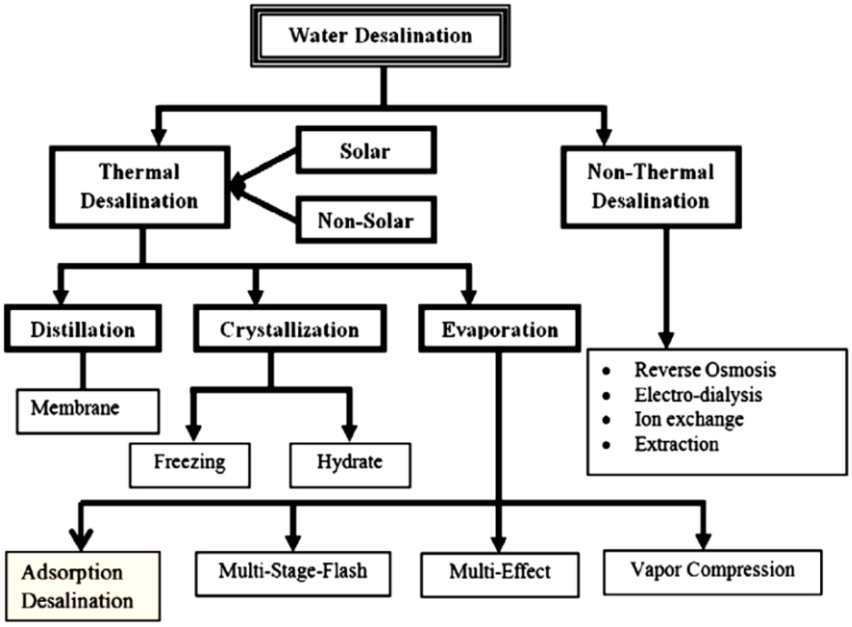

Figure 2-18 Classification of desalination processes [97]

Table 2.2 Energy costs comparison for different types based desalination [99].

Table 1 Energy costs comparison for various methods of desalination

Method of desalination	Thermal energy consumption kWh/m^3 (A)	Electric energy consumption kWh/m^3 (B)	Primary fuel input kWh/m^3, $C = (A/\eta_b + B/\eta_c)$	Energy cost of water US$ per m^3, $= 5*(C*3.6)/1055$ (GJ)
Multi-stage flash (MSF)	19.4	5.2	37.9	0.647
Multi-effect distillation (MED)	16.4	3.8	30.5	0.520
Vapor compression (VC)	—	11.1	29.2	0.497
Reverse osmosis (RO), single pass	—	8.2	21.5	0.366
Reverse osmosis (RO), double pass	—	9.0	23.7	0.403
Adsorption desalination	Free energy from waste heat	1. 5 (author's data)	3.9	0.067

All data are extracted from *Seawater Desalination in California, California Coastal Commission*, Chapter 1: Energy Use section, http://www.coastal.ca.gov/index.html. The conversion units of 1 AF ≡ 1345 m^3, 1 million BTU (1.055 GJ) of natural gas costs US$5 (adopted from Singapore's natural gas prices in 2005). The electricity conversion efficiency, η_c, of power plants is 38%, and the efficiency of boiler, η_b, is 80%.

2.3.1 Freeze desalination systems

2.3.1.1 Introduction

Freeze desalination can be used to produce potable water by cooling the sea/saline water to low temperature (lower than the freezing point of water) to produce ice crystal. During the

freezing process of saline water the pure water firstly freezes forming ice crystals leaving the salt behind. The equilibrium freezing point of a saline water decreases by increasing its salinity. The drop in the equilibrium freezing point of saline water compared to the freezing point of pure water (no salinity) is scientifically known as the Freezing Point Depression (FPD) as shown in Figure 2-19. The FPD is practically higher than the effective freezing temperature due to driving force temperature, which takes into account the heat exchange required to overcome thermal resistance [100]. Therefore, the freeze desalination system utilizes the phase change of sea water from liquid to solid state. The salinity of brine increases during the freezing process so it is very important to separate the ice crystal from the brine. A cleaning process of ice crystal should then be carried out to make sure there is no residual salt in the ice crystal. The ice crystal is finally melted to produce potable water [94].

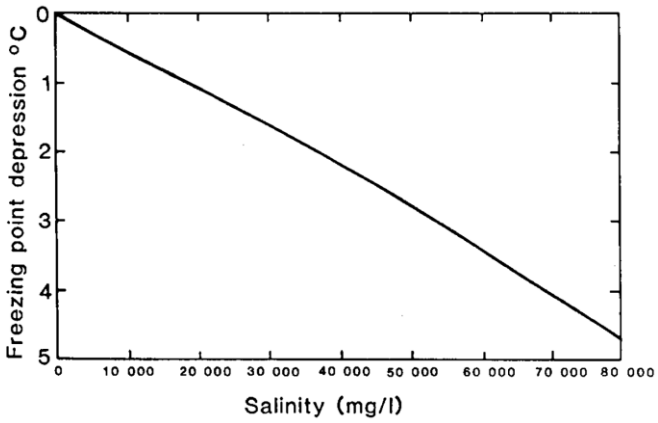

Figure 2-19 The freezing point depression of sea water [100].

A significant amount of energy is consumed in the cooling and separating processes of the freeze desalination system as reported by [101]. In order to minimize the energy consumption in freeze desalination systems, alternative systems are required to produce

fresh water. There are three types of freeze desalination systems namely; direct freezing, vacuum freezing and indirect freezing which are described in the followings sections.

2.3.1.2 Direct freezing process

A hydrocarbon refrigerant (like butane) is injected and brought in direct contact with the sea water using nozzles which throttle (depressurize) the liquid refrigerant from high to barometric pressure. During this process, the liquid refrigerant evaporates due to the sudden drop in the pressure of refrigerant extracting heat from sea water leading to lowering its temperature to less than the freezing point which then results in ice crystal formation. The brine slurry is also formed with the ice crystals as a mixture so it is pumped to the washing stage to separate the ice crystal from the brine slurry.

The freshwater is produced by transferring the ice crystal to the melting stage as shown in the Figure 2-20. The hydrocarbon refrigerant vapour in the freezer is recirculated using another compressor to be heated and circulated in the refrigeration cycle again [102].

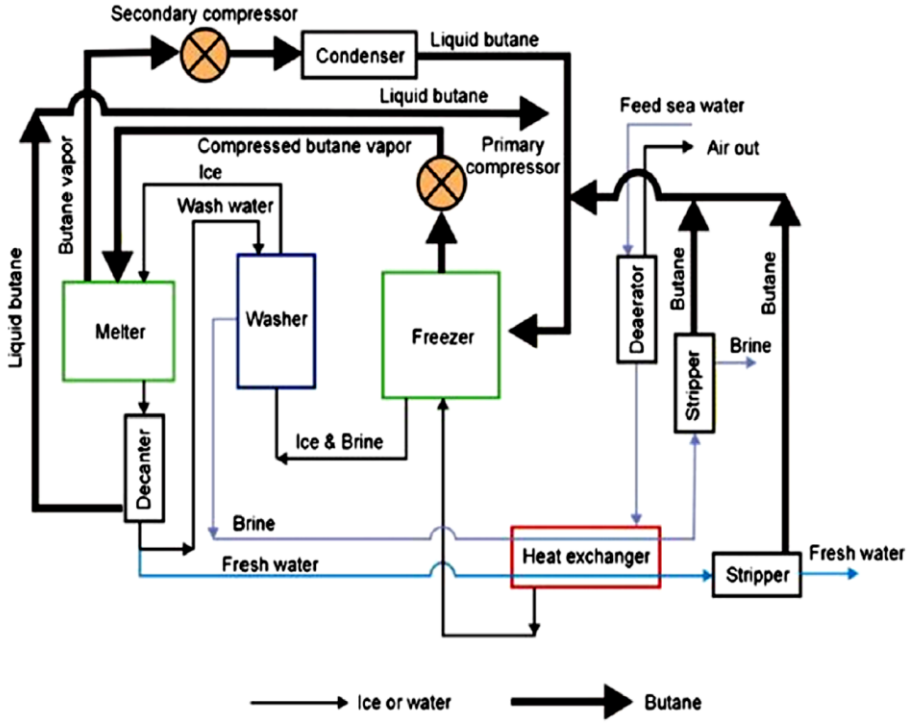

Figure 2-20 Schematic diagram of direct freezing process [102]

2.3.1.3 Vacuum freezing process

Figure 2-21 shows schematic of vacuum freeze desalination system proposed by Williams et al. 2015 [102]. In such system, vacuum is used to initiate boiling of the sea water which results in absorbing significant amount of heat from the sea water lowering its bulk temperature to below the freezing point and forming ice crystals. This is an energy efficient method of ice formation as evaporation of one kilogram of water could theoretically produce seven kilograms of ice based on the latent heat of vaporization being seven times higher than the latent heat of freezing. Therefore, using water as refrigerant leads to improved ice production, further to the advantages of reducing energy cost and global warming. The most important factor in the vacuum freezing system is the dissolved gases as they need to be removed to avoid any adverse effect on the overall operation of the system [102].

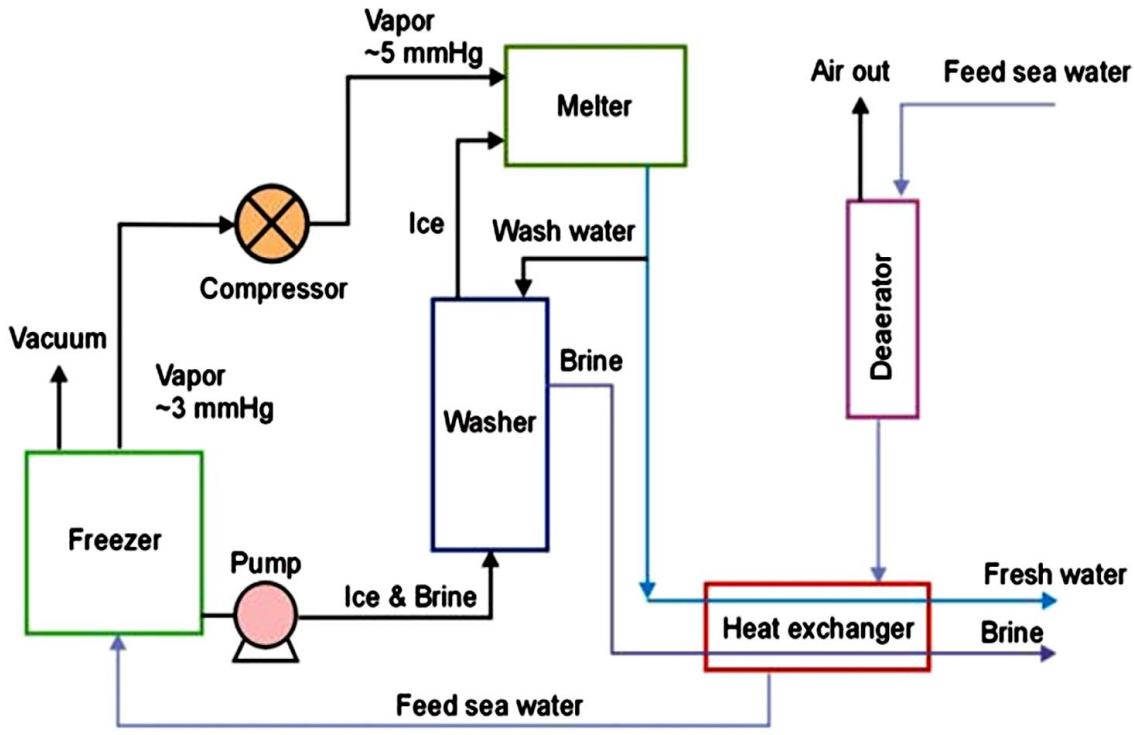

Fig. 4. Vacuum-freezing vapor compressor process [37].

Figure 2-21 Vacuum freezing process [102].

2.3.1.4 Indirect freezing process

In this system, there is no direct contact between the sea water and the refrigerant during the freezing process and the heat transfer between them is achieved through solid wall interface as shown in Figure 2-22 in which the refrigerant used in conventional vapour compression refrigeration or other systems circulates through channels fitted inside the freezer chamber. The incoming feed sea water firstly passes in the heat exchanger which work as a pre-cooler for decreasing the temperature of sea water before entering it to the freezer chamber, in which, further cooling is achieved to reach the freezing point and ice crystals formation. Brine slurry is also formed in the freezer chamber with the ice crystal as mixture to be pumped to the next stage where the ice crystals are separated from the brine slurry and washed. The washed ice is moved to the melting process which used heat from the condensing unit of the refrigeration system to produce fresh water.

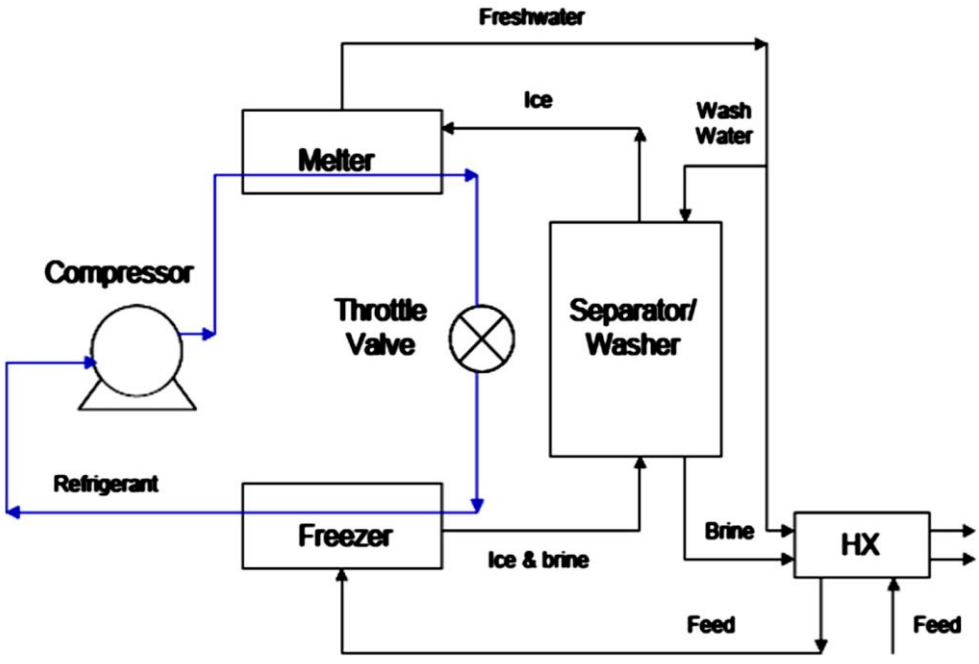

Figure 2-22 Schematic diagram of an indirect freezing process [102]

2.3.2 Adsorption desalination system

Adsorption desalination system provides an advantage of exploiting heat sources to produce potable water and cooling effect using solid sorption material like silica gel and zeolites [103]. There are many advantages to use the adsorption system for desalination application including, (1) it is environment friendly technology as it could be driven using low grade heat sources with temperature below 100°C thus reducing CO2 emissions and global warming; (2) lower corrosion and fouling factors in the evaporator compared to other desalination systems due to low evaporation temperature (<30°C); (3) there are limited moving parts; which leads to lower system's cost and maintenance; (4) adsorption desalination system offers the potential of producing distilled water and cooling as two useful outputs [97] using the same heat source; (5) it normally uses environment friendly materials [97]; (6) low consumption of electricity and lower biological and contamination materials produced through the production of water compared to membrane technique [103].

Many studies on adsorption desalination systems have been carried out as listed in Table 3.2. Which shows that the sea or brackish water are the only refrigerant used in the adsorption desalination system, while silica gel and zeolite are the only adsorbent materials used in such system. There are two main outputs that could be achieved from the adsorption desalination system using a single heat source which are cooling (>0°C) and potable water. The SDWP of adsorption desalination system is normally the major criteria of system's performance with values ranging from 0.98 to 26 cubic meters of potable water per day per ton of adsorbent material at evaporation temperature ranging from 5 to 30 °C as listed in Table 3.2. The table also shows that the adsorption desalination systems have been driven

using either solar or waste heat energy as a main input with wide range of desorption temperature, ranging from 50 to 195°C. The high temperature heat source is only used with zeolite 13X as an adsorbent. Some techniques have been investigated to improve the performance of the system in term of specific daily water production like using multi bed system, internal heat recovery between the condensers and evaporator [104], two stage mode [105], time-scheduling scheme [106] or heat and mass recovery [107]. Furthermore, combining the adsorption desalination system with other systems like vapour compression or multi-effect desalination systems are new ways to improve the daily water production of water.

Table 2.3 List of adsorption desalination systems

Ref.	Working pair	Outputs	SDWP [ton/day/ton_ads]	$m_{adsorbent}$ [kg/kg]	COP[-] /PR/ SCP [Rton/ton_ads]	T_{evap} [°C]	T_{des} [°C]	Notes	Heat source / Study
[103]	Silica gel / water	2	10	144	_	30	85	Four-bed system	waste heat
[108]	Silica gel / water	2	8.79	72	_/0.57/_	30	85	Two bed system	waste heat
[108]	Silica gel / water	2	10	144	_/0.6/_	30	85	Four-bed system	waste heat
[109]	Silica gel / water	2	4.7	_	0.26 /_/_	12	85	Four-bed system	waste heat
[105]	Silica gel / water	2	0.95	17.6	0.25/ _/_	45	85	2-stage mode with 4 beds	waste heat
[110]	zeolite AQSOA-ZO2 / water	2	6	1780	_/_/48	10	85	Two bed system	simulation
[110]	Silica gel / water	2	2.2	1780	_/_/20	10	85	Two bed system	simulation
[111]	zeolite AQSOA-ZO2 / water	1	15.4	3380	_/_/32.4	10	85	Four bed system with integrated evaporator/ condenser	simulation
[111]	zeolite AQSOA-ZO2 / water	2	12.4	3380	_	10	85	Four bed system with integrated evaporator/condenser	simulation
[112]	Silica gel / water	1	_	200	_/ 8 /_	5	65	Hybrid system (MED and Adsorption system)	simulation
[113]	Zeolite 13X / water	1	0.41 kg/ kg _ad	_	_/ 10.16/ _	10	195	Hybrid system: multi-effect desalination and adsorption heat	Solar

								pump	
[104]	Silica gel / water	1	4	13.5	_/_/_	30	85	Two bed system with internal heat recovery	solar
[114]	Silica gel / water	2	14	94	0.64/_/ 0.18	27	90	Hybrid system: mechanical vapour compression and adsorption system	simulation
[115]	Silica gel / water	1	10	36	/ 0.62	32	70	4 beds, internal heat recovery between the condenser and the evaporator	waste heat
[116]	Silica gel / water	2	4.4	5.60	0.55/ _/ _	15	85	4 bed, novel time-scheduling scheme	simulation
[117]	Silica gel / water	2	5.4	30.23	0.7 /0.618 /_	8 and 18	85	3 bed, 2 evaporator	simulation
[106]	Silica gel / water	2	8	36	65.44/ 0.68 / 0.44	10 and 24	85	4 beds, 2 evaporator	simulation
[2]	AQSOA-Z02 + water	2	8.2	36	/ _/ 44	10 and 25	85	Double stage adsorption cooling and desalination system	simulation
[98]	Silica gel / water	1	26	72	_/_/_	45	85	internal heat recovery between the evaporator and the condenser	simulation
[118]	Silica gel / water	2	_	_	_ /_/ _	25	50	Hybrid of MED and 2 bed adsorption cycle.	simulation
[107]	Silica gel / water	2	4.32		_/ 0.429 /_	12.2	85	2 beds, heat and mass recovery	
[119]	Zeolite / water	1	_	_	_	_	110	Hybrid 2 bed adsorption desalination heat pump system	simulation
[120]	Silica gel / water	2	_	_	0.55/ _/ _	10	85	4 bed	simulation
[121]	Silica gel / water	2	2.25	5.6	0.4/ _ /_		85	4 beds, single-stage AD system	simulation solar
[122]	Silica gel / water	1	15	144	_ /_/_	30	70	4 beds, internal heat recovery between the condenser and the	simulation

								evaporator.	
[99]	Silica gel / water	2	7		0.45/ 0.55/_	_	_	4 bed adsorption desalination system	simulation
[123]	Silica gel / water	2	3.6	36	_/_ / 25	10	85	4 bed adsorption desalination system	Waste heat

2.4 Summery

A comprehensive literature review was carried out regarding advances in adsorption ice making systems and the following provides a summary of the findings:

- The commonly used refrigerants in adsorption ice making systems are methanol, ammonia and ethanol which suffer from being flammable and/or poisonous. Very limited work was found on using water as refrigerant in ice making systems due to its freezing temperature. The presence of salt in seawater lowers its freezing point thus seawater can be used as refrigerant evaporating at temperature allowing production of ice. This research makes contribution to knowledge regarding the use of seawater as refrigerant in adsorption ice making system.
- Commonly used water adsorbent materials including silica gel and zeolite which suffer from relatively low uptake capabilities. Metal Organic Framework materials are new advanced adsorbent materials with a relatively high water adsorption uptake. CPO-27(NI) is a MOF material that has been shown to have water uptake double that of silica gel, chemically stable and commercially available. This research will make contribution to knowledge in using CPO-27(Ni) MOF material in adsorption ice making as refrigerant.
- Various methods were reported in the literature regarding enhancing the performance of adsorption ice making systems like advanced bed designs, various working pairs

and cycle configuration with heat and mass recovery. Also, few studies were reported on increasing the number of outputs from adsorption ice making system to include providing cooling for air conditioning and solar heat storage for heating purpose.

Increasing the number of outputs more than two have not been reported in the literature and this research provides the first study regarding the development of adsorption system for producing ice, ice slurry, cooling and water desalination.

- Adsorption desalination offers many advantages compared commonly used desalination technologies including low energy consumption and being environment friendly. Freeze desalination technology also offers the potential of providing potable water with low energy consumption as the latent heat of solidification is significantly lower than the latent heat of evaporation.

  Using the cooling effect of adsorption desalination systems to enable freeze desalination system have not reported been reported in literature and may offer enhance SDWP.

- Ice crystal suspected in saline water is also called ice slurry which has bed reported for use thermal energy storage with the advantage of reducing the size of refrigeration machine, reserving cooling effect, bring down electrical limit prerequisites and low energy cost compared to the conventional refrigeration system.

- Vacuum freezing desalinations system offers an advantage to use water as refrigerant as it could be theoretically produced seven kilograms of ice by evaporating one kilogram of seawater.

CHAPTER 3

Experimental Study of Single Bed Adsorption System Using CPO-27Ni with Potable and Sea Water as a Working Pair

3.1 Introduction:

Adsorption ice-making systems have been investigated as an alternative technique to the conventional vapour compression refrigeration systems as discussed in Chapter 2. The majority of research work on adsorption ice making systems has been achieved by producing ice as a single output or with cooling as a second output. Moreover, water has been highlighted to have a high latent heat of evaporation compared to the CFCs refrigerants but it has not been recommended to use as refrigerant in adsorption ice making systems due to its high freezing point temperature. To enhance the output of adsorption ice making systems, this chapter describes the development of novel adsorption ice making system that can be used to produce four outputs, namely: ice, cooling, ice slurry and fresh water. A single bed adsorption system using advanced (CPO-27(Ni)) MOF material as adsorbent and potable/sea water as refrigerant was used to demonstrate experimentally the production of the four outputs and evaluate the system performance at different operating conditions.

3.2 Test Facilities Description

Single bed adsorption system was developed to investigate the feasibility of producing ice, cooling, ice slurry and distilled water simultaneously. Figure 3-1 and Figure 3-2 show a schematic diagram and a pictorial view, respectively of the single bed adsorption system for

multi output. The test facility comprises an adsorber bed, a condenser and an evaporator as main components. The test facility also include auxiliary components to provide heating/cooling water system for the adsorber bed, chilled water/antifreeze circulating system for evaporator heat load and mains water for condenser cooling. The adsorber bed consists of a steel shell, plate and two rectangular finned tube heat exchangers. The heat exchangers are packed with an adsorbent material (CPO-27(Ni)) and fitted with the plate then located inside the shell. There are four tubes in each heat exchanger where the heating and cooling water flow during the desorption and adsorption processes, respectively. The flow of heating and cooling water within the adsorber bed is controlled using four solenoid valves and single pump with the opening and closing of solenoid valves are automatically controlled according to the desorption and adsorption processes.

Two shell and coil heat exchangers are used as evaporator and condenser with additional coil at the base of evaporator to enhance the heat transfer area during the boiling process. The evaporator and condenser are consecutively connected to the adsorber bed using two manual ball vales during the adsorption and desorption processes, respectively. The evaporator's and condenser's coils are connected with the chiller and main water line for circulating chilled water/antifreeze and cooling water through it during the adsorption and desorption processes, respectively. The mass flow rate of water/antifreeze and water in the evaporator's and condenser's coils are controlled using two solenoid valves and two ball valves, respectively. In addition, two vacuum pumps are connected in parallel and used to evacuate air from the adsorber bed, condenser and evaporator to achieve the required initial conditions. The adsorption system is fitted with measuring instruments like thermocouples, pressure transducers and flow meters to evaluate its performance at different operating conditions.

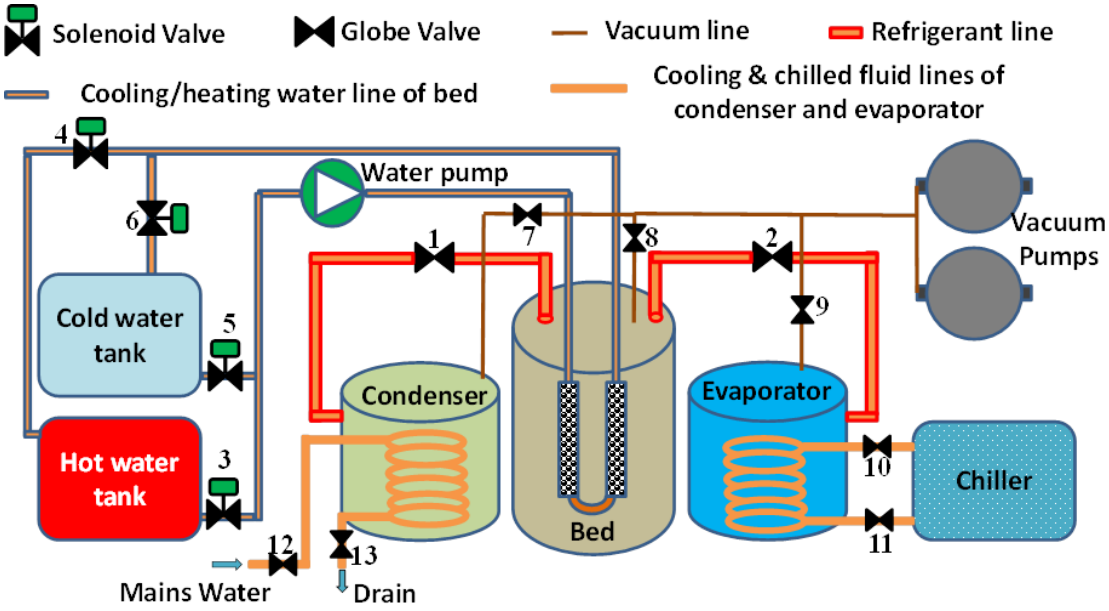

Figure 3-1 Schematic diagram of all test facility

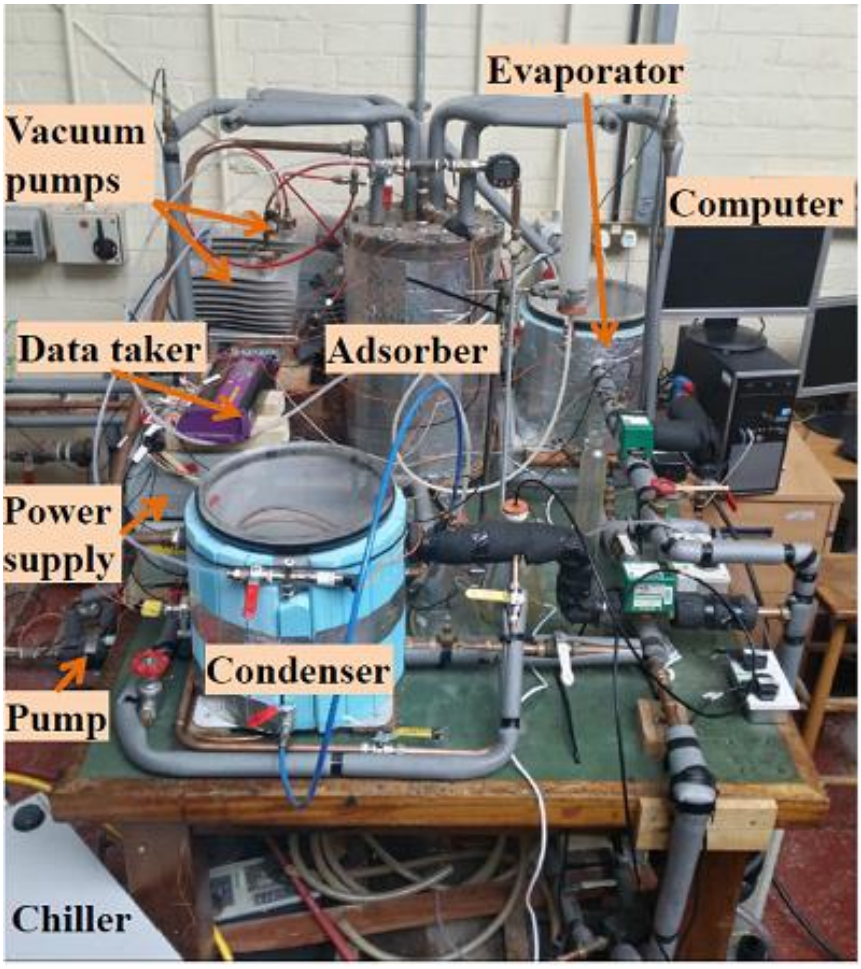

Figure 3-2 Pictorial figure of the whole test facility

Detailed descriptions of the main and auxiliary components of the system are given in the following sections.

3.2.1 Adsorber bed

The adsorber bed is constructed from heat exchangers, shell and plate. Two rectangular finned-tube heat exchanger modules manufactured by Weatherite Company are fitted in the shell to construct the adsorber bed. Figure 3-3 shows a pictorial diagram of the heat exchanger before packing with the adsorbent material consisting of four copper tubes fitted with 270 aluminium fins for enhancing the heat transfer between the heating/cooling circulated water and the adsorbent material. The design parameters of heat exchanger were listed by Shi B. 2015 [124]. The adsorbent material CPO-27Ni granules (see Figure 3-4) are packed in the spaces between the fins and pipes. The heat exchangers are covered using stainless steel mesh to prevent the adsorbent material falling off the fins.

The heating or cooling water circulates through two tubes of heat exchanger because the rest two tubes were used by [124] to fit electrical heaters which are modified and removed in this work. The tubes of heat exchangers are connected together at the lower end using U-bends while they are extended and passed through the steel plate using compression fittings at the upper end. The steel plate is used to seal the shell using flange and O-ring arrangement. The steel plate and the flange are provided with 24 bolts for adequate sealing. The steel plate is provided with eight holes for heat exchangers pipes, six holes for thermocouples and two holes for pressure transducer and vacuum pump. The steel shell is insulated using 20 mm thick ROKEWOOL material.

Figure 3-3 Pictorial figure of the rectangular finned heat exchanger (A) top view (B) side view

Packing Density = 480 kg/m^3

Total pore volume = 217 (cm^3/kg)

Granules size = 0.1075 mm

BET surface area = 1113 (m^2/g)

Pore mean diameter = 0.7 nm

Figure 3-4 Pictorial figure of CPO-27(Ni) MOF adsorbent material with its characterizations [84, 125]

3.2.2 Condenser

During the desorption process, the adsorber bed should be connected to the condenser to condense the refrigerant vapour. A shell and coil heat exchanger with transparent lid is fitted in the test facility to serve as condenser as shown in Figure 3-5. The shell consists of a steel container (320mm OD; 340mm height and 3mm wall thickness) and transparent acrylic lid. The steel container is fitted with three holes for mains water (inlet and outlet

connection); one hole for thermocouples; one hole for fitting pressure transducer and one hole for connecting to vacuum pump. A KF flange is welded through the condenser's wall to pass two thermocouples (Type K), one fitted on the base and the second one is located at the middle of condenser to measure the refrigerant liquid and vapour temperatures, respectively. The transparent lid seals the pressure inside the steel container using a rubber gasket, where during the vacuuming process the lid compresses on the rubber gasket as the pressure becomes lower than the atmospheric pressure. The coil is formed as helical shape using 8mm OD copper tube with 8 turns of 220mm OD and pitch of 30 mm. The mains water circulates in the coil to absorb the heat of condensation from refrigerant vapour flowing from the adsorber bed. The condenser is insulated to reduce the heat losses to the surrounding.

Figure 3-5 Pictorial figure of helical coil inside condenser

3.2.3 Evaporator

The evaporator has the same configuration as that of the condenser; however, there is an additional spiral coil fitted in the base of the steel container (see Figure 3-7) to be immersed

in the liquid refrigerant to enable effective evaporation. The spiral coil is formed from 4 m long copper tube as shown in Figure 3-6. During the adsorption process, the refrigerant liquid in the evaporator absorbs the heat from the chilled water/antifreeze at certain pressure and temperature leading to the refrigerant evaporation with the vapour flowing to the adsorber bed to be absorbed by the adsorbent material. This leads to drop in the outlet temperature of water/antifreeze in the evaporator's coil. For investigation purposes, the chiller was connected with the evaporator coil to simulate the cooling load of the test facility. Two litres of saline water is charged in the evaporator as the main refrigerant which covered the spiral coil, while potable water is charged into stainless steel cups (see *Figure 3-7*) with volume of 30 ml each. The cups are fitted in the refrigerant liquid using wire frame structure to prevent any movement during the evaporation process as shown in Figure 3-8. Furthermore, the cups are provided with open ends cone shape caps, which are formed using aluminium foil (see Figure 3-8), to make sure that the splashed drops of water from the cups during the evaporation process will be dropped down to the cups. Ice slurry and solid ice are produced from the saline and potable water, respectively.

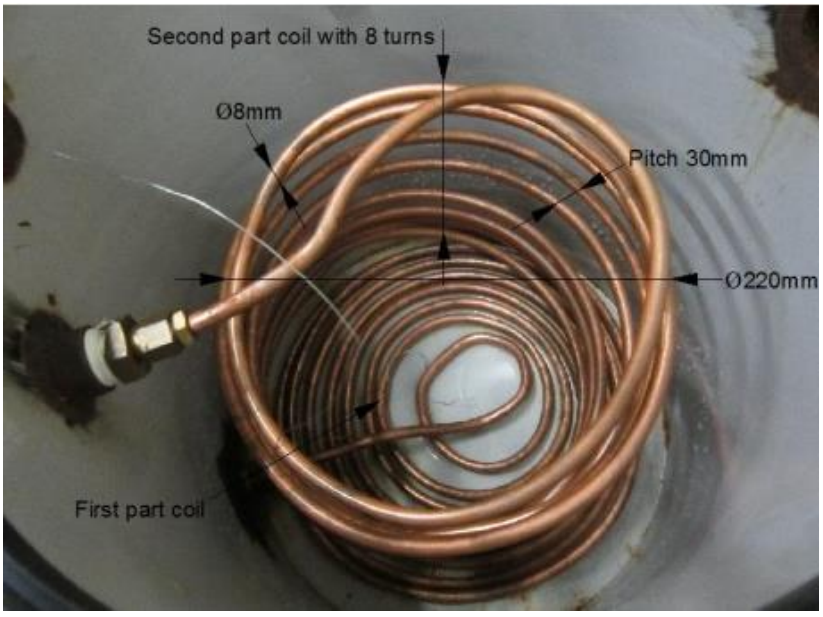

Figure 3-6 Helical and spiral coil inside evaporator

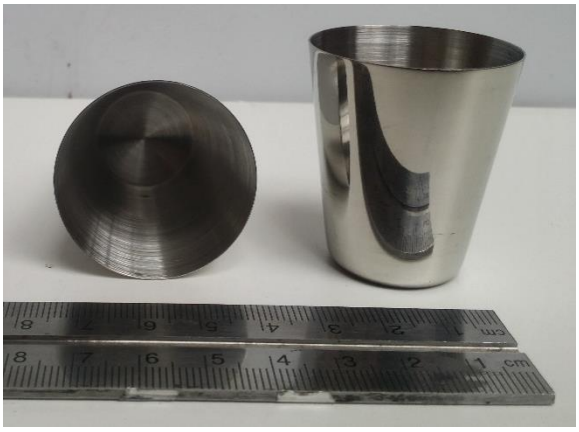

Figure 3-7 Stainless steel cups

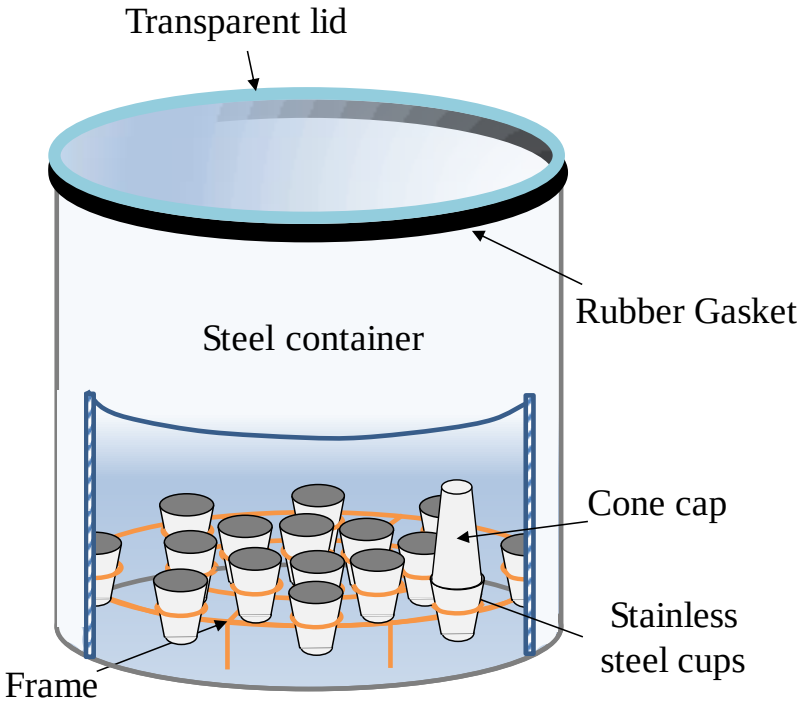

Figure 3-8 Schematic diagram for the evaporator (the coil does not show

3.2.4 Chiller unit

A one HP chiller (CU-700) manufactured by the Betta-Tech company (see Figure 3-9) is connected to the evaporator's coil to provide the thermal energy required for the

evaporation of refrigerant at low temperature <0℃. The chiller could be operated at wide range of temperature from -15 to 70 ˚C where a refrigeration system and heater are built in the chiller unit to provide a constant input temperature to the evaporator's coil. The chiller was filled with water/antifreeze that was prepared by mixing 10% pure Monopropylene Glycol with 90% fresh water to achieve a temperature of -10℃. The chiller is provided with liquid pump for circulating the water/antifreeze, where the maximum mass flow rate of the pump is 15 litre/min at zero head and pressure up to 0.5 bar.

Figure 3-9 Photograph of chiller unit

3.2.5 Electric heaters and control unit

To investigate the performance of the single bed adsorption system for multi outputs applications at different condensing temperatures, four OMEGALUX® electric rope heaters are wrapped around the mains water pipe (see Figure 3-10), connected to the inlet of the condenser. The linear wattage of the rope heater is about 4 Watt/in where the length and diameter of each heater are up to 3 m and 0.005 m, respectively. The heaters temperature is

controlled using four N322 PID controllers from Novus Company, as shown in Figure 3-11 (A) and (B). The PID controllers are connected with J-type thermocouples, which are fitted on the tube's wall to sense the temperature and switch off the heater when the temperature exceeds the setting temperature and vice versa, with an accuracy of 3˚C.

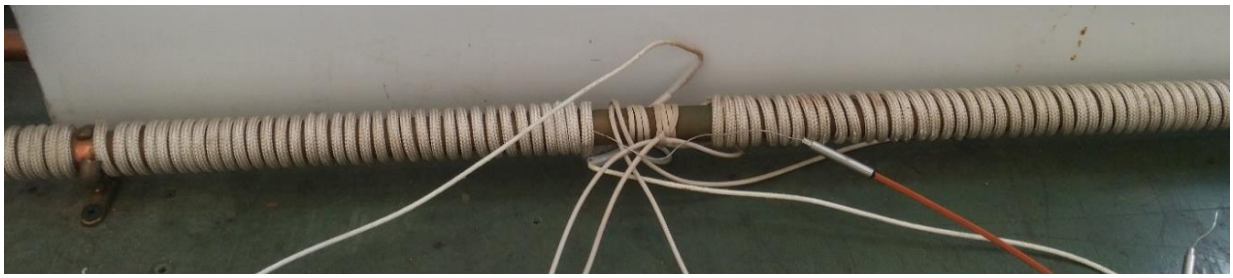

Figure 3-10 Electric heater wraps around main water line

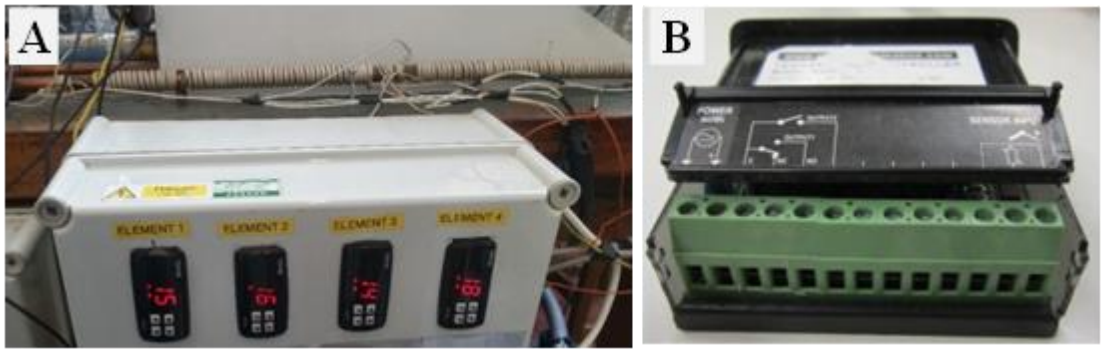

Figure 3-11 (A) Control box (B) PID controller

3.2.6 Heating/cooling water circulating system

Two tanks are used to provide hot or cold water to the adsorber bed using the same water pump. During desorption or adsorption modes, the adsorber bed will be connected to the heating or cooling water tank, respectively. The heating water tank is constructed from stainless steel with rectangular shape and dimensions of 0.7×0.5×0.6 m, in which, two 9000W electric heaters are fitted. The heating water tank is insulated with 0.1 m thick ROKEWOOL material to reduce the heat losses to the surrounding. A plastic tank with capacity of 200 litres was used as cooling water tank. Both tanks are fed using mains water

line and the water levels in both tanks are controlled using float valves. An SS-9R-MD pump from March May Ltd (see Figure 3-12) is fitted at the outlets lines of both tanks to circulate the heating or cooling water based on the running mode. The mass flow rate of the pump is up to 60 L/min at maximum pressure of 6 bar.

Figure 3-12 Photograph of the pump

3.2.7 Valves

Four valves are required to control the circulation of the heating and cooling water to switch the operation of the adsorber bed from desorption to adsorption processes and vice versa. Motorized-valves with two ports (type SMV2530 from the Inta Company) were used to achieve this task as shown in Figure 3-13. As shown in the Figure 3-1, motorized valve 5 and 6 are used to connect the bed with the cooling water tank, while solenoid valves 3 and 4 are used to connect the bed with the heating water tank. The motorized valves 10 and 11 were used at the inlet and outlet of the evaporator's coil to control the flow of water/antifreeze. A pair of manual ball valves is used to control the flow of the mains water through the condenser's coil (12, 13). Regarding the refrigerant vapour side, two manual ball valves are used to connect the bed with either the condenser or the evaporator during the desorption or adsorption processes, respectively.

The motorized valves 3,4,5,6,10 and 11 are controlled using an NI 6008 control board from national instrument company as shown in Figure 3-14. The control board is linked with a computer using LabVIEW program, in which, the required time for closing and opening the valves could be set to vary cycles numbers, switching and cycle time. The control board operates at low voltage output signals of 0 or 5 V, therefore, a couple of relays are used as an interface between the control board and the valves which operate at 230V.

Figure 3-13 Motorized-ball valve

Figure 3-14 NI6008 control board

3.2.8 Vacuum pumps

Two Edwards nXDS15i dry scroll vacuum pumps are connected to the test facility as shown in Figure 3-15 to vacuum the system and to reach a required pressure of refrigerant in the bed, condenser and evaporator based on a certain temperatures. The vacuum pumps

were connected to the bed, condenser and evaporator using 6mm diameter hard hoses with ball valves to evacuate each part individually.

Figure 3-15 Vacuum pumps

3.2.9 Measuring devices

Temperature, pressure and mass flow rate are measured at various locations in the test facility to enable evaluating the performance of the system. This section describes the measuring devices used in the test facility.

3.2.9.1 Thermocouples

Many thermocouples are fitted at different points in the adsorption bed, in the liquid and vapour refrigerant inside the condenser and evaporator, inlets and outlets of circulated heating and cooling water, inlet and outlet of the mains water used in the condenser's coil, inlet and outlet of water/antifreeze in the evaporator's coil. The thermocouples are required for measuring the temperatures which are used for evaluating the performance of the test facility.

Five T-type thermocouples from Omega Engineering Ltd. with sheath diameters of 1.5 mm (see Figure 3-16) are fitted in the adsorber bed, namely; two thermocouples were inserted

through the metal mesh to touch the adsorbent material in each heat exchanger as shown in Figure 3-17. One thermocouple was suspended in the adsorber shell to measure the temperature of refrigerant vapour. The thermocouples could be used for measuring temperature up to 260˚C. The wires of thermocouples were passed through the adsorber plate using compression fitting, and then were connected to the data taker.

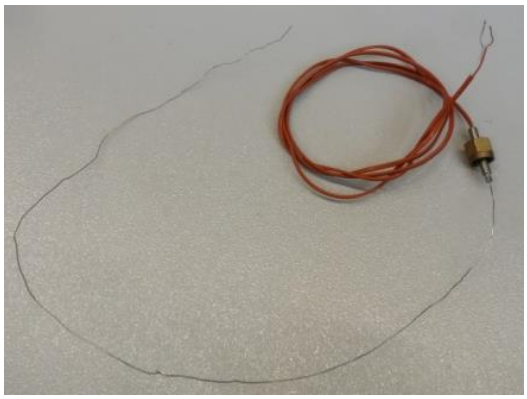

Figure 3-16 T-type thermocouple

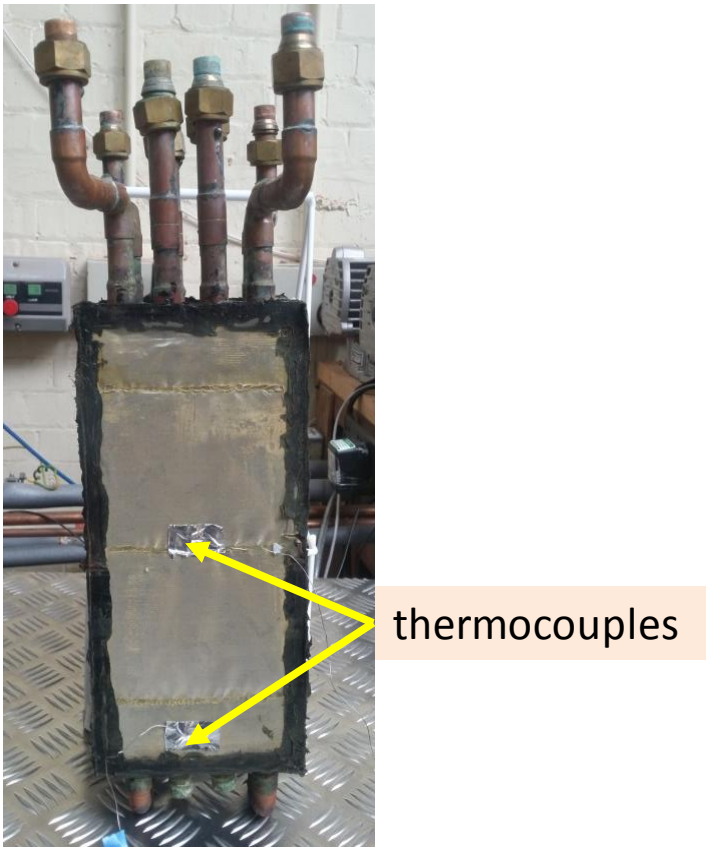

Figure 3-17 Packed adsorption bed with thermocouples

In the evaporator, two T-type thermocouples were used to monitor the vapour and liquid temperature of refrigerant and passed through the evaporator's shell. In the condenser, two K-type thermocouples were used to measure the refrigerant liquid and vapour temperatures using KF type K thermocouple feedthrough with flange as shown in *Figure 3-18*. T- type and K-type thermocouples were used to measure the surface and fluid temperatures in the system.

Figure 3-18 Feedthrough with KF flange

Six Platinum RTD probes from Omega Ltd. with 100mm length and 6 mm diameter are used at the inlet and outlet of the heating-cooling to the adsorber, the mains water pipe to the condenser's coil and the water/antifreeze of the evaporator's coil. The RTD probes are fitted using compression fittings as shown in *Figure 3-19* to measure the temperatures of circulated water in the system.

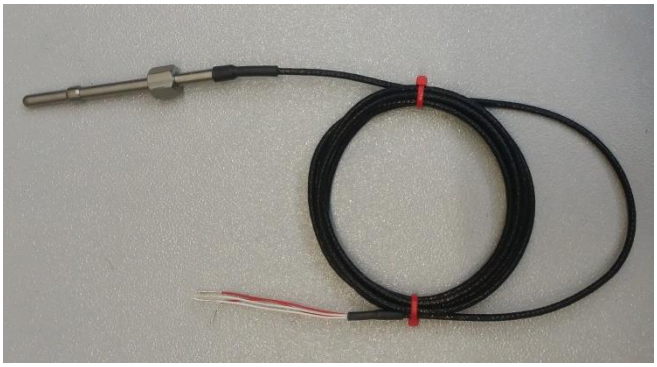

Figure 3-19 RTD sensors

3.2.9.2 Pressure transducers

Three pressure transducers were used to monitor and record the pressure inside the test facility. The adsorber bed, evaporator and condenser were fitted with 4 to 20 mA current output pressure transducers from Omega Engineering Ltd. with pressure range from 0 to 350 mbar and accuracy of ±0.087 kPas. The current signals from pressure transducers are converted to voltage using 100 ohms resistance because the data taker requires voltage inputs. The wiring diagram of the pressure transducers is shown in *Figure 3-20*.

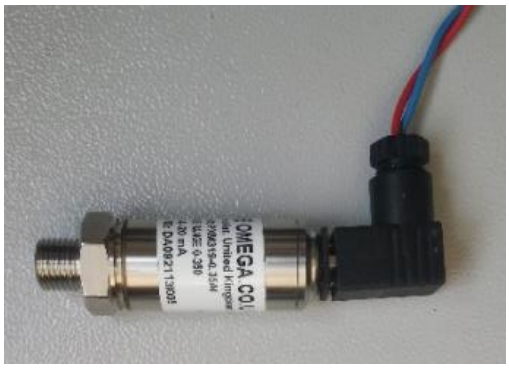

Figure 3-20 Pressure transducers

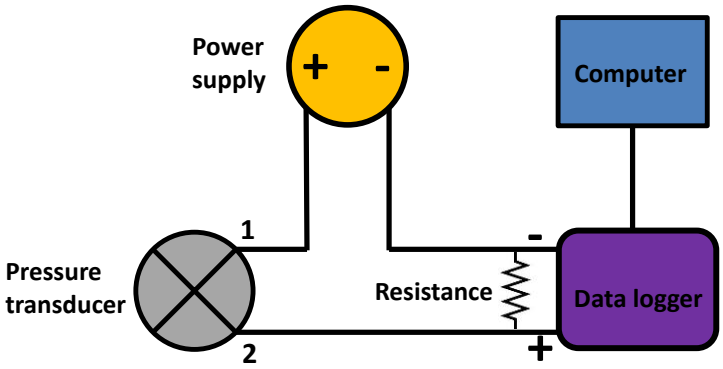

Figure 3-21 Electrical wiring diagram of pressure transducer

3.2.9.3 Data taker

The whole listed measuring devices are logged using a DataTaker DT85 with sensor input of ± 30V as shown in Figure 3-22. The DataTaker is connected with a computer to save the logged data each 4 second. The data of pressure transducers and thermocouples are identified in the software of DataTaker based on the pressure ranges and the types of thermocouples, respectively.

Figure 3-22 Data taker

3.2.9.4 Flow meters

The mass flow rate of heating /cooling water is measured using FLC-H14 from Omega Engineering Ltd. as shown in Figure 3-23. The range of the flow meter is from 0 to 57 LPM with measurement accuracy of ±1LPM. The mass flow rate of water/antifreeze and mains

water line were measured using Parker PET liquid flow indicator, as shown in Figure 3-23, with flow rate range from 2 to 30 LPM and an error of ±1.5 LPM.

Figure 3-23 Flow meters

3.3 Measuring devices calibration

All measuring instruments were calibrated using standard methods before being fitted in the test facility to achieve accurate results in term of different outputs from the test facility. All thermocouples (T-type, K-type and RTD) were calibrated against alcohol thermometer. They were gathered together in a beaker which was filled with water and heated using an electrical heater with a wide range of temperature based on a setting of thermostat as shown in Figure 3-24. The thermocouples were connected with a data taker as shown in Figure 3-25 for recording the data and uncertainties of all thermocouples were determined as shown in Table 3.1. The pressure transducers were also calibrated against standard pressure gage which is fitted in the calibration kit as shown in Figure 3-25. The pressure

transducer is connected with the data taker to collect the data and to evaluate their accuracy as shown in Figure 3-26 and Figure 3-27.

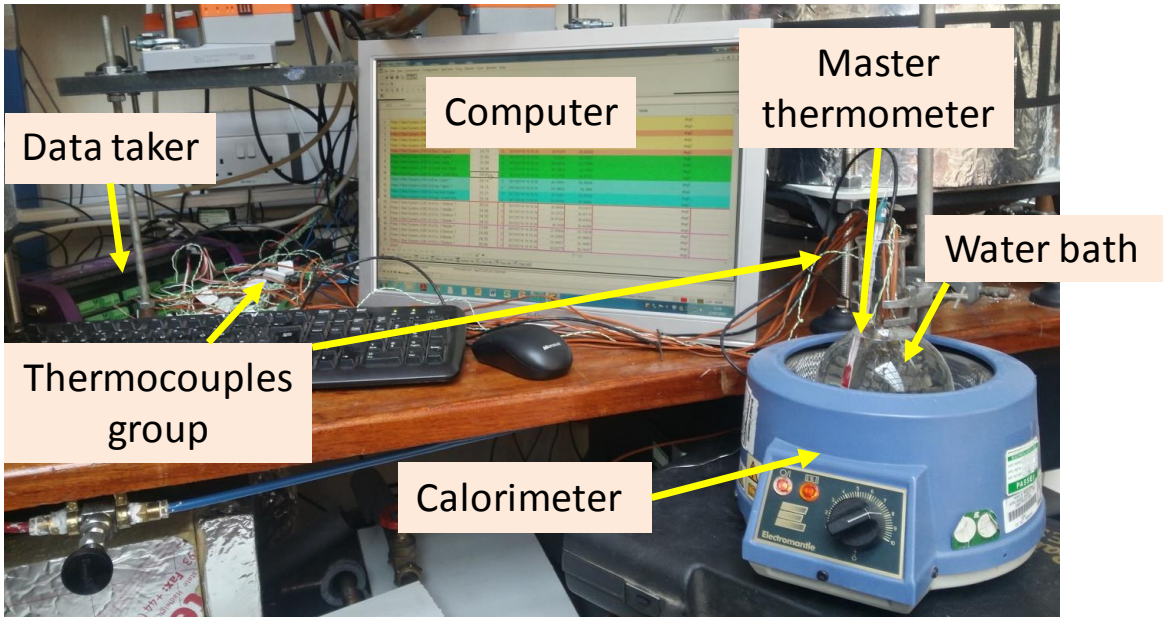

Figure 3-24 Thermocouples calibration

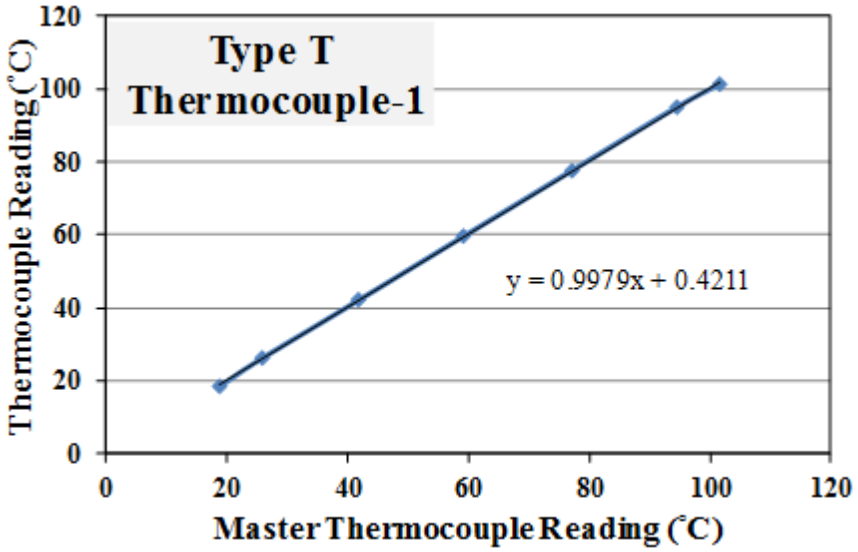

Figure 3-25 Thermocouple calibration chart

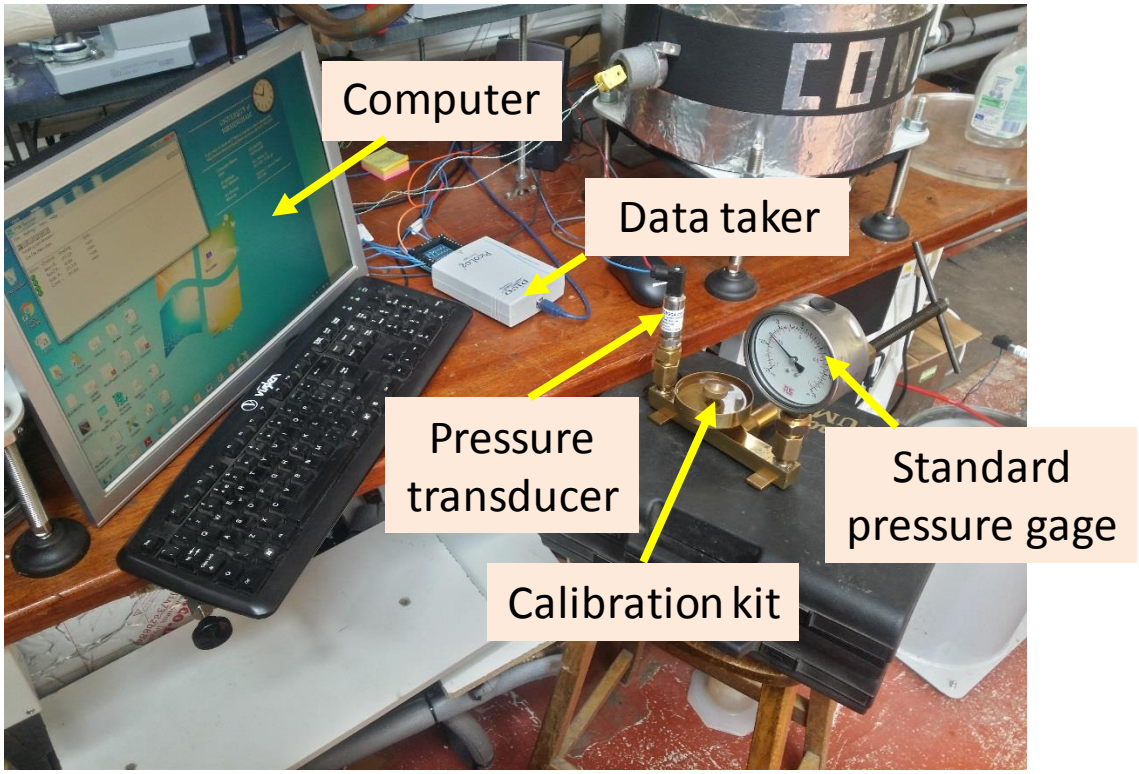

Figure 3-26 Pressure transducer calibration

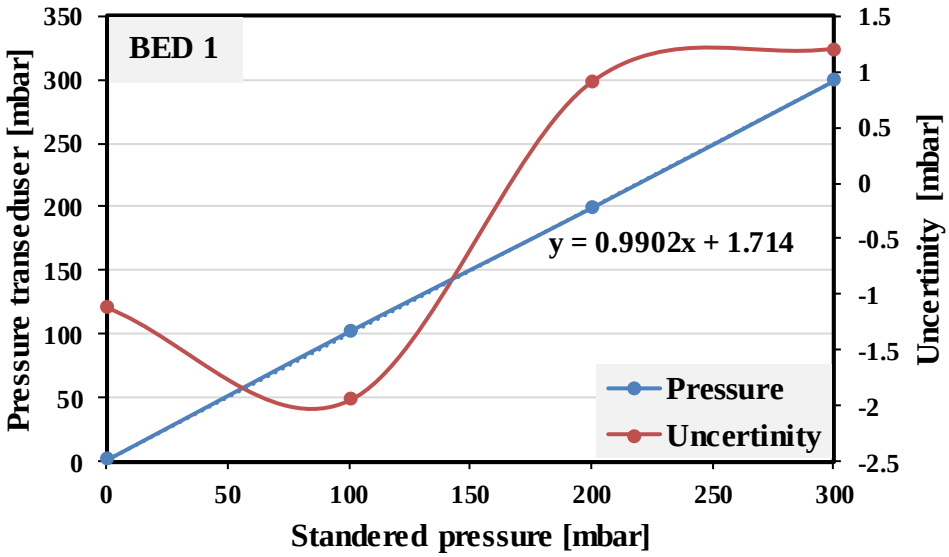

Figure 3-27 Pressure transducer calibration

Table 3.1 Uncertainties of the all thermocouples, pressure transducers and balance of the single bed adsorption system

	Item Name		Number	Location	Curve fit formula	Absolute Uncertainty
Single Bed System	**Temperature - Thermocouples**	**Type T**	T-1	Bed/heat exchanger 1/Middle	$0.9979*T_{ref.} + 0.4211$	±0.544 ˚C
			T-2	Bed/heat exchanger 1/Bottom	$0.9974* T_{ref} + 0.4028$	±0.514 ˚C
			T-3	Bed/heat exchanger 2/Middle	$0.9975* T_{ref} + 0.4521$	±0.574 ˚C
			T-4	Bed/heat exchanger 2/Bottom	$0.9982* T_{ref} + 0.3488$	±0.52 ˚C
			T-5	Bed/ vapour	$0.9986* T_{ref} + 0.2925$	±0.509 ˚C
			T-6	Evaporator/ liquid refrigerant	$0.9982* T_{ref} + 0.5613$	±0.75 ˚C
			T-7	Evaporator/ vapour refrigerant	$0.999* T_{ref} + 0.5628$	±0.77 ˚C
		Type K	T-8	Condenser/ liquid refrigerant	$0.9942* T_{ref} + 0.6683$	±0.71 ˚C
			T-9	Condenser/ vapour refrigerant	$y = 1.0003x + 0.3074$	±0.6971 ˚C
		RTD	T-10	Bed/ inlet water-heat exchanger	$0.9976* T_{ref} - 0.0318$	±0.52 ˚C
			T-11	Bed/ outlet water-heat exchanger	$0.998* T_{ref} - 0.1153$	±0.61 ˚C
			T-12	Evaporator/ Inlet antifreeze-coil	$0.9898* T_{ref} + 0.5812$	±0.42 ˚C
			T-13	Evaporator/ outlet antifreeze-coil	$0.9874* T_{ref} + 1.0529$	±0.71 ˚C
			T-14	Inlet water- condenser coil	$0.9896* T_{ref} + 0.9158$	±0.715 ˚C
			T-15	outlet water- condenser coil	$0.9883* T_{ref} + 1.0894$	±0.69 ˚C
	Pressure Transducer		P-1	Bed	$1.003*P_{ref} + 0.3251$	±1.05mBar
			P-2	Condensar	$1.0012*P_{ref} + 1.465$	±2.1 mBar
			P-3	Evaporador	$1.0021*P_{ref}- 0.032$	±1.1 mBar
	Balance				0.9977*m + 3.4408	±0.08g

3.4 Test rig commissioning

After assembling the test rig, it was commissioned to ensure achieving the required operating conditions through the following (i) air leakage testing to achieve the operating vacuum pressure (ii) thermocouples and pressure transducers were connected to the data logger/PC and checked to ensure reading equal values (iii) all the mentioned valves can operate at the required times and open/shut within the recommended time (iv) ensuring the hot water, chilled water and mains water circulating system produce the flow rates required for testing. The following sub sections will describe the above mentioned commissioning steps.

3.4.1 Air leakage

To achieve the operating vacuum pressure of 2 mbar at temperature of 24˚C, all the components of the test rig have to be sealed, vacuumed and tested over a period of time to ensure minimal leakage. Three techniques were used to detect the leakage in the current system based on the position of the leakage as follows:

3.4.1.1 Paste method

This technique was used in the joints like tube-fitting, valve-fitting and gasket-shell. It requires applying thick white colour paste (like toothpaste) to the joints after vacuuming the system. If there is a small leakage, tiny holes form in the paste, and hence, the leakage point could be recognised. If the leakage was significant, the paste clearly collapses and could be detected easily.

3.4.1.2 Thin-transparent diaphragm method:

This technique was used with the upper plate of adsorber bed before connecting the hot/cooling water pipes (see Figure 3-28). This means that the upper surface of the plate is a flat surface with eight holes, in which, the heat exchangers beds were connected underneath the plate using compression fittings. The plate and the heat exchangers were fitted with the shell using rubber gasket and bolts. In order to check for any leakage at the connection between the heat exchanger beds and the compression fittings underneath the plate, the adsorber bed was connected to the vacuum pump and vacuumed to 2 mbar at 24˚C. Then thin-transparent diaphragm was placed over the plate to cover the eight holes by wiping the top surface of the plate with any liquid (like water) to provide a proper seal between the diaphragm and the plate. If leakage in the compression fittings exists, the diaphragm will be pulled down forming bubbles identifying areas of leakage.

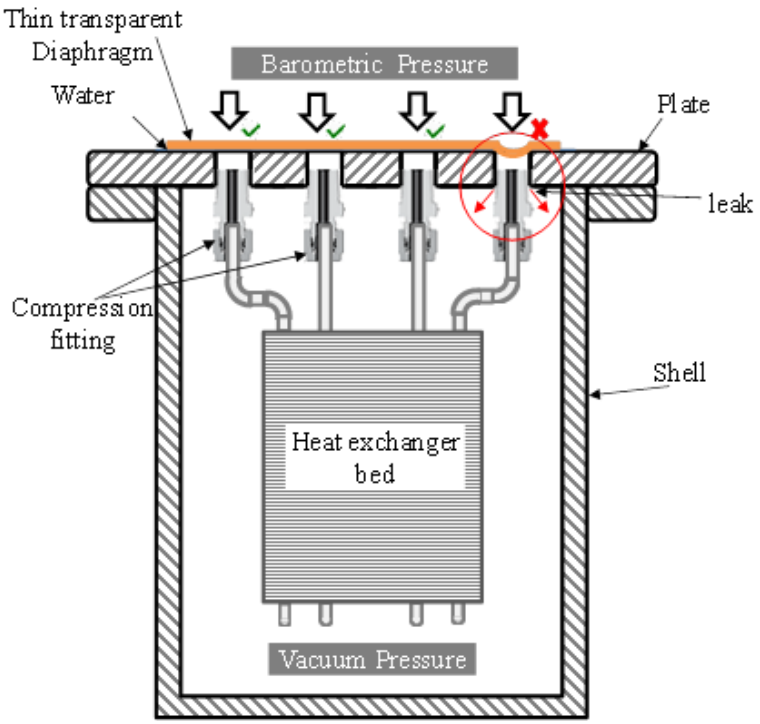

Figure 3-28 Diaphragm method for detecting a leak in the system

3.4.1.3 Submerging method:

This method was specially used for testing leakage in the condenser or evaporator of the adsorption system by filling them with water and submerging all expected leakage points, and then put the transparent cover on the container, connect to the vacuum pumps and vacuum to saturation pressure of water based on the water temperature. In case there is any leakage, it will be clearly shown via transparent lid, where bubbles form at the leakage points. In this method, it is required to take into account bubbles formed due to boiling process during evacuation period.

After identifying all leakage points and sealing them, the whole test facility was left under vacuum for two days and there was no significant increase in pressure with maximum change of 1 mbar. This is adequate to enable carrying out performance testing.

3.4.2 Thermocouples and pressure transducers consistency

The calibrated thermocouples and pressure transducers were connected to the data taker and monitored for a period of 30 minutes to make sure that they measure similar temperature and pressure values. Then the thermocouples and pressure transducers were tested by circulating the heating/cooling water through the test facility to ensure all thermocouples show the correct response to temperature changes.

3.4.3 Motorized valves operation and timing

The motorized valves were connected to the control board and Lab View program was developed to operate the system with specified switching and desorption/adsorption times. The motorized valves were tested by operating the test facility to check open and shut within the recommended times.

3.4.4 Fluid circulating system

The heating/cooling water systems were tested by circulating the fluid in the adsorber bed to make sure there is no leakage and produce the required range of flow rates. The main water pipe and water /antifreeze system were also connected and test by circulating the fluids in the condenser and the evaporator.

3.5 Experimental Testing

The experimental testing method includes two processes. The first process is preparing the test facility to enable starting the tests at the same conditions. The second process is carrying out the performance testing at various operating conditions.

3.5.1 Preparation process

To ensure reliable results, all the tests were carried out at the same initial conditions achieved through the preparation procedure outlined below:

a) Connect the heating water system to the adsorber bed by opening valves 3 and 4 (see Figure 3-1 and Table 3.2) to circulate the hot water. Meanwhile, connect the adsorber bed to the vacuum pumps by opening valve 8 to desorb any refrigerant from the adsorbent material. Once the pressure and temperature inside the adsorber bed reach 7mbar and 85^0C. Then the valves (3, 4 and 8) will be closed at the end of this step.
b) Connect the condenser to the vacuum pump by opening valve 7 and once the pressure inside the container reaches 2mbar at ambient temperature of 24^0C, close the valve.
c) Dissolve the required mass (70 grams) of sea salt in two litres of deionized water to obtain saline water (seawater) with total dissolved solids of 35000 ppm using.

d) Pour the two litres of seawater in the evaporator and immerse the required number of the 30mL stainless steel cups (4, 8, 12, 16 or 20 cups) filled with potable water.

e) Switch on the chiller and connect it to the evaporator's coil by opening valves 10 and 11 to cool down the refrigerant liquid temperature to 1^0C. The evaporator will then be connected to the vacuum pump for five minutes by opening valve 9. At the end of this task, valves 9, 10 and 11will be closed.

Table 3.2 Control sequence and valves operation for the test facility

	Description	Time (min)	Valve 1	Valve 2	Valve 3	Valve 4	Valve 5	Valve 6	Valve 7	Valve 8	Valve 9	Valve 10	Valve 11	Valve 12	Valve 13
Preparing Period	Bed-vacuum pump	_	M	M	A	A	A	A	M	M	M	M	M	M	M
	Condenser-vacuum pump	_	M	M	A	A	A	A	M	M	M	M	M	M	M
	Evaporator-vacuum pump	_	M	M	A	A	A	A	M	M	M	M	M	M	M
Operation period	Switching time-precooling	3	M	M	A	A	A	A	M	M	M	M	M	M	M
	Adsorption-evaporation	16	M	M	A	A	A	A	M	M	M	M	M	M	M
	Switching time-preheating	3	M	M	A	A	A	A	M	M	M	M	M	M	M
	Desorption-condensation	16	M	M	A	A	A	A	M	M	M	M	M	M	M

A	Closed valve/Automated control (LabView)	M	Closed valve/ manually control
A	Opened valve/Automated control (LabView)	M	Opened valve/ manually control

3.5.2 Performance testing process

The testing procedure consists of eight steps, as follows:

a) Connect the evaporator and the condenser to the chiller and the mains water line by opening valves 10, 11, 12 and 13 to circulate the water/antifreeze and cooling water and adjusting thermostat of the chiller to the required evaporator condition.

b) Connect the adsorber bed with the cooling water system (liquid side) by opening valves 5 and 6 to achieve a pre-cooling during the specified switching time.

c) At the end of switching time, open valve 2 to connect the adsorber bed with the evaporator (refrigerant vapour side) to start the adsorption process, continue the circulation of cooling water in the adsorber bed to extract the heat generated during the adsorption process through half the cycle time. At the end of this task, close valves 2, 5 and 6 to isolate the adsorber bed from the evaporator and cooling water system.

d) Open valves 3 and 4 to connect the adsorber bed with the heating water system (liquid side) to start pre-heating the adsorber bed during the same switching time as that of pre-cooling.

e) After the period of pre-heating, the adsorber bed was connected to the condenser by opening valve 1 to start the desorption process during the same half cycle time, while the heating water continue to circulate in the adsorber bed to provide the heat required during the desorption process. At the end of this task, close valves 1, 3 and 4 to isolate the adsorber bed from the condenser and hot water system.

f) The tasks from (b) to (e) were repeated for the specified number of cycles complete one test.

g) Open the transparent lid of the evaporator for collecting the stainless steel cups to weight the mass of solid ice required to calculate the specific daily ice production (SDIP). Also separate the brine of seawater from the ice slurry to be weighted and calculate the specific daily ice slurry production of (SDSP).

h) Open the transparent lid of the condenser for collecting the fresh water and weight it to calculate the specific daily distilled water production (SDWP).

3.6 System performance analysis

In this section, the methodology used to evaluate the system performance in terms of coefficient of performance (COP), SDIP, SDSP and SDWP using the measured data is described as follows:

a) The coefficient of performance (COP) for cooling is defined as the ratio of effective cooling achieved in the evaporator and the heat used in the desorption process. The calculation was based on the temperatures of heating liquid and water/antifreeze side as given by,

$$COP = \frac{Q_{evap}}{Q_{heat}} \quad (1)$$

Where Q_{evap} is the cooling rate achieved during the adsorption time. Q_{heat} is the heat used for the pre-heating and desorption processes of the adsorber bed. Both parameters are evaluated using equations (2) and (3) as follows,

$$Q_{evap} = \frac{\dot{m}_{AF}\, C_{p_{AF}}}{t_{at}} \int_0^{t_{at}} \left(T_{AF,in} - T_{AF,out}\right) dt \quad (2)$$

$$Q_{heat} = \frac{\dot{m}_{w,hot}\, C_{p_{w,hot}}}{t_{hct}} \int_0^{t_{hct}} \left(T_{hot,w,in} - T_{hot,w,out}\right) dt \quad (3)$$

Where the parameters $\dot{m}$ (kg/s), C_p (kJ/kg/K), t (sec) and T (˚C) are the mass flow rate, specific heat constant at constant pressure, time and temperature, respectively. The subscription w, hct, at, AF, in, out, denote water, half cycle time, adsorption time, water/antifreeze, inlet and outlet, respectively.

b) The Specific Daily Ice Production (SDIP) was calculated using the collected mass of solid ice from the evaporator using fresh water in the cups. The required time between two batches was taken as 8 min for collecting the ice and the evacuating process in

task (e) of the preparation procedure plus the time required for the specified number of cycles as follows:

$$SDIP = \frac{m_{ice,batch} \times 60 \times 24}{(t_{cycle-time} \times N_{cycle/batch} + t_{preparing}) \times m_{ads.}} \quad (4)$$

c) The Specific Daily Ice Slurry Production (SDSP) was calculated based on the collected mass of ice slurry from the evaporator (sea water side). The required time for preparation between two batches was also taken into account as follows:

$$SDSP = \frac{m_{ice-slurry,batch} \times 60 \times 24}{(t_{cycle-time} \times N_{cycle/batch} + t_{preparing}) \times m_{ads.}} \quad (5)$$

d) The Specific Daily Fresh Water Production (SDWP) was calculated based on the collected mass of fresh water from the condenser. The required time between two batches was also taken in to account as follows:

$$SDWP = \frac{m_{water,batch} \times 60 \times 24}{(t_{cycle-time} \times N_{cycle/batch} + t_{preparing}) \times m_{ads.}} \quad (6)$$

The uncertainty in the SDIP, SDSP, SDWP were estimated based on the calibration of a scale and a beaker which were used to measure the outputs, while for the COP, it was assessed based on the calibration of the thermocouples and flow meter.

3.7 Results

In this section, the performance of the single bed adsorption system for producing ice, ice slurry, cooling and fresh water is experimentally investigated at various operating parameters. Table 3.3 shows the initial conditions that were used in all the tests carried out in this parametric study. The temperature and pressure profiles of the single bed adsorption system are shown in Figure 3-29 and Figure 3-30.

Table 3.3 Operating conditions for the parametric study

Parameter	Value	Unit
Ambient temperature	23	˚C
Average temperature of inlet tap water	15	˚C
Average temperature of inlet chilled antifreeze	-1	˚C
Average temperature of heating water	95	˚C
Average temperature of cooling water	20	˚C
Mass flow rate of heating/cooling water system	7.3	L/min
Mass flow rate of chilled anti-freeze	5	L/min
Mass flow rate of tap water in condenser	5	L/min
Specific heat of water	4.18	kJ/kg/K
Specific heat of anti-freeze	4.1	kJ/kg/K
Total adsorbent mass	670	gram
Preparing time	8	min
Volume of sea water in evaporator	2	L

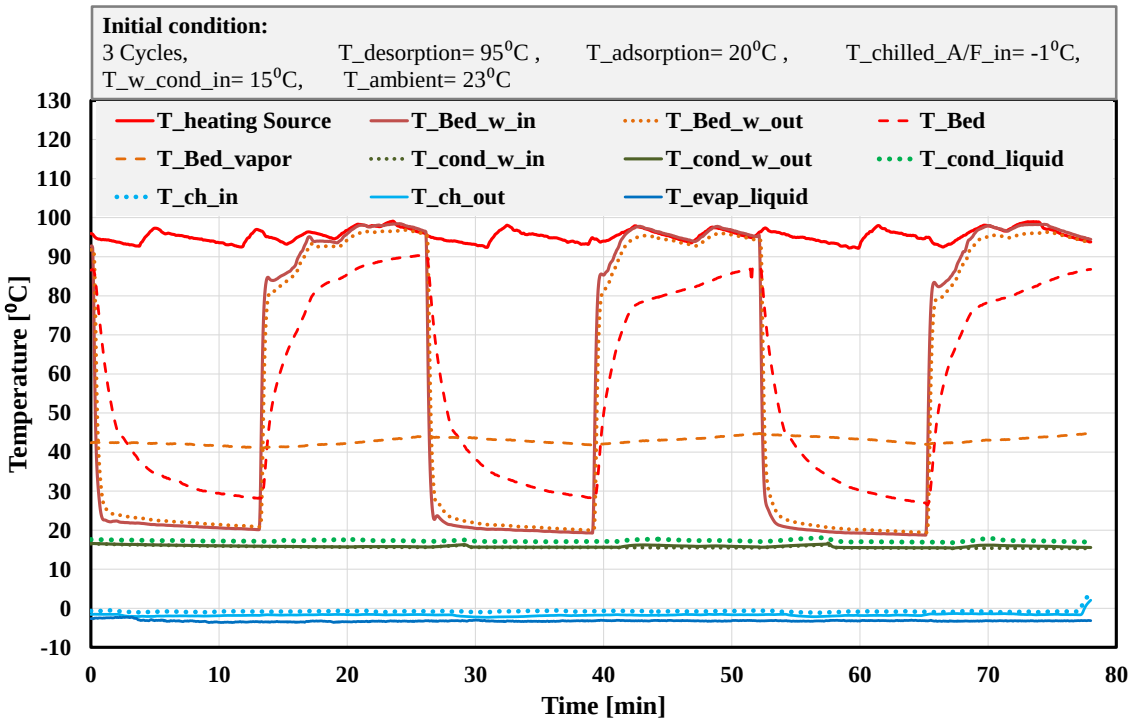

Figure 3-29 Cyclic temperature distribution at the adsorber bed, condenser and evaporator of single bed adsorption system

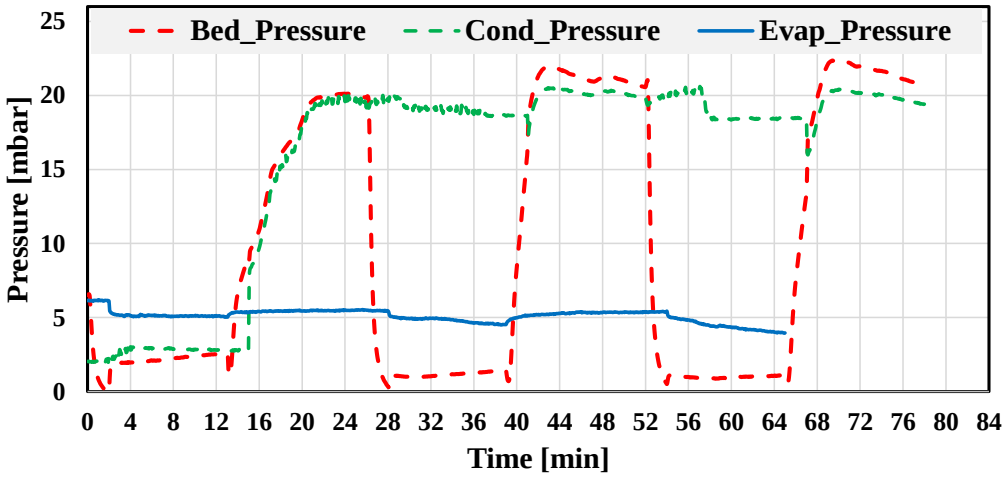

Figure 3-30 Cyclic pressure distribution at the adsorber bed, condenser and evaporator of single bed adsorption system

3.7.1 Volume of potable water in the evaporator

Figure 3-32 (A), (B), (C) and (D) show the effect of fresh water volume in the evaporator on the SDIP, SDSP, SDWP and COP, respectively. The experimental result in Figure 3-32 (A) shows that increasing the volume of fresh water in the evaporator results in increasing the SDIP. The rate of increase is from 30 to 40% per 120 ml of fresh water (four cups (120 ml)) in the range of 120 to 480 ml. This is because the fresh water crystallizes before the sea water, this helps to obtain an enhancement in ice production see Figure 3-31 by adding more volume of fresh water. The rate of increase in SDIP decreases to 10% per 120 ml by increasing the volume of fresh water from 480 to 600 ml. This is due to the configuration and size of evaporator, as by adding more cups of fresh water, the space available for the cups will be reduced. Therefore, an ice layer can easily to form and obstruct the boiling process of sea water. Hence consequently, the evaporation-adsorption process will decrease, leading to the reduction of SDIP. The maximum SDIP produces in this study is significantly higher than that produces by Wang et al. [13].Wang et al produces 2.6

ton/day/ton_ads at desorption and evaporation temperature of 95℃ and -15℃, while the maximum SDIP achieved is 10 ton/day/ton_ads at higher evaporation temperature of -1℃.

Figure 3-32 (B) shows a drop in the SDSP by increasing the volume of fresh water in the evaporator. Increasing the volume 120, 240, 360, 480 and 600 ml, the drop in SDSP increased by 2.8, 4.4, 15.3 and 16.9%, respectively. The reason for this drop in SDSP is due to the reduction in the surface of sea water in the evaporator by adding more cups of fresh water. As a result, the formed ice layer is hard to break due to the increase of surface tension of sea water which means that the evaporation process will be reduced by adding more cups.

Figure 3-32 (C) shows the variation in SDWP due to the increase in volume of fresh water, where no significant change in SDWP was observed with maximum difference of only 8%. The reason for this could be that there is no significant change in the operating conditions of the condenser and it is clear that the change in volume of fresh water inside the evaporator has no significant effect on the circulated water vapour from the adsorber to the condenser. The maximum value of SDWP is 1.4 ton/day/ton of adsorbet, which is comparable to those reported by [114] using silica gel/ water at desorption and evaporation temperature of 90˚C and 27 ˚C, respectively. Although significantly higher SDWP values were reported in literature, however these have been obtained at higher evaporation temperature with no other outputs from the system. This is because the condensed amount of water vapour significantly increases with the increase in the evaporation temperature > 10˚C [122, 126]. However, the SDWP in current study is addressed as a by-product outcome.

Figure 3-32 (D) shows the effect of fresh water volume on the COP of the single bed adsorption system. It can be seen that the COP increases by increasing the volume of fresh water, the maximum COP (0.205) achieved was at 480 ml of fresh water. This is because by increasing the volume of fresh water, the potential of evaporation will be improved in term of cooling effect according to the freeze point of fresh water. However, it can be seen from the figure that the COP decreases by adding more volume of fresh water above 480ml. This is due to the reduction in evaporation-adsorption process, as the potential of generated vapour to pass through the adsorber bed will be decreased by forming an ice layer on the top surface of the refrigerant (seawater). In other words, by adding more cups more than 16 (480 ml) the exposed surface of saline water will be reduced and the ice will easily form leading to reduction the evaporation-adsorption process.

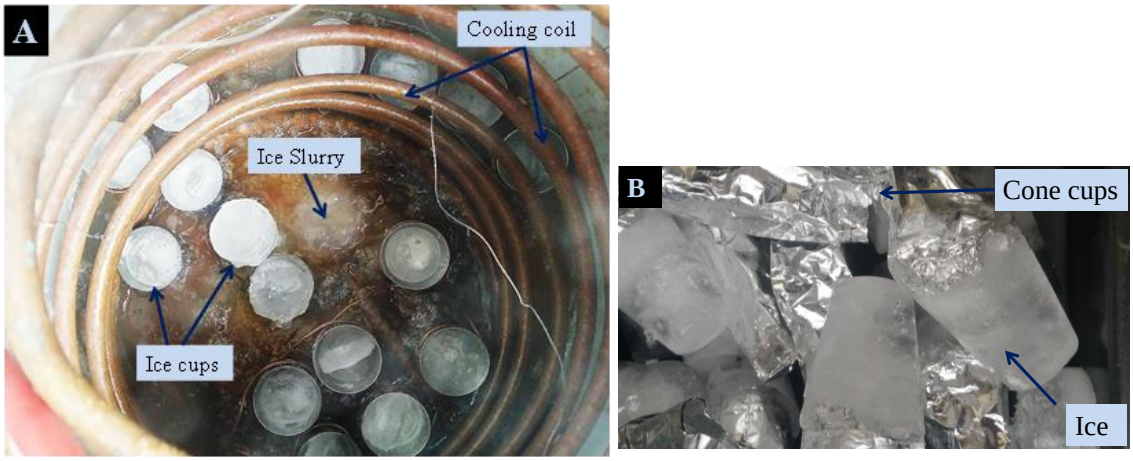

Figure 3-31 Pictorial view in the evaporator (A) ice cups with saline water (B) collected ice

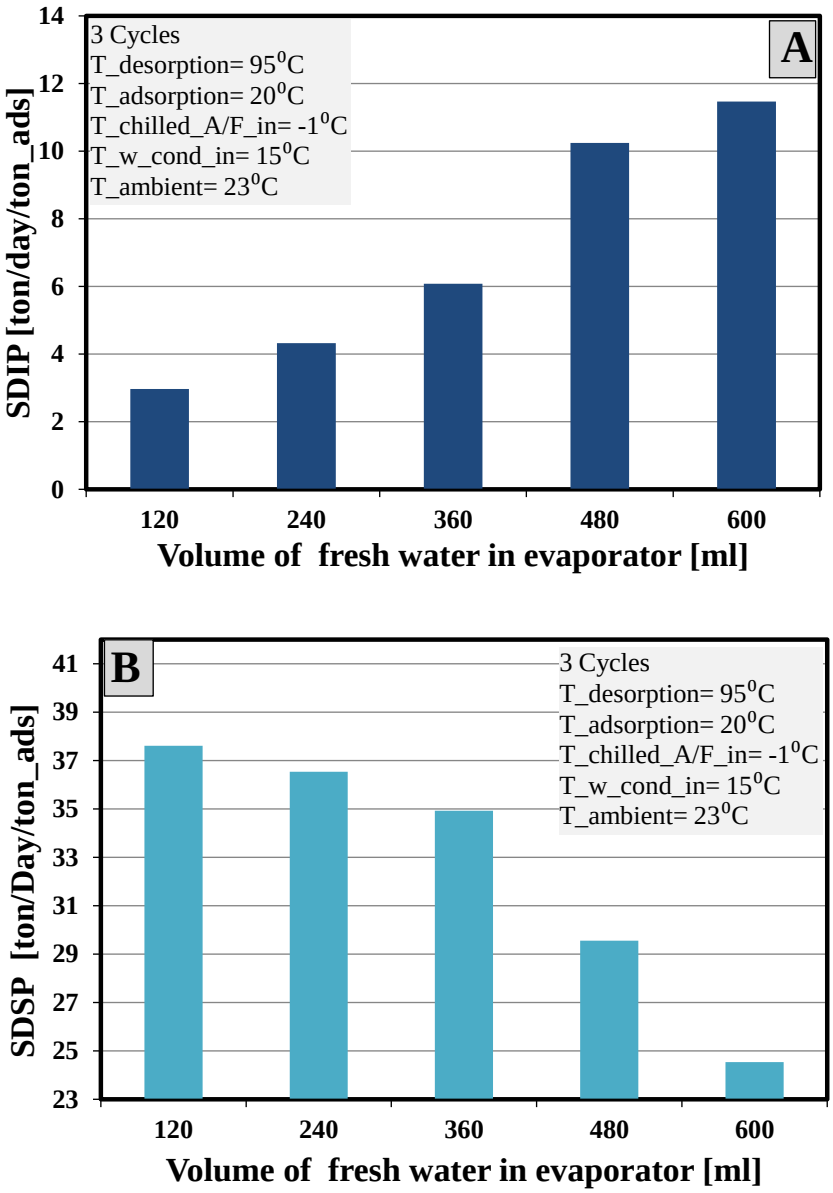

Figure 3-32 Effect of potable water volume in the stainless steel cups on each of (A) SDIP, mass of solid ice and fresh water in the evaporator, (B) SDSP in the evaporator, (C) SDWP, and (D) COP

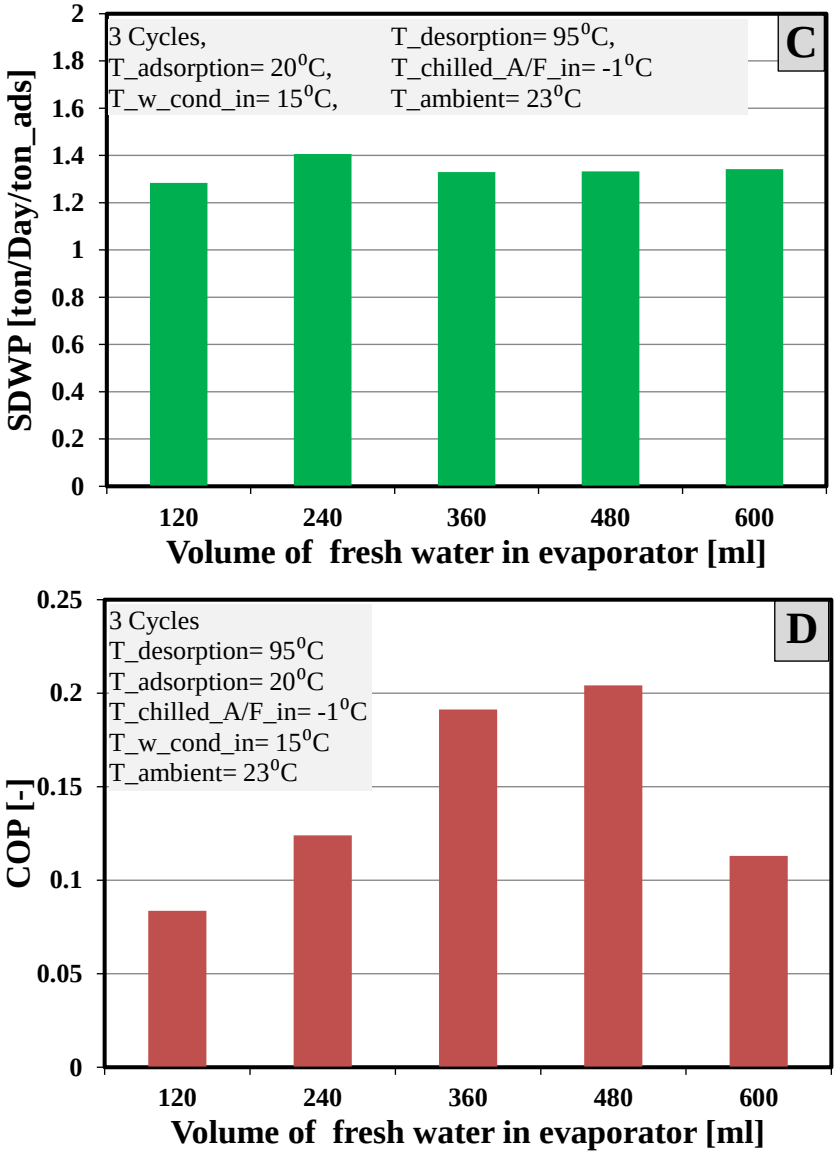

Figure 3-32 (Continued: effect of potable water volume in the stainless steel cups on each of (C) SDWP and (D) COP)

3.7.2 Salinity Effect of Sea Water

Figure 3-33 shows the salinity effect of water (as the refrigerant) in the evaporator on the performance of the single bed adsorption ice making-water desalination system. As shown in *Figure 3-33* (A), it is clear that the maximum SDIP is at 35×10^3 ppm based on maximum mass of the produced ice in cups per batch. The SDIP increased by 7.7% when the salinity was increased from 20×10^3 to 35×10^3 ppm. This is due to water evaporating for longer time

before starting to freeze in the evaporator. Then the SDIP decreased at 1.3% per 15×10^3 ppm by increasing the salinity from 35×10^3 to 65×10^3 ppm. The main reason of this drop is the decrease in the freezing point depression due to the increase in salinity as shown in Figure 2-19.

Figure 3-33 (B) shows that there was increase in the SDSP and SDWP up to 60% and 6.3% by increasing the salinity from 20 to 35 ppm, respectively. The same trend was shown in *Figure 3-33* (C) but with smaller effect on the COP. The reason for this is that the period of evaporation-adsorption processes is relatively increased by lowering the freezing point of water. In contrast, the SDSP, SDWP and COP are moderately decreased by increasing the salinity of water from 35×10^3 to 65×10^3 ppm. This could be caused by changing the physical properties of saline water where the boiling temperature of water increases by increasing the salinity of water.

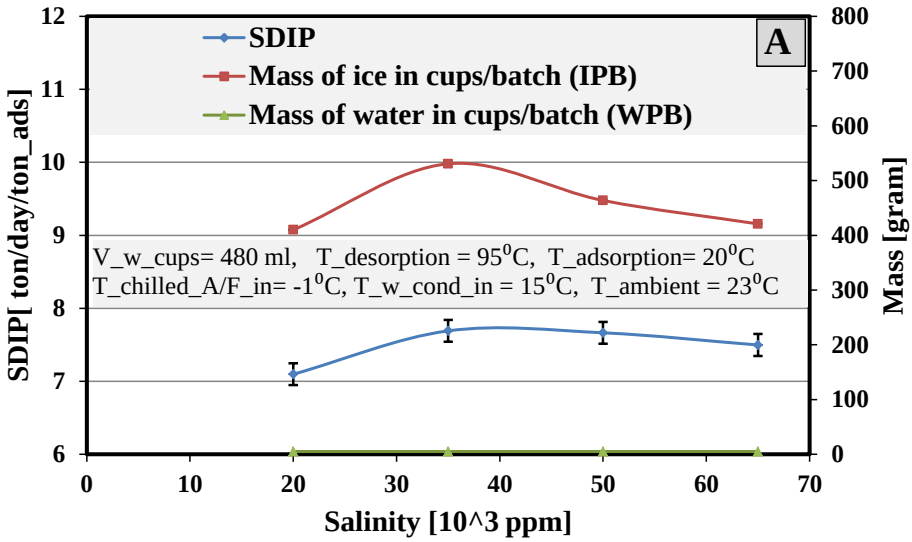

Figure 3-33 Effect of water salinity on each of (A) SDIP, mass of solid ice and fresh water in the evaporator, (B) SDSP in the evaporator and SDWP in the condenser, and (C) COP of cooling

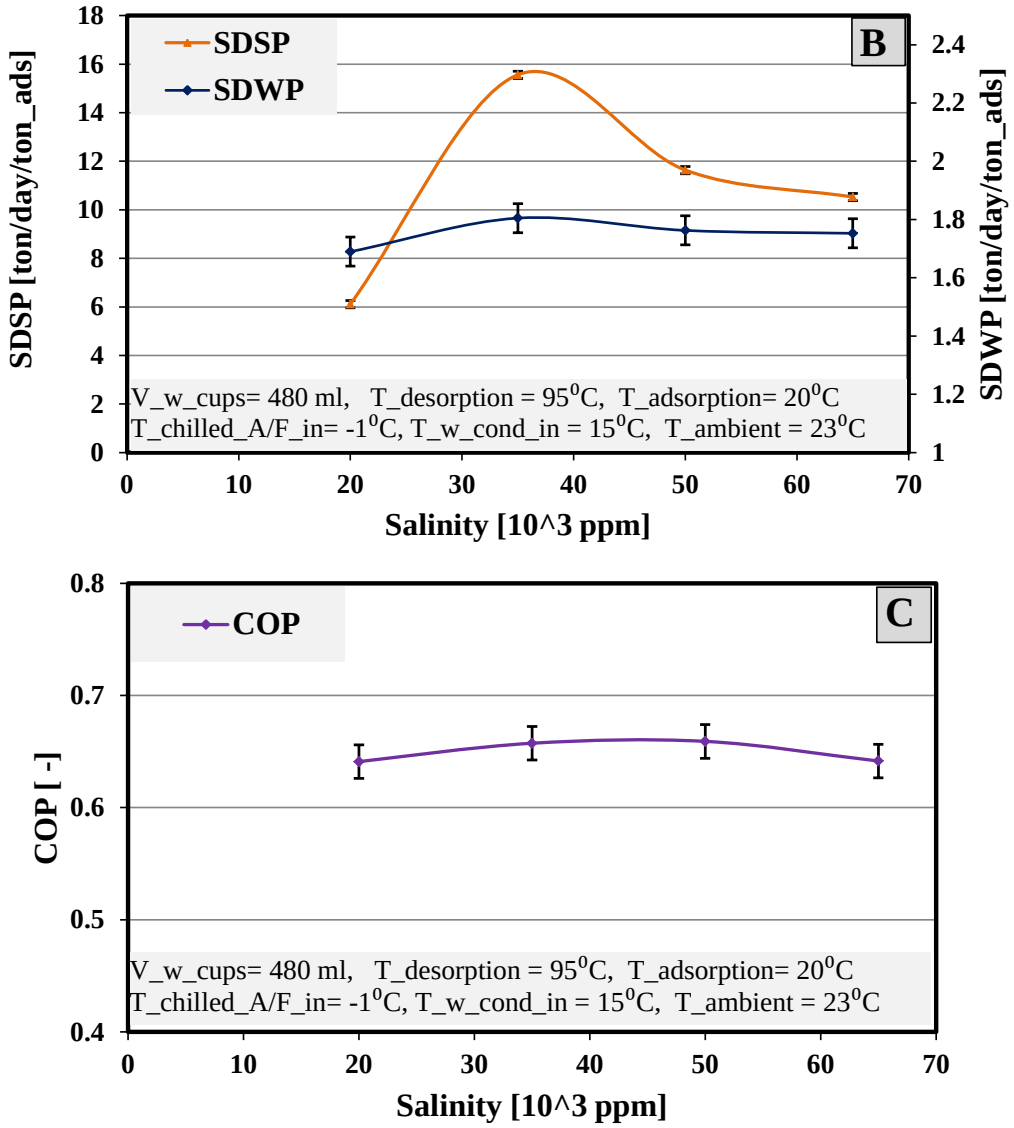

Figure 3-33 (Continued: effect of water salinity on each of (B) SDSP in the evaporator and SDWP in the condenser, and (C) COP of cooling)

3.7.3 Effect of cycle's number

Figure 3-34 shows the effect of cycle's number on the performance of the single bed adsorption ice making – water desalination system in terms of the COP, SDIP, SDSP and SDWP. It could be seen from Figure 3-34 (A) that the SDIP has fluctuated considerably with maximum and minimum values of 9 to 7.5 ton/day/ton_ads, respectively,

by increasing the cycle's numbers from 1 to 4. Despite this trend, the mass of solid ice in stainless steel cups per batch increased considerably by increasing the cycle's numbers. This increase is caused by the batch run time, as it is increased by increasing the number of cycles. The reason behind the fluctuation is probably due to the rate of increase in the ice mass against the decrease in the batch number per day by increasing the cycle numbers. For example, the batch run time of one and four cycles is 34 and 112 mins (including the preparation time) while the batch number is 24 and 13 per day, respectively, with the same number of the cups was used in both tests, this means that the same volume of fresh water at different run times. Figure 3-34 (A) shows that there was water in the stainless steel cups after 1st, 2nd and 3rd cycles while all the water in the cups changed to solid ice during the 4th cycles. This is due to the improvement in ice production per batch, as the solidity of ice is directly proportional with the number of cycles due to the longer time of cooling effect applied to the same amount of fresh water in the16 cups.

Figure 3-34 (B) shows that the SDSP significantly decreased by 30.4%, 15.3% and 12.8% by increasing the number of cycles from one, two, three to four cycles, respectively. Despite of this drop in SDSP, the mass of ice slurry increased by 30.9%, 26.6% and 11.8% per one batch by increasing the cycle's number from 1 to 4, respectively. This is due to the run time per day, where the rate of increase in ice slurry per batch does not overcome the increase in run time, which has negative effect on the SDSP as the number of batches produced per day decreases. The increase in the mass of ice slurry per batch is due to the high potential of seawater (as refrigerant) to freeze in evaporator, as the time available for the evaporation process increases, leading to the increase in the amount of ice slurry per batch.

As shown in Figure 3-34 (C), the cycle's number affects the cooling COP where the COP remains relatively constant by increasing the number of cycles from one to two, then decreases significantly (60%) by increasing the number of cycles to three and decreases further by increasing the number of cycles to four. This reduction in COP could be attributed to the increased ice slurry formation on the surface of the saline water refrigerant thus reduction the evaporation process.

Figure 3-34 (D) shows that there was an enhancement in the SDWP up to 78% and 24 % per one cycle by increasing the cycle's number from one to three cycles, respectively. In the same figure, there was a drop in the SDWP after the third cycle. However, despite this drop, the mass of distilled water in condenser is significantly increased per one batch by increasing the number of cycles. The main cause of this drop is the reduction in the number of batches achieved during daytime by increasing the number of cycles at the same operating conditions. The figure also shows that one cycle per batch produced small amount of water (4 grams) in condenser due to the adsorbent in the bed has low potential to release the vapour to the condenser as some of refrigerant remained in the adsorbent, which needs longer time to release the vapour to the condenser.

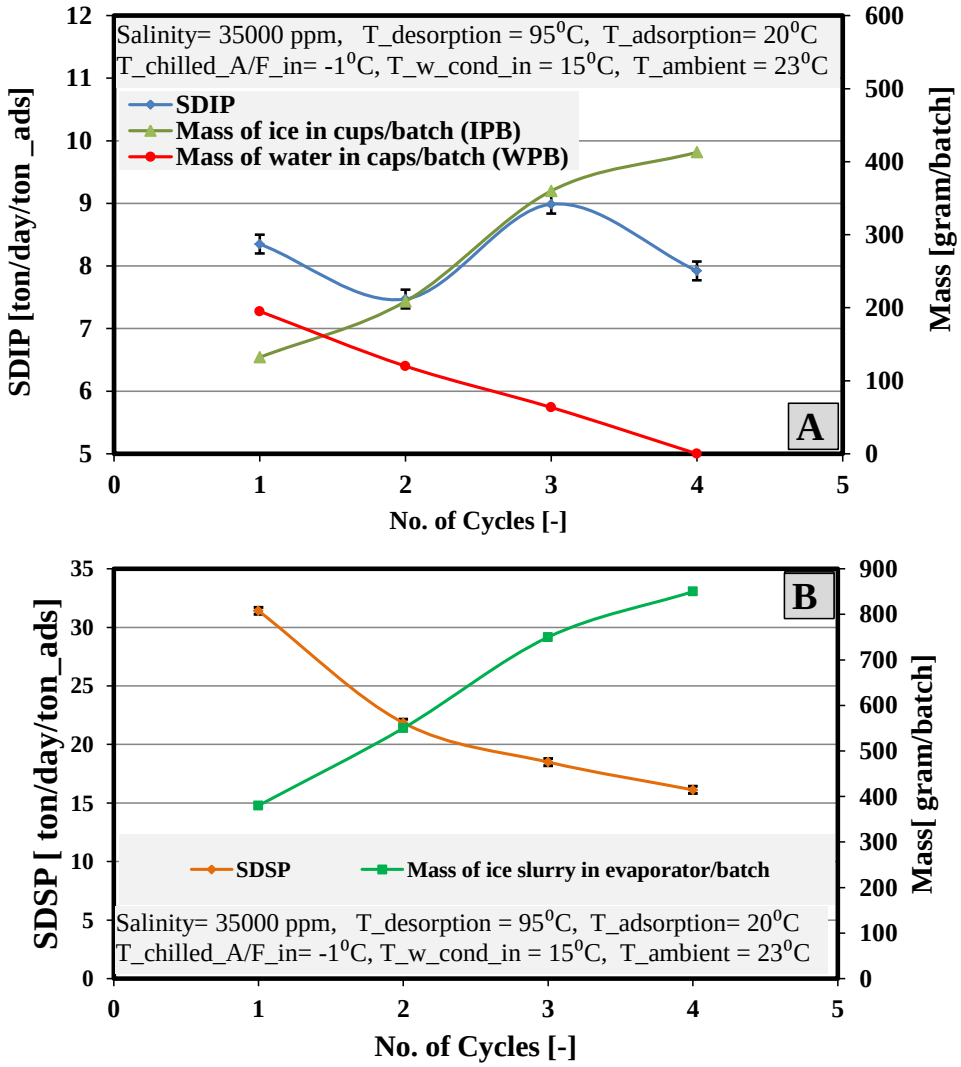

Figure 3-34 Effect of cycle's number on each of (A) SDIP, mass of solid ice and fresh water in the evaporator, (B) SDSP and mass of ice slurry in the evaporator, (C) SDWP and mass of fresh water in the condenser, and (D) COP

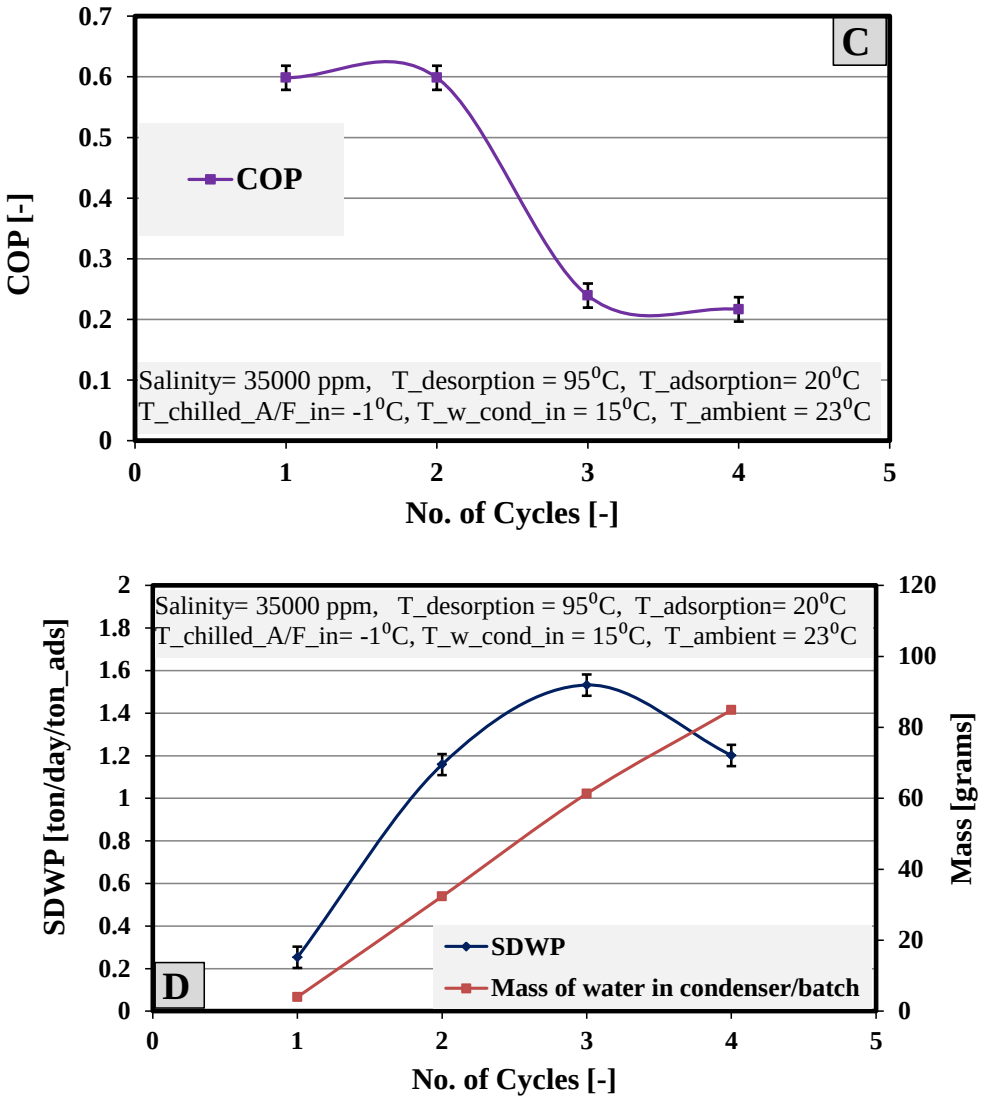

Figure 3-34 (Continued: effect of cycle's number on each of (C) SDWP and mass of fresh water in the condenser, and (D) COP)

3.7.4 Effect of Switching Time

Figure 3-35 shows the effect of switching time on the SDIP, SDSP, SDWP, and COP using three cycles per batch. Figure 3-35 (A) shows that increasing the switching time from one minute to two minutes increased the SDIP by 7.9% but further increasing the switching time to 3 and 4 minutes resulted in little change in the SDIP. Increasing the switching time allowed preheating/precooling the adsorbent material for the desorption/adsorption process. However, significant increase in the switching time reduces the number of batches

produced per day thus counteracting the enhancement of the desorption/adsorption processes. Figure 3-35 (A) also shows that the amount of water in the stainless steel cups inside the evaporator decreased by 39%, 25% and 0% per one minute by increasing the switching time from one to four minutes, respectively.

Figure 3-35 (B) shows an increase in the SDWP by increasing the switching time to reach a maximum value at 2.5 minutes and then it decreased. After this point, the mass of water in the condenser per batch reached steady state while the SDWP decreased by increasing the switching time.

Figure 3-35 (C) shows that by increasing the switching time from one to four minutes, the rate of enhancement in the COP per one minute is 15.4%, 24% and 8%, respectively. The reason for this enhancement in the COP is that increasing the period of pre-cooling and pre-heating processes from one to four leads to enhancing the adsorption and desorption processes in the beds, respectively, thus, a large amount of refrigerant vapour will be adsorbed and desorbed.

As shown in Figure 3-35 (D), the SDSP decreased with a maximum rate of 6.3% per one minute by increasing the switching time. Despite this decrease in SDSP, there was a small increase in the mass of ice slurry per one minute of 1.7%, 6.6% and 0.3% by increasing the switching time from one to four minutes, respectively. This is caused by contradictory effect of increasing switching which results in decreasing the number of batches per day but results in enhancing the adsorption/desorption process thus increasing the mass of slurry ice in the evaporator.

From the above discussion, a switching time of 3 minutes can be considered as optimum switching time producing optimum outputs.

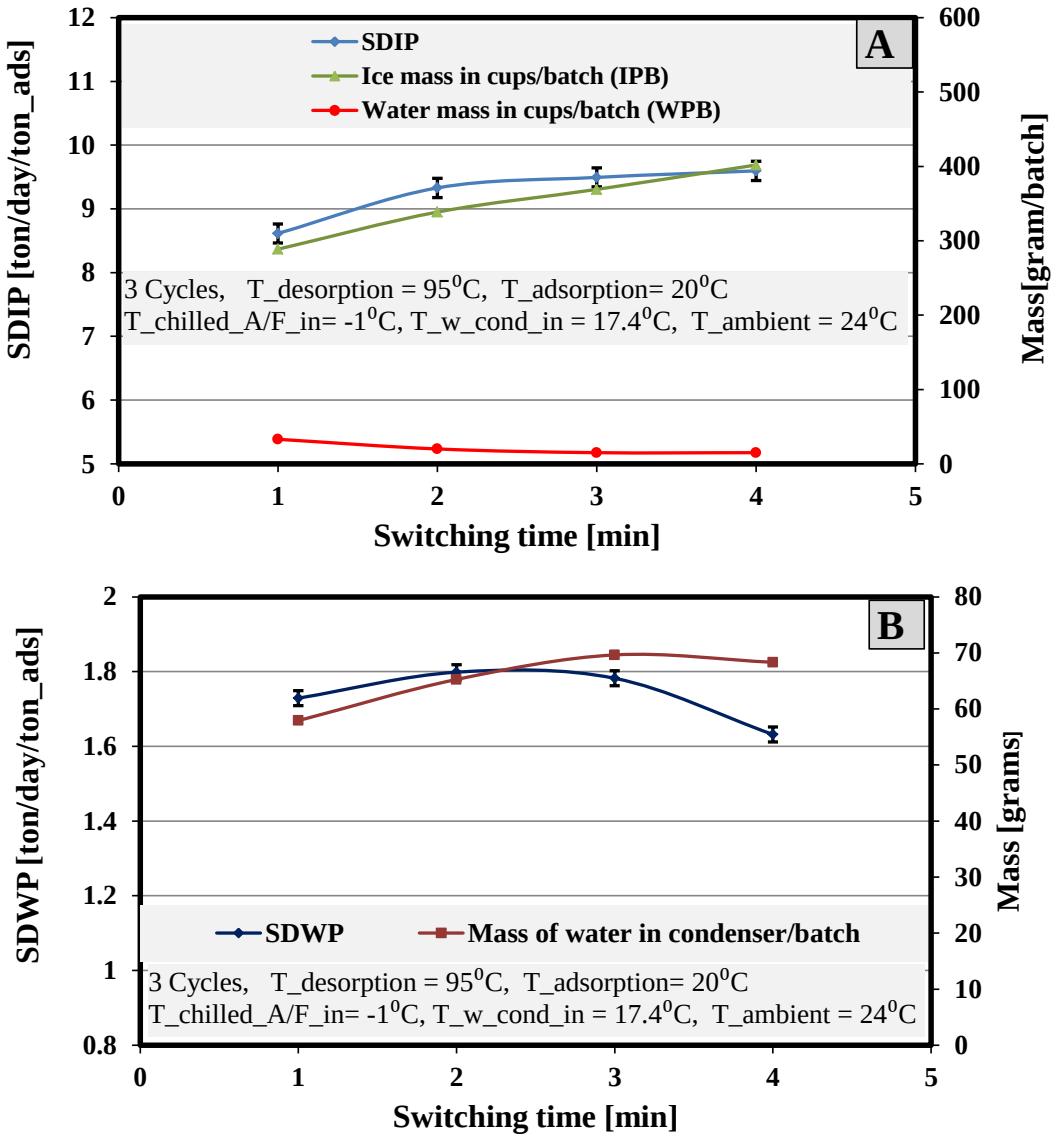

Figure 3-35 Effect of switching time on each of (A) SDIP, mass of solid ice and fresh water in evaporator, (B) SDSP and mass of ice slurry in evaporator, (C) COP of cooling and (D) SDSP and mass of ice slurry in the evaporator.

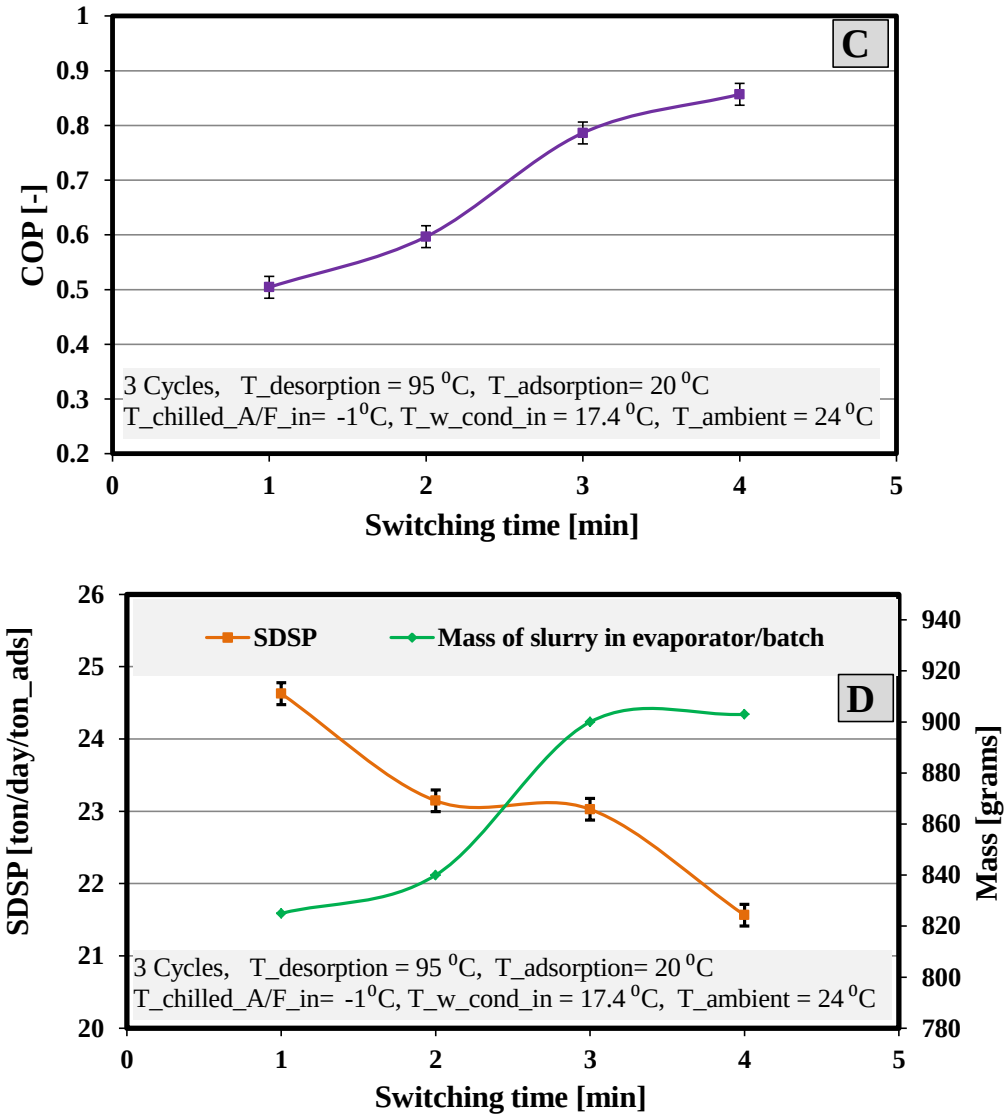

Figure 3-35 (Continued: effect of switching time on each of (C) COP of cooling and (D) SDSP and mass of ice slurry in the evaporator).

3.7.5 Effect of adsorption/desorption timeFigure 3-36 shows the effect of adsorption and desorption time (ADT) on the SDIP, SDSP, SDWP and COP using the optimum switching time of 3 minutes as stated above. Figure 3-36(A) shows a significant increase in the SDIP of 14.7% by increasing the ADT from 9 to 11 minutes; however, there was a drop in the SDIP of 2%, 4.9% and 3.4% as the ADT increased from 11, 13, 15 and 17 minutes, respectively. The main reason behind this drop is the decrease in the batch number per day by increasing the ADT. Despite this drop in SDIP, the mass of solid ice in the stainless steel

cups increased by 25 %, 9.7%, 5.7% and 0.8% as the ADT increased from 9, 11, 13, 15 and 17 minutes, respectively. The main reason for this increase is the longer time of adsorption and desorption per batch which leads higher amounts of refrigerant vapour being adsorbed and desorbed, respectively, however this increase couldn't compensate the decrease in the batch number per day. Here, it is worth mentioning that all water in the cups becomes ice at ADT of 15 and 17 minutes. Figure 3-36(B) shows that the SDWP increased by up to 35% by increasing the ADT from 9 to 11 minutes which can be attributed to a higher amount of desorbed vapour from the adsorbent material. The rate of increase in the SDWP fluctuates moderately as the ADT increased from 11 min to 17 min with a maximum rate of ±9% per two minutes of the ADT. The same trend was shown by Ali et al. (2016) [2], however with higher rate of SDWP due to higher evaporation temperature of 10℃. The reason for this fluctuation could be that the adsorption and desorption rates will be reduced after certain ADT values based on the characterization of the adsorbent material (see section Figure 2-3). Figure 3-36(C) shows a significant increase in the COP of the system based on cooling effect by up to 20% and 10% as ADT increased from 9 to 11 and 13 minutes, respectively. Then, the COP slightly dropped by increasing the ADT from 13 to 15 minutes. The main reason of this drop is the higher rate of desorption heat associated with increasing the ADT which inversely affect the COP of the system. Increasing the ADT from 9 to 15 minutes increased the average change in the antifreeze temperature from 2.25 to 2.6, 2.7 and 2.85 K, respectively. After 15 min, the COP slightly decreased by 3.4 % due to the decrease in the average drop of antifreeze temperature from 2.85 to 2.2 K. Figure 3-36(D) shows that the mass of ice slurry sharply increased by up to 22 % as the ADT increased from 9 to 11 minutes. In contrast, the SDSP decreased by 9.6% with the same ADT change. The reason for this decrease is that increasing the ADT results in higher amount of

evaporated refrigerant thus increasing the amount of heat extracted from the water/antifreeze. But, the increase in the ADT has an adverse effect on the SDSP as any increase in the ADT leads to decreasing the number of batches per day. It could be noticed that the SDSP fluctuated within maximum and minimum values of 17.8 to 15.7 ton/day/ton_ads, respectively, by increasing the ADT from 11 to 17 minutes.

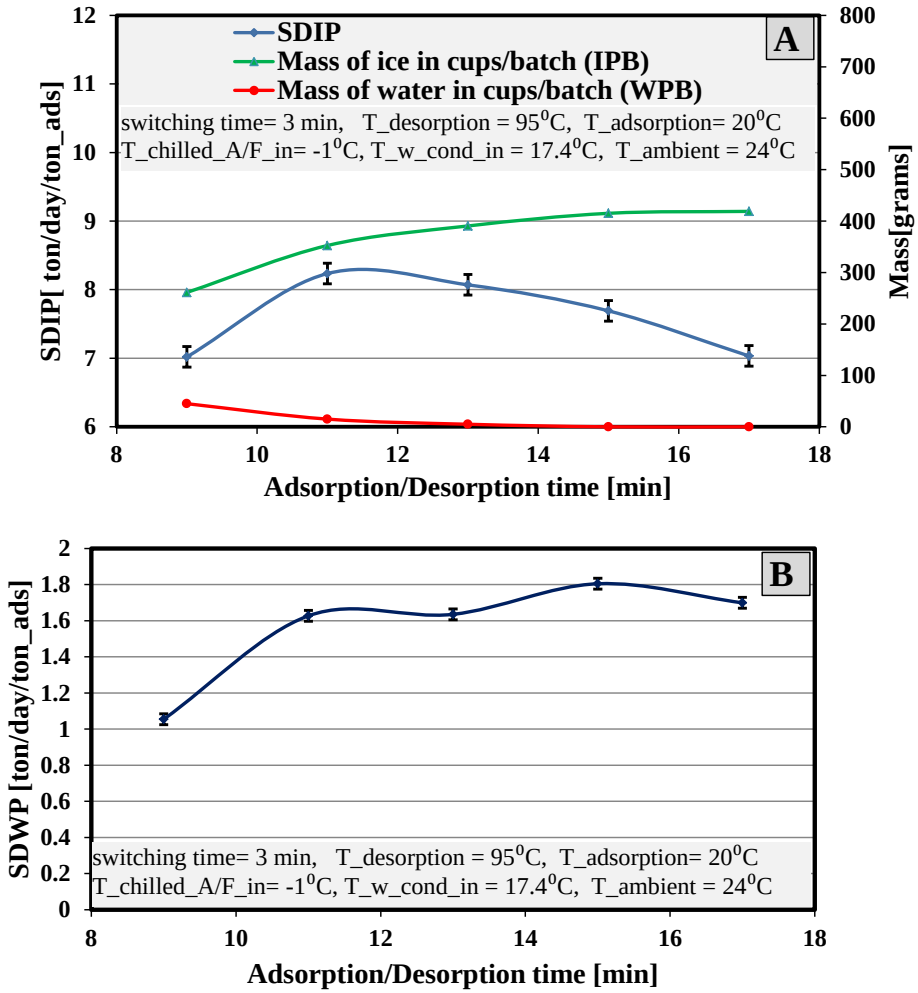

Figure 3-36 Effect of adsorption/desorption time on each of (A) SDIP, mass of solid ice and fresh water in the evaporator, (B) SDWP in the evaporator, (C) COP of cooling and temperature drop in the evaporator, and (D) SDSP and mass of ice slurry in the evaporator.

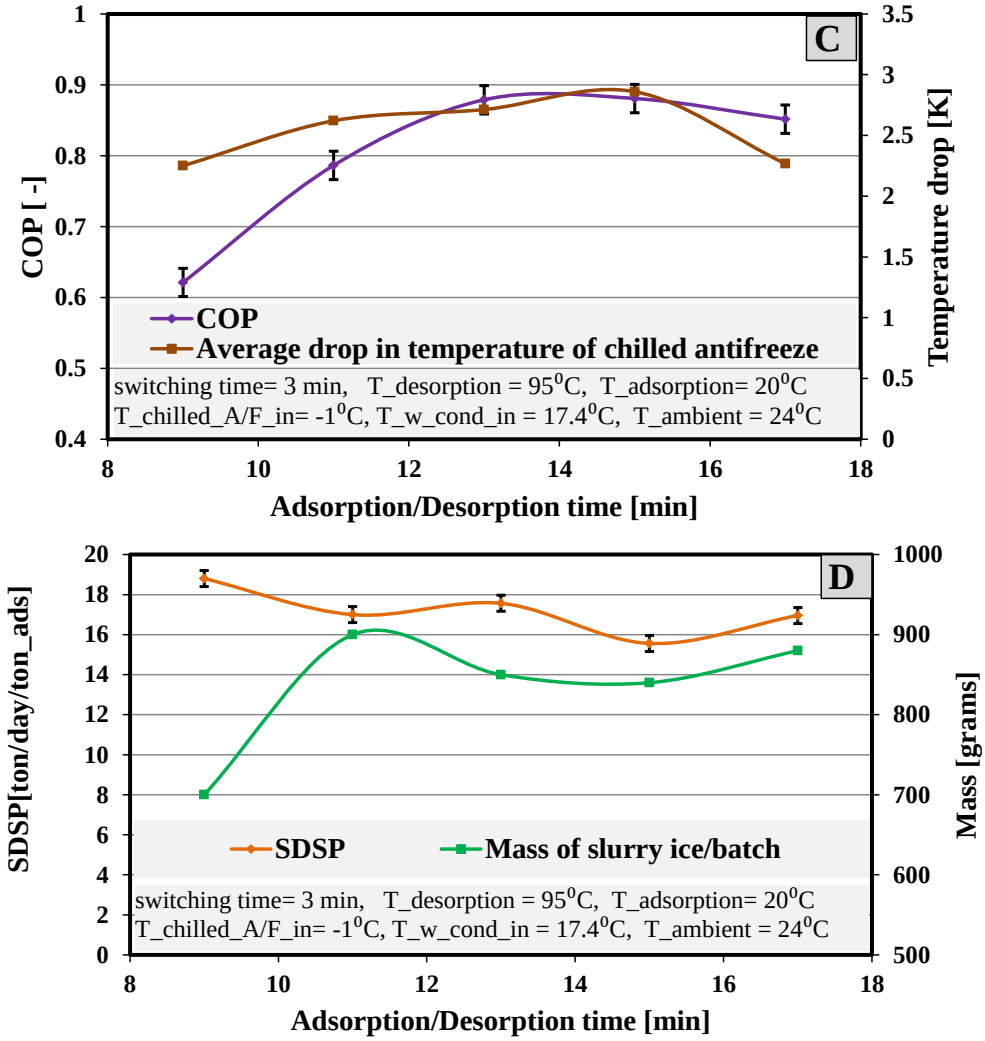

Figure 3-36 (Continued: effect of adsorption/desorption time on each of (C) COP of cooling and temperature drop in the evaporator, and (D) SDSP and mass of ice slurry in the evaporator).

3.7.6 Effect of desorption temperature

Figure 3-37 (A), (B) and (C) show the effect of desorption temperature on the performance of single bed adsorption system in term of SDIP, SDSP, SDWP and COP. Desorption temperature is normally investigated by researchers to find the optimum temperature as it is the driving temperature of the current system [127] and [128]. Figure 3-37 (A) shows an increase in the SDIP of 11% and 7.9 % by increasing the desorption temperature from 88 to

93 and 98˚C due to the increase in the production of ice in the stainless steel cups. This increase in the SDIP is because the amount of refrigerant vapour flow from the bed to the condenser during the desorption-condensation process increases by increasing the desorption temperature, this in turn dries the adsorbent material to adsorb a higher amount of refrigerant vapour from the evaporator during the evaporation-adsorption process.

Figure 3-37 (B) shows a small increase in the SDSP up to 10% by increasing the desorption temperature from 88˚C to 93˚C, and then there was a smaller decrease in the SDSP of 2% by increasing the desorption temperature from 93˚C to 98˚C. A significant increase in the SDWP up to 26% and 19% are shown in Figure 3-37 (B) by increasing desorption temperature form 88˚C to 93˚C and 98˚C, respectively. The same trend was theoretically investigated by other researchers with higher rate of SDWP of about 9 ton/day/ton of adsorbent [2] and 8 ton/day/ton of adsorbent [1] due to the higher evaporation temperature of 10℃ and desorption temperature of 90℃ . The main cause of this increase in SDWP is the high amount of refrigerant vapour generated from the adsorber bed to the condenser as it increases by increasing desorption temperature during the desorption-condensation process.Figure 3-36 (C) shows a significant increase in the COP of the single bed adsorption system of 39% and 20% by increasing the desorption temperature from 88˚C to 93˚C and 98˚C. The reason for this increase in the COP is that the adsorbent material has a potential to adsorb a higher amount of refrigerant vapour at higher desorption temperature.

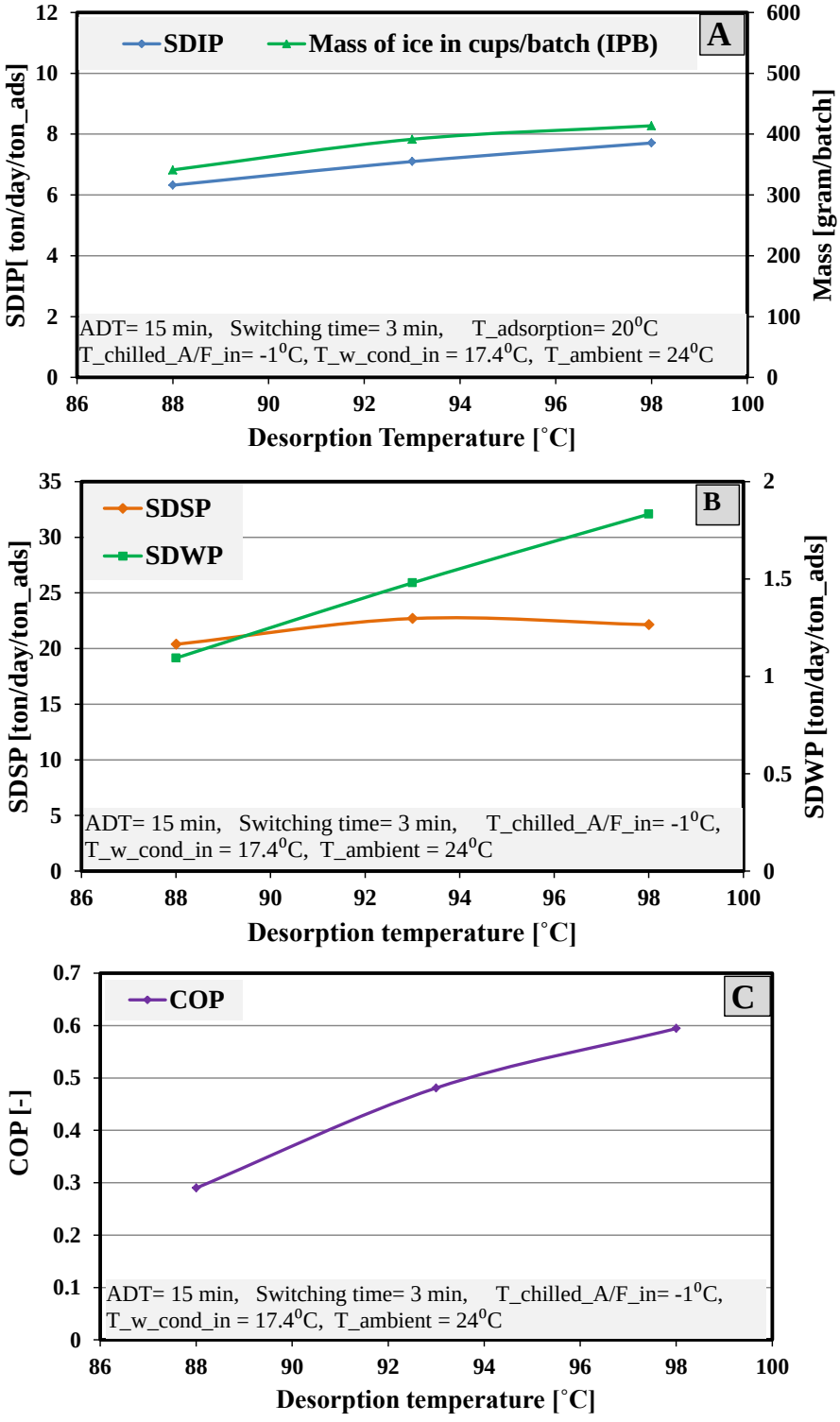

Figure 3-37 Effect of desorption temperature on the (A) SDIP, (B) SDSP and SDWP and (C) COP of the single bed adsorption refrigeration system

3.7.7 Effect of water/antifreeze temperature

Figure 3-38 (A), (B) and (C) show the effect of water/antifreeze inlet temperature to the evaporator on the performance of the single bed adsorption system in term of SDIP, SDSP, SDWP and COP. The evaporator temperature is one of the most important parameters in this study as it directly affects the production of ice and slurry ice in the evaporator. Figure 3-38 (A) shows a small increase in the SDIP of 5% by increasing the evaporator temperature from -3˚C to -1˚C. This increase in SDIP could be due to the reduction in the slurry ice formation at high evaporation temperature which leads to increasing the potential of evaporation process on the upper surface of saline water in the evaporator, which in turn increases the cooling of the potable water in the stainless steel cups. A significant decrease in the SDIP of 34% and 31% can be observed in Figure 3-38 (A) by increasing the evaporator temperature from -1˚C to 1˚C and 3˚C, respectively. The reason for this reduction is that the crystallization phenomenon becomes weaker as the evaporator temperature increases.

Figure 3-38 (B) shows a significant reduction in the SDSP of 35%, 58% and 50% by increasing the evaporator temperature from -3˚C to -1˚C, 1˚C and 3˚C, respectively. This reduction in the SDSP is due to increasing the evaporator temperature above the freezing point of the saline water. A significant increase in the SDWP of 21%, 13% and 17% could be deduced from Figure 3-38 (B) by increasing the evaporator temperature from -3˚C to -1˚C, 1˚C and 3˚C, respectively. The same trend was found by Ali et al. 2016 [106] but with higher SDWP of 2.5 ton/day/ton of adsorbent at 5˚C compared to 2.3 ton/day/ton of adsorbent from the current system at 3 ˚C. The main cause of the stated increase in the SDWP is the increase in the evaporation process of the saline water by increasing the evaporation temperature, which help to move more refrigerant vapour from the evaporator

to the adsorber beds. This in turn leads to increasing the desorbed vapour of refrigerant from the bed to the condenser during the desorption-condensation process.

Figure 3-38 (C) shows a significant increase in the COP of the current system by 53%, 38% and 18% as the water/antifreeze inlet temperature in evaporator increases from -3˚C to -1˚C, 1˚C and 3˚C, respectively. The same trend was shown by Allouhi et al. (2016) [29] and Song et al (2014) [33] but with lower COP of 0.138 [29] compared to 0.8 of the current system at the same evaporation temperature of 2˚C. The main cause of this increase in the COP is an increase in the evaporation process inside the evaporator due to increasing the water/ antifreeze temperature. In addition, the reduction in ice layer formation on the top of the saline water at higher evaporation temperatures contributes to this increase in the COP. Based on the stated results, the optimum evaporator temperature for the next parametric study is at -1˚C taking into account the best ice production.

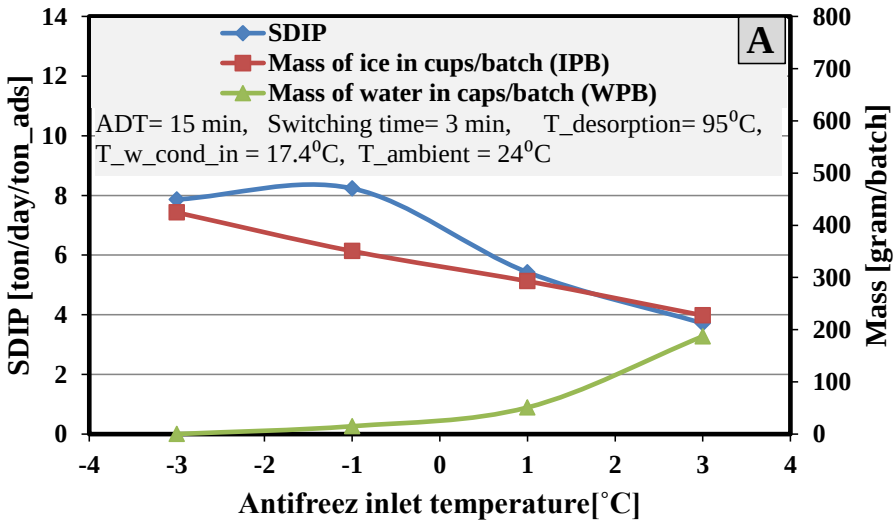

Figure 3-38 Effect of antifreeze inlet temperature on the (A) SDIP, (B) SDSP and SDWP, and (C) COP of the single bed adsorption refrigeration system.

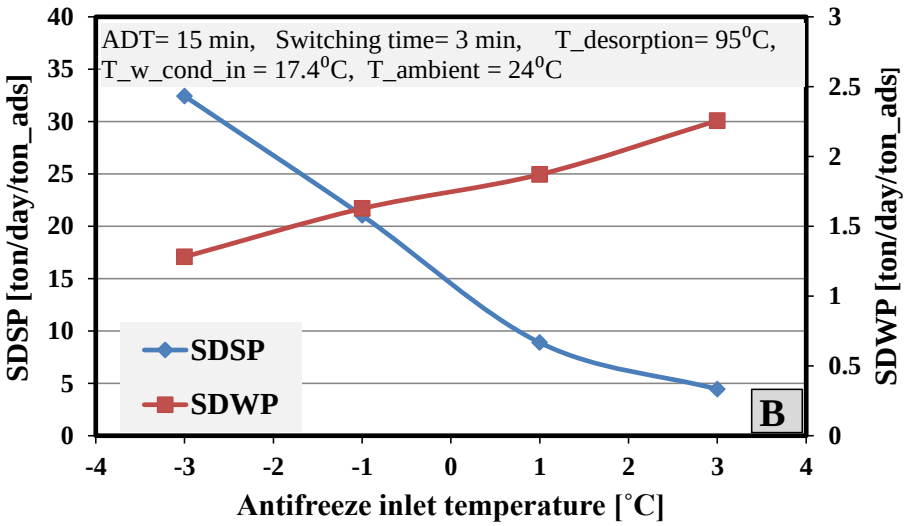

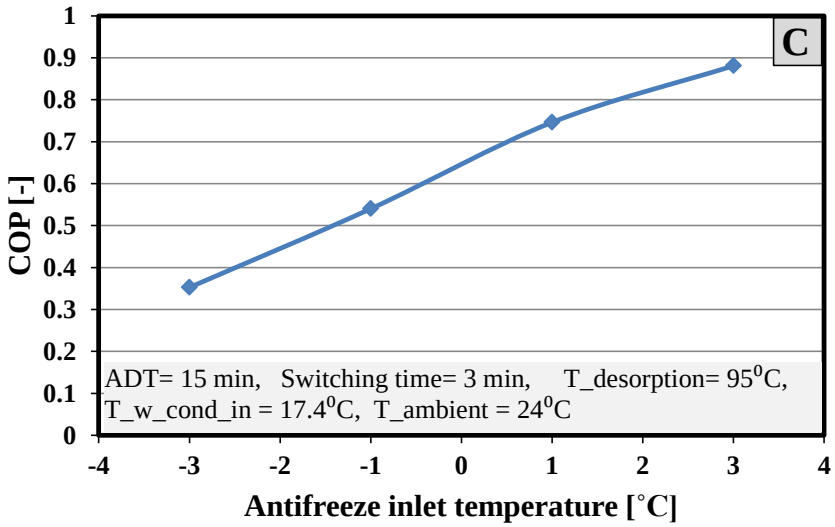

Figure 3-38 (Continued: effect of antifreeze inlet temperature on the (B) SDSP and SDWP (C) COP of the single bed adsorption refrigeration system).

3.7.8 Effect of condensation temperature

Figure 3-39 (A), (B) and (C) show the effect of condensation temperature on the performance of the single bed adsorption system in terms of SDIP, SDWP, SDSP and COP at evaporation temperature of -1˚C, desorption temperature of 95˚C, ADT of 15 minutes and switching time of 3 minutes. The condensing temperature directly affects the performance of the current system through its effect on the desorption-condensation process. The results were obtained using mains water temperature of 17.5˚C. Figure 3-39

(A) shows a reduction in the SDIP of 10% and 5% per 2.5˚C increase in the condensation temperature form 17.5˚C to 20˚C 22.5˚C, respectively. The main reason for this reduction is the relatively lower potential of refrigerant desorption at high condensing temperature.

Figure 3-39 (B) shows insignificant reduction in the SDSP of the current system of 1% and 3% by increasing the condensing temperature form 17.5˚C to 20˚C and 22.5˚C, respectively. However, significant reduction in the SDWP of 6% and 44.4% could be seen from Figure 3-39 (B) by increasing the condensing temperature form 17.5˚C to 20˚C and 22.5˚C, respectively. The reason for the significant reduction in the SDWP is that the rate of condensation is relatively low at high condensing temperature.

Figure 3-39 (C) also shows significant reduction in the COP of the single bed adsorption system of 29% and 62% by increasing the condensing temperature form 17.5˚C to 20˚C and 22.5˚C, respectively. The same trend was theoretically found by Allouhi et al (2016) [29] with COP of 0.135 obtained at 24 ˚C but at higher evaporation temperature of 5 ˚C. The main reason of this significant reduction is that the low rate of condensation caused by the low amount of desorbed refrigerant, which leads to decreasing the cooling effect in the evaporator during the evaporation-adsorption process.

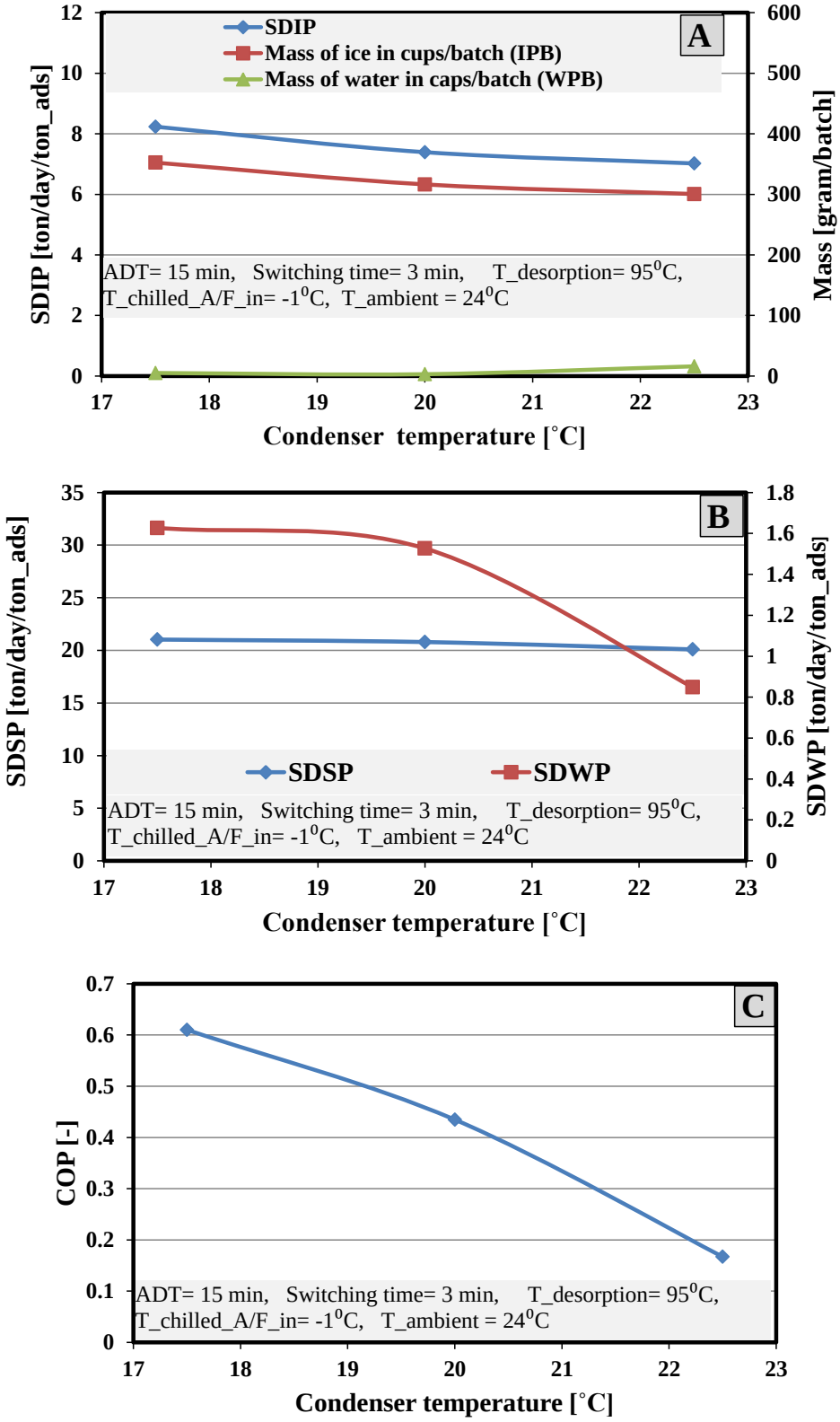

Figure 3-39 Effect of condensing temperature on the (A) SDIP, (B) SDSP and SDWP and (C) COP of the single bed adsorption refrigeration system

3.8 Summery

A detailed description of the single bed adsorption system for multi output applications has been given in this chapter by describing all components of the test facility and explaining the procedure used to carry out the performance testing. The performance of the single bed adsorption system has been experimentally investigated in terms of production of ice, cooling, ice slurry and distilled water. A parametric study has been experimentally investigated to determine the optimum operating conditions for best multi outputs production. Therefore, seven parameters have been investigated in this chapter, namely, volume of potable water and water salinity in the evaporator, cycles number, switching time, adsorption/desorption time, desorption temperature, antifreeze temperature and condensing temperature. Using 2000 mL of seawater with salinity of 35000 ppm, the optimum number of ice cups is 16 cups (480 ml of potable water). The optimum number of cycles, switching time and adsorption-desorption time are 3 cycles, 3 min and 15 min, respectively. It is concluded that the single bed adsorption ice making system could achieve maximum SDIP of 8.2 ton/day/ton of adsorbent which is 3.15 times higher than the maximum value produced by Wang et al (2001) [13]. There is a significant enhancement in the SDWP (26%) and COP (39%) by increasing the desorption temperature from 88 ˚C to 93 ˚C. The optimum evaporation temperature is -1 ˚C based on the salinity of seawater of 35,000 ppm.

CHAPTER 4

Experimental Study of Two Bed Adsorption System Using CPO-27(Ni) with Potable and Saline Water as a Working Pair

4.1 Introduction

This chapter provides a detailed description of the whole components of the automated two bed adsorption cooling system using CPO-27(Ni) MOF material and potable-saline water as a working pair. The aim of this experimental work was to practically investigate the potential of using adsorption system to produce multi-outputs including ice, desalinated water, ice slurry and cooling. The overall performance of two bed adsorption system at low evaporation temperature below 0˚C was evaluated at different operating conditions in terms of daily production of ice, ice slurry and desalinated water, in addition to cooling. The two bed system offers a continuous adsorption system as opposed to the intermittent operation of the single bed system. Therefore, it was built to investigate the potential of enhancing the performance of multi outputs in terms of SDIP, SDSP, SDWP and cooling, compared to the single bed adsorption system in described Chapter three.

4.2 Description of the Test Facility

Two-bed adsorption system for multi-outputs production was developed as a fully automated system to investigate the performance of the test facility using CPO-27(Ni) and potable-saline water as a working pair. Schematic and pictorial diagrams of the test facility are shown in Figure 4-1 and Figure 4-2. The test facility consists of two adsorber beds, a condenser and an evaporator. The adsorber beds adsorb and desorb the refrigerant therefore,

they should connect with the evaporator and condenser, respectively. To extract or supply the heat load of the various components of the system, heating and cooling water systems, mains water supply and a chiller were connected as alternative components with each of the adsorber beds, the condenser and evaporator, respectively. Each adsorber bed consists of a steel shell and plate to which two heat exchangers packed with an adsorbent material of CPO-27Ni are fitted.

The heating or cooling water circulate through the tubes of heat exchanger using two pumps to heat up or cool down the adsorbent material during the desorption or adsorption processes, respectively. Four automated valves are automatically controlled by control board operated using Lab View software to manage the flow of heating or cooling water for each adsorber bed based on the desorption or adsorption processes. The mains water and chilled water/antifreeze circulate through the coils of the condenser and evaporator to absorb and add heat during the condensation and evaporation processes, respectively. Regarding the refrigerant vapour lines, the adsrber beds are alternately linked with the condenser and the evaporator using four vacuum valves (9 – 12) controlled using four automated actuators to open and close at certain times. In order to evacuate the main components from air, they were connected to the vacuum pump using manifold with eight manual vacuum valves to make sure that the evacuation process of each component could be carried out separately.

Many measuring instruments were fitted to the main components at different locations to measure their pressure and temperature variation with time. Four flow meters are fitted in the heating, cooling, mains water and water/antifreeze circuits for measuring the mass flow rate of circulated fluids. All pressure transducers and thermocouples in the system were

connected to a computer using a data logger connected to personal computer to monitor and save the temperature and pressure readings to be used for evaluating the system performance.

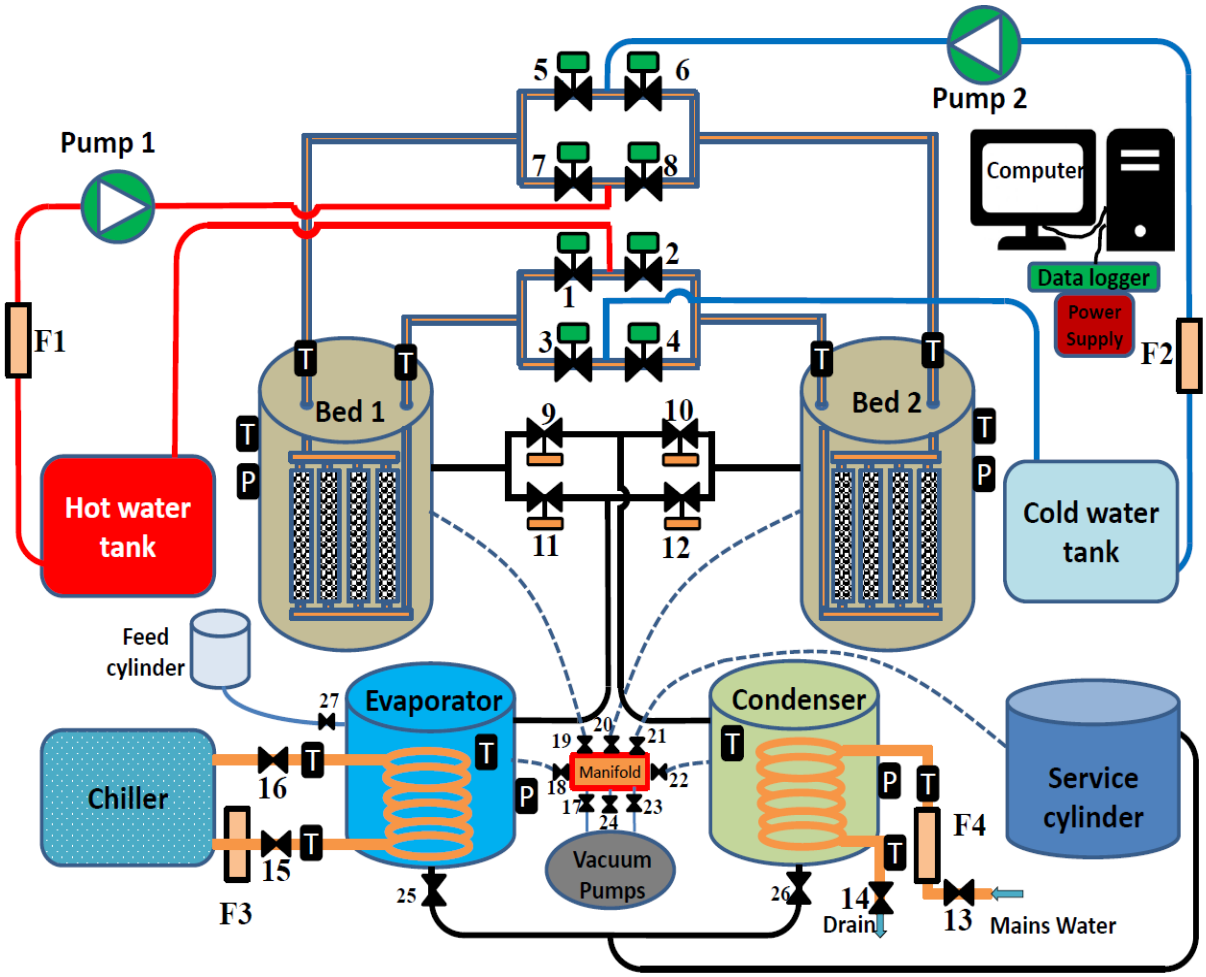

Figure 4-1 A schematic design of the two-bed adsorption of multi-output application

Figure 4-2 Pictorial view of the two-bed adsorption system

4.2.1 Adsorber beds

Two identical adsorber beds are constructed and used in the test facility, which form the chemical compressor that circulates the refrigerant in the cooling system. Each adsorber bed consists of a steel cylinder, a plate and two heat exchangers as shown in Figure 4-3.

4.2.1.1 Cylinders

The cylinder was designed with nominal diameter of 330mm and height of 600mm. Based on refrigerant vapour, the adsorber beds were connected with the measurement instruments, vacuum line, the condenser and the evaporator. Two pairs of KF flanges with diameters of 40mm and 25mm were welded on the side wall of the cylinder to enable connecting the cylinder to various devices thus level achieving the required vacuum.

4.2.1.2 Plate

The plate was machined with eight holes to connect the heating/cooling water pipes with the two heat exchangers using straight compression fittings on both sides of the plate (see Figure 4-3). On the upper side, the straight fittings are connected to manifolds of copper tubes (see Figure 4-3) via compression fittings. The seal the plate was fitted to the cylinder using 18 * M10 bolts and a rubber O-ring thus ensuring good vacuum sealing.

4.2.1.3 Heat exchangers

Each adsorber bed was fitted with two heat exchangers. Each heat exchanger was formed of six copper tubes which pass through rectangular thin fins of aluminium. The copper tubes are connected together at both ends by welding two rectangular headers of copper tubes to serve as the inlet and outlet of the heating/cooling water as shown in Figure 4-3. The spaces between the fins and the copper tubes were filled with 585grams of the CPO-27Ni per heat exchanger. Both adsorber beds were provided with four heat exchangers with a total of 2340 grams of the CPO-27Ni material. The adsorber beds were insulated using a fully flexible sheet of black Nitrile Rubber with thickness of 25mm and thermal conductivity of 0.037 W/m/K at 20˚C to reduce the heat losses to the surrounding.

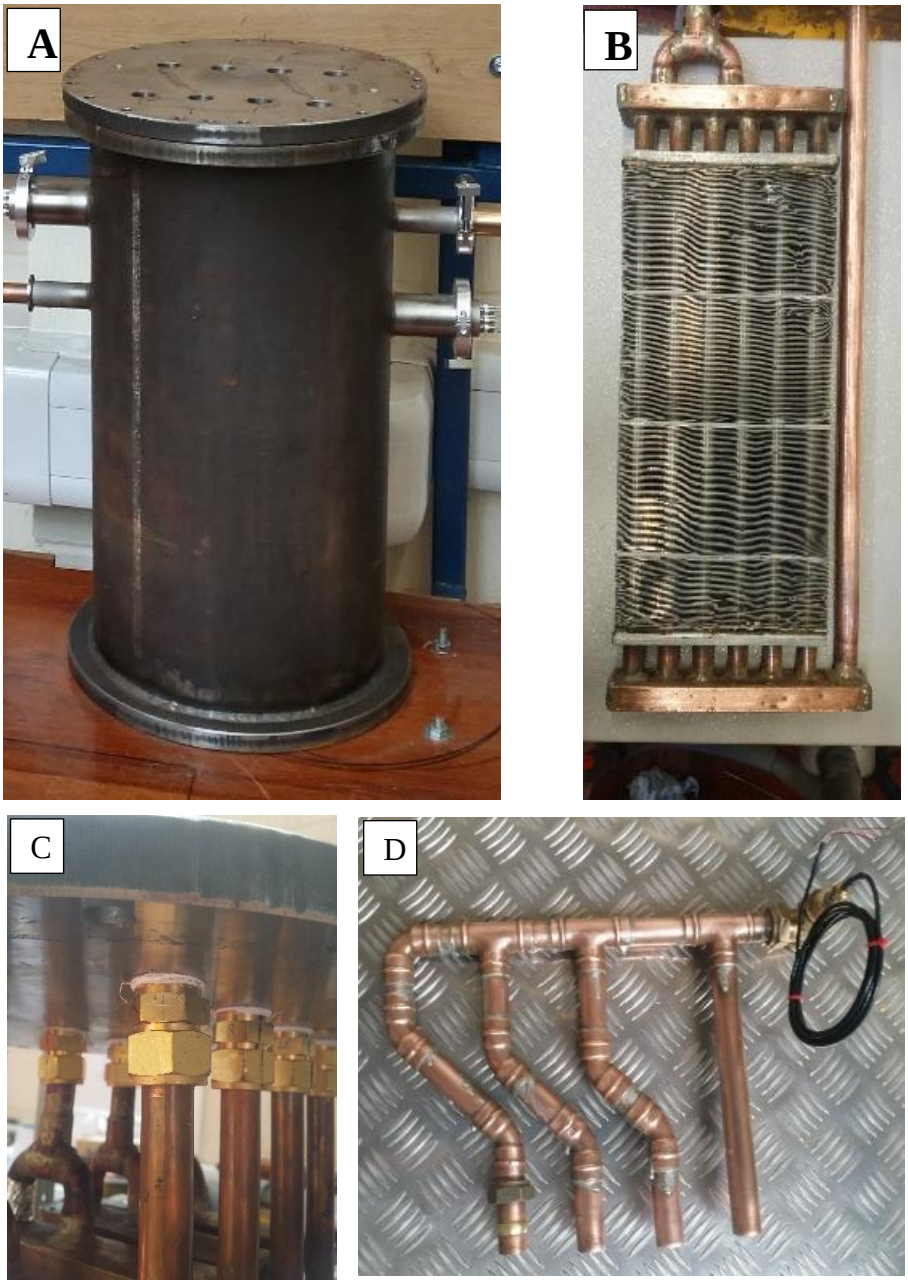

Figure 4-3 Components of the adsorber beds (A) Steel shell and plate, (B) Heat exchanger, (C) straight fitting on bottom side of plate, (D) Manifold

4.2.2 Condenser

The condenser in this test facility consists of a stainless-steel shell, a transparent led and a coil as shown in Figure 4-4. The shell with diameter of 320mm and height of 340mm was connected to the asdorber bed, evaporator, mains water inlet & outlet, vacuum pump and

measuring instruments, using six holes machined in the shell wall. To ensure achieving appropriate sealing of the condenser, KF flanges were welded at three positions to connect the vapour line, vacuum line and feedthrough thermocouples. The base of the shell is formed as a concave shape to ensure that the condensate refrigerant can be drained effectively through a stainless steel fitting connected to the centre of the base. During the condensation process, the liquid refrigerant is collected in the concave base as distilled water which could be collected at the end of each run by opening the valve which was fitted at the concave base. The inlet and outlet of mains water line are connected to the coil to absorb the heat of condensation. In order to avoid the condensate drops from upper tubes fall on the lower part of the coil, it was formed as a cone shape using 10 m long copper tube with diameter of 8mm (see Figure 4-4). Two hollow cone coils with different diameters were fitted in the condensers shell. The transparent led was used to enable observation of the condensation process. In order to reduce any heat transfer through the shell walls, the stainless-steel shell was insulated using black Nitrile Rubber with thickness of 25mm as shown in Figure 4-2.

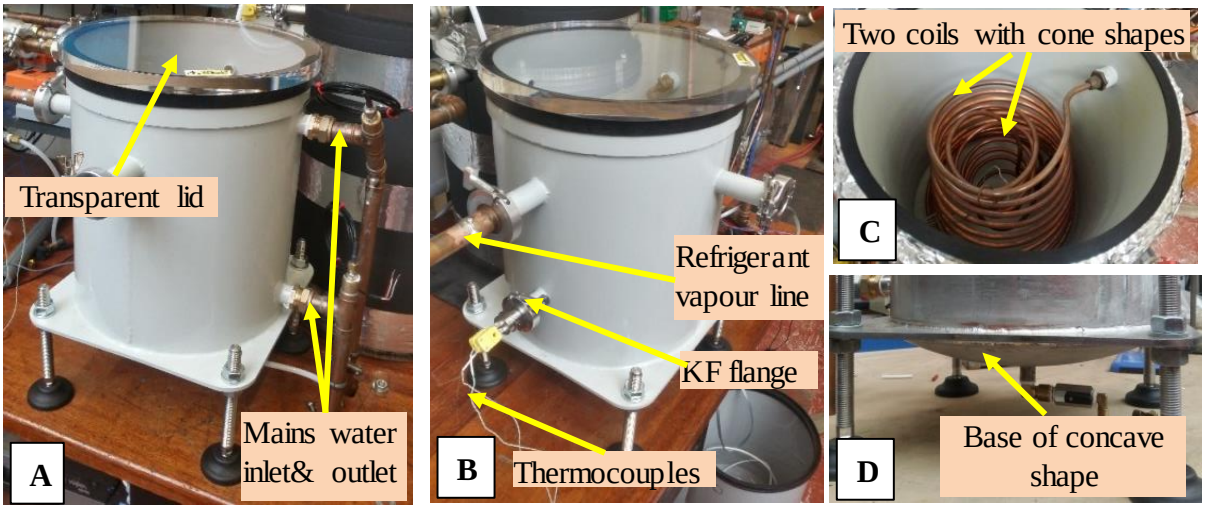

Figure 4-4 Condenser (A) Mains water inlet & outlet (B) Vapour line and KF flange (C) Coils (D) Base

4.2.3 Evaporator

The evaporator was constructed in similar manner to that of the condenser using stainless steel shell, transparent lid and a copper tube coil as shown in *Figure 4-5*. However, the tube coil was made as two layers of spiral coils fitted at the base of the shell to make sure that coils are immersed in the refrigerant liquid for better heat transfer. A copper tube of 8mm diameter and 10m long is used to form the two coils. The coils are connected to the chiller to circulate water/antifreeze through the coil to simulate the supplied load and control the evaporator operating temperature and pressure. Regarding the vapour side, the evaporator is alternately connected with one adorber bed to enable continuous adsorption process. The evaporator is charged with saline water which acts as a refrigerant and used to produce ice slurry. Also, stainless steel cups with volume of 33mL each (see *Figure* 4-6) filled with potable water for producing ice were immersed in the saline water refrigerant. Temperature and pressure measuring instruments are fitted in the evaporator using KF fitting.

Figure 4-5 Evaporator

Figure 4-6. Stainless steel cups

4.2.4 Service cylinder

A steel cylinder with diameter and height of 320 and 340mm, respectively (see Figure 4-2) was used in the test facility to collect the distilled water from the condenser or the brine water and molten slurry ice from the evaporator using the manual valves fitted on the concave bases of the condenser and the evaporator. The service cylinder was only used at the end of each test. The condenser and the evaporator were pressurized to the atmospheric pressure during the collection processes to ensure the pressure inside the service cylinder in lower than that of the evaporator or condenser.

4.2.5 Chiller, heating/cooling water systems and pumps

The chiller and the heating/cooling water systems in the test facility were described in section 3.2.4 and 3.2.6, respectively. Heating and cooling water are circulated through the adsorber beds using two centrifugal pumps MXHM 203E from Calpeda (see *Figure 4-7*) fitted in-line with heating and cooling water tanks. The pump capacity was chosen based on the systems pressure losses where the required maximum mass flow rate of a single pump is 25 L/min.

Figure 4-7 Water pump

4.2.6 Condenser cooling water

The condenser was cooled using mains water to extract the heat of condensation. The mains water line was connected to the inlet of the condenser's coil while the outlet of the coil was connected to the drain. During experimental tests, the temperature of mains water was monitored to ensue steady temperature values with minimum variation.

4.2.7 Motorized valves

Eight motorised-ball valves (typeCWX-25S from TOFINE Group CO.), as shown in Figure 4-8, are fitted in the system as shown in Figure to direct the heating and cooling water to and from the adsorber bed. Four valves are fitted in the supply line to circulate the heating/cooling water to the adsorber beds, while the remaining four valves are used in the return line to circulate the heating/cooling water from the adsorber beds. All the motorized valves are controlled using Lab View and control board (NI 9482).

Figure 4-8. Motorized- ball valve

4.2.8 Actuators-vacuum valves

Four ball valves (see Figure 4-9) were fitted in the refrigerant vapour lines connecting the adsorber beds with either the condenser or the evaporator. The ball valves were fully automated to open or close via shaft adapter using actuators with 90˚ turn. The actuators (LM24A from Belimo) as shown in Figure 4-9 were electrically controlled by the control board which in turn is activated using Lab View.

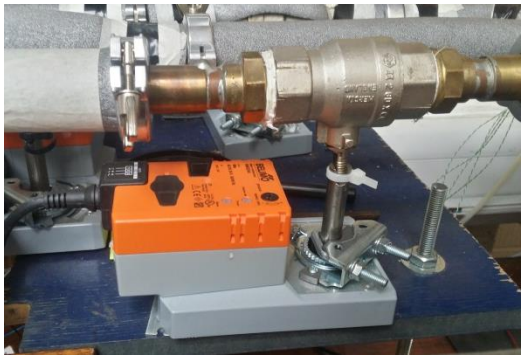

Figure 4-9 Vacuum-ball valve and automated actuator

4.2.9 Vacuum pump

An oil lubricated vacuum pump (type LC. 106 with capacity of 2.2 kW) as shown in Figure 4-10 is used to maintain the pressure inside the components of the test facility at the

same initial vacuum condition. The vacuum pump is required during preparation period to initiate the system operation. The vacuum pump was connected to manifold to enable vacuuming the various components of the system either individually or collectively, where there is a vacuum valve to connect to each of the main components.

Figure 4-10 Vacuum pump

4.2.10 Measuring instruments

Many measuring devices were used to determine the performance of the test facility including temperature, pressure and flow rates sensors. The collected data of temperature and pressure is saved in the data logger to be used in the calculation of the system performance. A detailed description of the various measuring devices used and their position in the test facility is given in the following section.

4.2.10.1 Thermocouples

Two types of thermocouples are used in the test facility. Ten Platinum RTD probes from Omega Ltd (see Figure 4-11) with an accuracy of ±0.5 ˚C are fitted at the inlet and outlet of

the heating/cooling fluids to the adsorber beds, the condenser's coil and the evaporator's coil to measure the temperature of the circulated water through them. Also eight Type K thermocouples (see Figure 4-12) were fitted in the adsorber beds to measure the temperature of adsorbent material at two points, refrigerant vapour and the cylinder's wall. Other four Type K thermocouples are fitted in the condenser and the evaporator to measure the vapour and liquid temperature of the refrigerant. All type K thermocouples are connected to the data logger using the thermocouples, feedthrough (see Figure 4-12) with KF flange which are recommended for vacuum applications.

Figure 4-11. RTD thermocouple

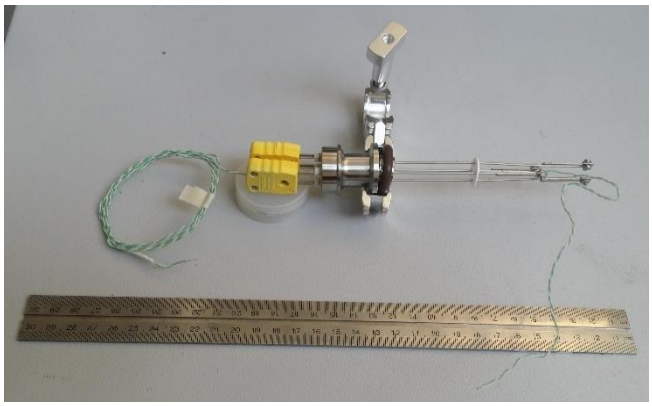

Figure 4-12. Type K thermocouples with KF feed through

4.2.10.2 Pressure Transducers

Four pressure transducers from Omega (PXM319-0.35AL from OMEGA®) (see Figure 4-13) are fitted in the adsorber beds, the condenser and the evaporator to measure the refrigerant pressure. The operating pressure of the transducers is from 0 to 350 mbar corresponding to current output ranging from 4 to 20 mA with accuracy of ±0.25%. The pressure transducers were activated with DC voltage of 15 to 30 volt using XKTtsueecrr 24 Volt power supply and connected with the data logger to save the data via the computer.

Figure 4-13 Pressure transducer

4.2.10.3 Data Acquisition

The same data taker which was used in the single bed system (section 3.2.9.3) is used in the current test facility to collect the signals from all thermocouples fitted in the system. The software of data taker was setup to identify the various thermocouples based on their type and measured parameter based on the types of thermocouples. The signals of the pressure transducers are logged using a Pico Logger 1012 voltage data logger (see Figure 4-14) with voltage rate of 0-2.5 V and accuracy of 0.5% @12 bits. Four resistances of 100 ohm each are fitted in the electrical board of the PicoLogger in order to convert the transducer current output to volt signal as required by the PicoLogger. The PicoLogger was connected with the computer via USB to monitor and save the measured data.

Figure 4-14 Pico Log

4.2.10.4 Control board

Two electromechanical relay (NI 9482 and NI cDAQ-9174 from National Instrument Company) as shown in Figure 4-15 were used to control the automated valves and the actuators used in the test facility. This control board is activated using a program developed in LabView environment.

Figure 4-15 Control board

4.2.10.5 Flow meters

Four flow meters are fitted in the test facility to measure the flow rate of the heating and cooling water through the heat exchangers of the adsorber beds, the mains water through the condenser's coil and the water/antifreeze through the evaporator's coil. Regarding the

circulated water through the adsorber beds, two of FLC-W14 flow meter from OMIGA® (see Figure 4-16 (B)) with scale from 0 to 57 LPM and accuracy ±5% were used. The other two flow meters are of Parker PET flow meters (see Figure 4-16 (A)) with scale of 2 to30 LPM and accuracy of ±5% were installed at the inlet of the condenser and the evaporator.

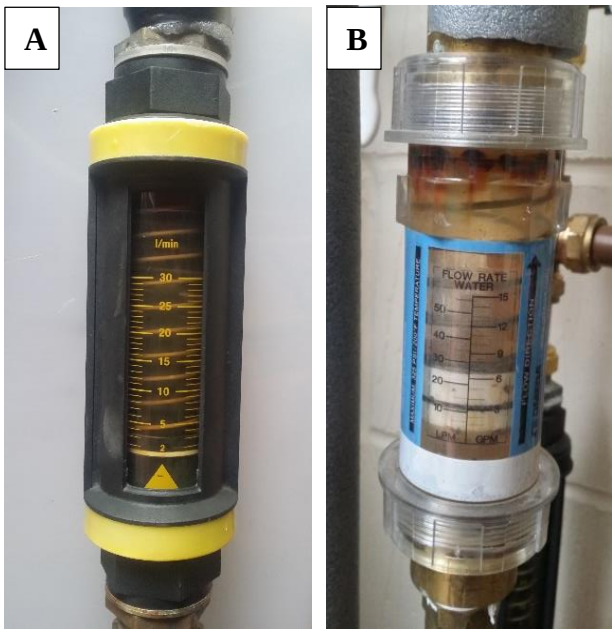

Figure 4-16 Flow meter (A) Parker and (B) Omega

4.2.10.6 Scale and measuring cylinder

A scale was used to weight the mass of ice collected from the evaporator after each run. The measuring cylinder was used to measure the volume of distilled water, brine water and molten ice slurry separately.

The all measuring instruments used in the two bed system were calibrated using the same method in section 3.3 to determine the absolute their uncertainties as shown in Table 4.1.

Table 4.1 Uncertainties of the all thermocouples, pressure transducers and balance of the double bed adsorption system

	Item Name		Number	Location	Curve fit formula	Absolute Uncertainty
Double Bed System	**Temperature - Thermocouples**	**Type K**	T-1	Bed1/heatexchanger/ Middle	0.9992* T_{ref} + 0.0756	±0.34˚C
			T-2	Bed1/heatexchanger/ Bottom	0.9984* T_{ref} + 0.3155	±0.44˚C
			T-3	Bed1/ vapour	0.9954* T_{ref} + 0.3141	±0.39˚C
			T-4	Bed2/heatexchanger/ Middle	0.9996* T_{ref} + 0.1244	±0.40˚C
			T-5	Bed2/heatexchanger/ Bottom	0.9991* T_{ref} + 0.286	±0.39˚C
			T-6	Bed2/ vapour	0.9982* T_{ref} + 0.5613	±0.45˚C
			T-7	Evaporator/ liquid refrigerant	0.999* T_{ref} + 0.5628	±0.31˚C
			T-8	Evaporator/ vapour refrigerant	1.0004* T_{ref} - 0.0022	±0.31˚C
			T-9	Condenser/ liquid refrigerant	0.9986* T_{ref} + 0.2881	±0.4 ˚C
			T-10	Condenser/ vapour refrigerant	0.9975* T_{ref} + 0.1942	±0.4 ˚C
		RTD	T-11	Bed1/ inlet water-heat exchanger	0.9782* T_{ref} + 1.7507	±0.53 ˚C
			T-12	Bed1/ outlet water-heat exchanger	0.9988* T_{ref} - 0.0978	±0.49˚C
			T-13	Bed2/ inlet water-heat exchanger	0.9989* T_{ref} - 0.0896	±0.44˚C
			T-14	Bed2/ outlet water-heat exchanger	0.989* T_{ref} + 0.6352	±0.48˚C
			T-15	Evaporator/ Inlet antifreeze-coil	0.9939* T_{ref} + 0.4948	±0.47˚C
			T-16	Evaporator/ outlet antifreeze-coil	0.9961* T_{ref} + 0.352	±0.45˚C
			T-17	Inlet water- condenser coil	0.9983* T_{ref} + 0.1519	±0.41˚C
			T-18	outlet water- condenser coil	0.9955* T_{ref} + 0.7703	±0.35˚C
	Pressure Transducer		P-1	Bed 1	0.9902*P_{ref} + 1.714	±1.95 mBar
			P-2	Bed 2	0.999*P_{ref}+ 1.027	±1.18 mBar
			P-3	Condensar	0.9997*P_{ref}+ 0.144	±0.5 mBar
			P-4	Evaporador	1.0036*P_{ref} + 0.5134	±1.5 mBar
	Balance				0.9977*m + 3.4408	±0.08g

4.3 Experimental testing

Once the test facility was constructed and all measuring devices were fitted, commissioning processes were undertaken to ensure that all components can operate at the required condition.

4.3.1 Leakage test

The system was designed for operating at pressure below atmospheric one. Therefore, to ensure that there are no leakages through the numerous fittings on the refrigeration flow circuit, a comprehensive procedure was followed for leakage testing using the methods described in section 3.3.1. After sorting out all leakages in the system, each of the adsorber beds, the condenser and evaporator was connected to vacuum pump separately and evacuated to 2 mbar at 24 ˚C and the pressure monitored for 24 hours to make sure that there is a negligible increase in the pressure (±2 mbar).

4.3.2 System preparation procedure

Once the test facility is ready for testing, a preparation procedure is preferred before each run to ensure the same starting conditions as follows:

1. Fill the heating and cooling water tank with water and wait until the water level reaches the desired level.
2. Switch on the heaters and adjust the heater thermostat to the required desorption temperature.
3. Switch on the computer and run the LabView software using the preparation mode to open the solenoid valves 1, 2, 7 and 8 to prepare the adsorber beds for drying process.

4. Switch on pump 1 of heating water tank to circulate the hot water in the adsorber beds.
5. In order to track the temperatures and the pressure in the test facility, activate the data taker and PicoLogger software's and wait until the temperatures of the adsorber beds reaching to maximum value.
6. Switch on the vacuum pump, and then open valves 17, 18, 21 and 22 to remove any water vapour that is inside the adsorber beds. Based on the initial conditions, the drying process will be stopped once the temperature and the pressure reach 95˚C and 15 mbar, respectively.
7. Close valves 17, 18, 21 and 22 to isolate the adsorber beds from the vacuum pump then switch off the vacuum pump.
8. Cover the condenser with the transparent lid, and then open valves 13 & 14 to circulate the mains water through the condenser's coil.
9. Switch on the vacuum pump and open valves 17, 22 and 23 to vacuum the condenser.
10. Once the pressure in the condenser reaches 12 mbar at temperature of 10^{o}C, close the valves 17, 22 and 23 and then switch off the vacuum pump.
11. Fill the feed cylinder with 1100 ml of refrigerant then open valve 27 for a short time to make sure that there is no air in the connecting tube between the feed cylinder and the evaporator.
12. Repeat tasks 8 to 11 but for the evaporator by opening the valve 18 instead of 22, and the valves 15& 16 instead of 13 & 14 to circulate the water/antifreeze through the evaporator's coil after switching on the chiller at the required temperature.

13. Gently open valve 27 to feed 1000 ml of refrigerant from the feed cylinder to the evaporator and avoid generating a vortex during the feeding task to avoid any air comes inside the evaporator, and then close valve 27.
14. Refill the feed cylinder with 1000 ml of refrigerant.
15. Repeat task 14.
16. Repeat tasks 15 and 16 until reaching the required level of refrigerant and submerging the evaporators coil with refrigerant (around 3 litres).

4.3.3 Operating procedures

After the preparation procedure, the test rig is ready for performance testing as follows:

1. Set the thermostat of the chiller and the hot water tank on the desired temperature.
2. Switch on Pump 1 and Pump 2.
3. Open valves 13 and 14 to circulate the mains water to the condenser.
4. Start the LabVIEW operation mode to operate Bed 1 and Bed 2 in desorption and adsorption modes, respectively. Accordingly, valves 1, 4, 6 and 7 should be automatically opened to circulate the heating and cooling water in Bed 1 and Bed 2, respectively.
5. Set the LabVIEW on the desired switching time, adsorption-desorption time and number of cycles to start the operation mode.
6. Run the LabVIEW program.
7. The first operation mode is the switching mode which automatically starts by closing valves 1, 4, 6 and 7 and simultaneously open valves 2, 3, 5 and 8 for connecting Bed 1 and Bed 2 with the cooling and heating water systems to cool down and heat up, respectively.

8. At the end of switching time, the second operation mode is adsorption-desorption which starts by automatically opening valves 10 and 11 to connect refrigerant vapour lines from Bed 1 and Bed 2 to the evaporator and the condenser. Therefore, the refrigerant vapour will flow from the evaporator to adsorber bed 1 and from adsorbed bed 2 to the condenser during the evaporation-adsorption and desorption-condensation processes, respectively.
9. The third operation mode is switching time of desorption/adsorption which starts at the end of the second operation mode. Adsorber bed 1 and adsorber bed 2 are connected with the heating and cooling water systems to heat up and cool down during the switching time, respectively. Accordingly, valves opened in tasks 7 and 8 will be closed and valves 1, 4, 6 and 7 will be simultaneously.
10. At the end of the third operation mode, the fourth operation mode (desorption-adsorption) automatically starts by opening valves 9 and 12 to move the refrigerant vapour to and from the condenser and the evaporator during the desorption-condensation and evaporation-adsorption processes, respectively.
11. Tasks from 7 to 10 are repeated based on the number of cycles.
12. At the end of last cycle time, all valves close.
13. Save all temperatures and pressure data from data taker and PicoLogger.
14. Make sure to switch off the chiller, the heater, Pump 1 and Pump 2 and then close the valves 13, 14, 15 and 16.

4.4 Results

The measured temperature, pressure and flow rate data were used to analyse the system performance based on the production of ice, ice slurry, distilled water and cooling. The

method of calculating the Specific Daily Ice Production (SDIP), Specific Daily Ice Slurry Production (SDSP) and Specific Daily Water Production (SDWP) and the System cooling coefficient of performance (COP) were described in Chapter 3 section 3.6. Different parametric including number of cycles, switching time, adsorption/desorption time, mass flow rate of heating & cooling water and water/antifreeze temperature were investigated to determine the optimum operating conditions for the two bed adsorption system using CPO27(Ni) to produce several outputs.

4.4.1 Number of cycles:

The number of cycles is a vital parameter that affects the performance of the system based on the developed technique in the evaporator. Various numbers of cycles were investigated to determine the optimum value for production of ice, ice slurry, cooling and distilled water The system is operated based on batch production of the multi output from the system according to the current configuration of the evaporator. The study in this section was carried out at the operating conditions shown in Table 4.2. Figure 4-17 (A), (B) and (C) show the effect of cycle's number on the SDIP, SDWP, COP and SDSP of the two bed adsorption ice making-desalination system. Figure 4-17 (A) shows a drop in the SDIP of 17% by increasing the cycle's number from 1 to 3 due to the use of a constant volume of potable water in the stainless steel cups used to produce ice. Furthermore, the operating time of one patch increases by increasing the number of cycles which decreases the number of batches per day at the same amount of potable water in the cups. However, it can be noticed from Figure 4-17 (A) that there is an increase in the mass of ice and a decrease in the non-frozen water in the stainless steel cups. It is clear from the same figure that all the potable water in the stainless steel cups was changed to ice for the case of three cycles,

however, the evaporation process starts to deteriorate at the end of the third cycle due to the ice formation on the upper layer. Therefore, no advantage is expected to run the system with cycle's number higher than three.

Figure 4-17 (B) shows an improvement in the SDWP at average of 12.7 % per cycle by increasing cycle's number, because the adsorbent material contains a certain amount of the adsorbed refrigerant especially at the first cycle's number and then this amount decreases with the increase in cycle's number. The figure also shows a slight drop of 7.8% in the COP by increasing the number of cycles from one to two, because the adsorbent material has a potential to adsorb a relatively higher amount of refrigerant during the first cycle of evaporation-adoption process; accordingly, a slightly higher amount of cooling is produced over the first cycle which leads to higher COP. A significant increase of up to 37 % in the COP was noticed when the number of cycle changes from two to three. This is due to the increase in the cooling of the water/antifreeze due to ice formation in the saline water

Table 4.2. Initial conditions

Parameter	Value	Unit
Adsorbent mass (both generators)	2.34	kg
Desorption temperature (hot water tank)	95	°C
Adsorption temperature (mains water)	11	°C
Condenser temperature (mains water)	11	°C
Evaporator temperature (chiller)	-1	°C
Heating & cooling water flow rate (beds)	12	L/min
Cooling water flow rate (mains water-condenser)	4	L/min
Antifreeze flow rate (chiller-evaporator)	4	L/min
Adsorption/Desorption time	15	min
Switching time	3	min
Single cycle time	36	min
Volume of sea water in evaporator	3	L
Volume of potable water in stainless steel cups (evaporator)	0.48	L

refrigerant. Figure 4-17 (C) shows that the mass of ice slurry increases with the increase in the cycles number. It increased from 0.45 to 0.6 to 0.85 kg by increasing the cycle number from one to two to three, respectively. The main reason of this increase is relatively longer evaporation-adsorption time which leads to produce much amount of the ice slurry per batch. However, Figure 4-17 shows that the SDSP decreases by 24% by increasing the cycle number from one to two and by 5% by increasing the cycle's number from two to three. The main reason of this decrease in the SDSP is the number of batches per day which decreases by increasing the number of cycles at the same amount of saline water in the evaporator.

Based on the above described results, three cycles are chosen as optimum cycle number to investigate the next parametric study in order to achieve an optimum condition of the two bed ice making-desalination system.

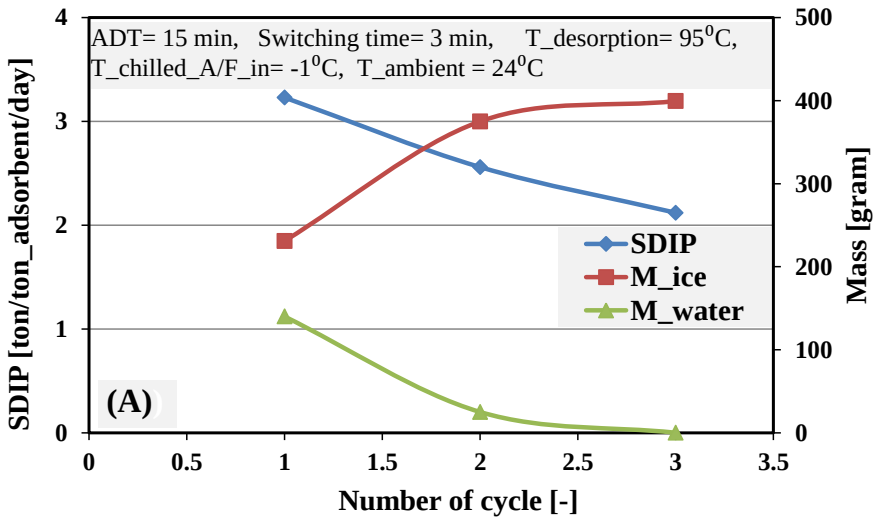

Figure 4-17 Effect of cycle's number on the performance of two bed adsorption ice making-desalination system based on the (A) SDIP, (B) SDWP and COP, and (C) SDSP

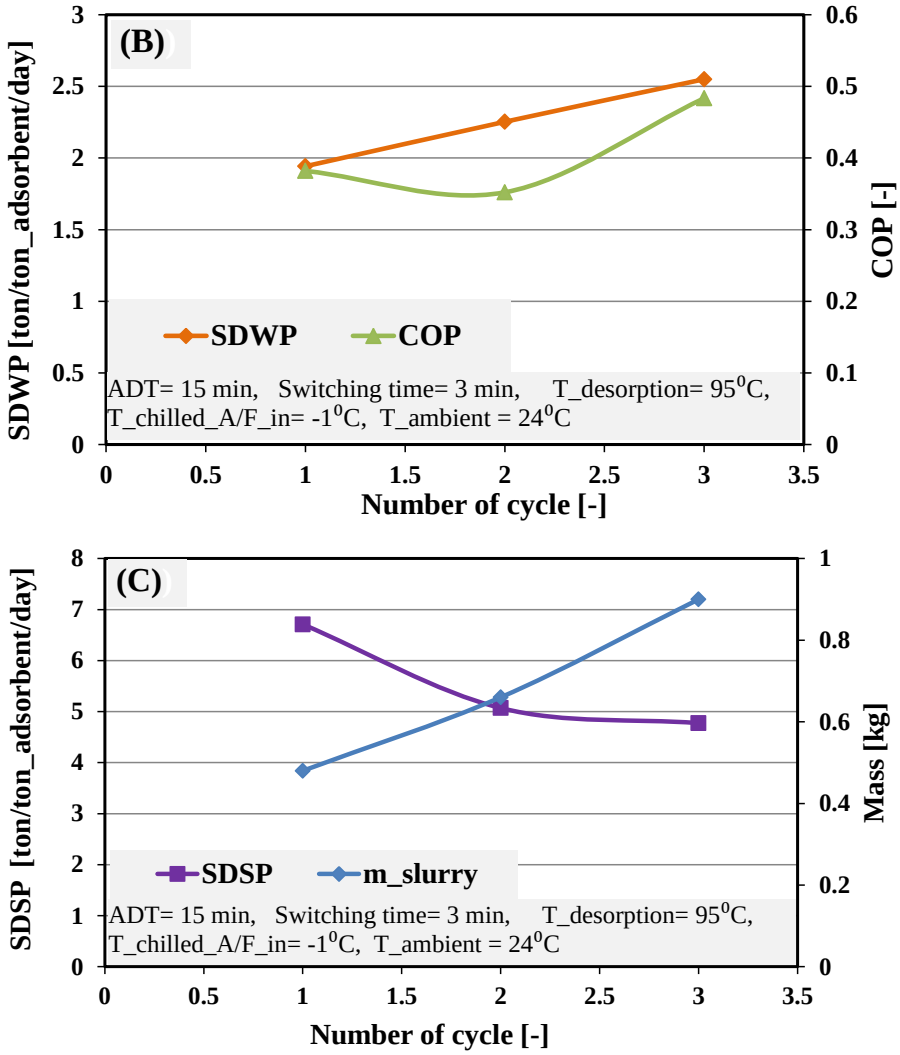

Figure 4-17 (Continued: effect of cycle's number on the performance on the (B) SDWP, COP and (C) SDSP)

4.4.2 Switching time

The switching time is an important parameter which needs to be optimised as it is needed to prepare the adsorbent materials inside the beds for the adsorption and desorption processes. The initial conditions, used in this parametric study, are listed in Table 4.2 while various switching time. Figure 4-18 (A), (B) and (C) show the effect of the switching time on the performance of the two bed adsorption ice making-desalination system in terms of the SDIP, SDWP, COP and SDSP. Figure 4-18 (A) show a slight increase in the SDIP of 5%

by increasing the switching time from one to two minutes. The reason for this increase is that the adsorbent material in the beds requires a certain time for reaching the required temperature and pressure. Figure 4-18 (A) shows no significant change in the mass of ice and non-frozen water in the stainless steel due to increasing the switching time.

Figure 4-18 (B) shows an increase in the SDWP by 12.2% and 18% per one minute by increasing the switching time from 1 to 2 then from 2 to 3 minutes, respectively. This increase is because the adsorbent material adsorbs and desorbs a higher amount of the refrigerant from the evaporator and to the condenser by increasing the switching time as the cooling and heating processes will be longer, respectively. As the switching time increases from 3 to 4 minutes a rapid decrease of 41% in the SDWP is shown in Figure 4-18 (B) due to the cooling and heating processes during the fourth minute is less effective so the daily water production will be reduced by increasing the switching time more than three minutes. Figure 4-18 (B) also shows that there was an increase in the COP of 25% per a minute by increasing the switching time from one to three minutes, because the adsorbent material has a potential to absorb and desorb a higher amount of refrigerant during the adsorption and desorption processes according to longer period of pre-cooling and pre-heating, respectively, which enhances the cooling effect in the evaporator. And then there was an insignificant decrease when the switching time increased from three to four minutes. The reason for this decrease is that any increase in switching time, after the beds reaches to desire temperature and pressure, is counted as a waste time which effects on the performance of system.

Figure 4-18 (C) shows that there is no significant variation in the SDSP and the mass of slurry ice by increasing the switching time from one to two minutes, however there is a

slight increase in the SDSP and the mass of slurry ice of 6% per one minute by increasing the switching time from two to four. The main cause of this increase is the potential of high adsorbing and desorbing processes of the refrigerant with the adsorbent material by increasing the switching time.

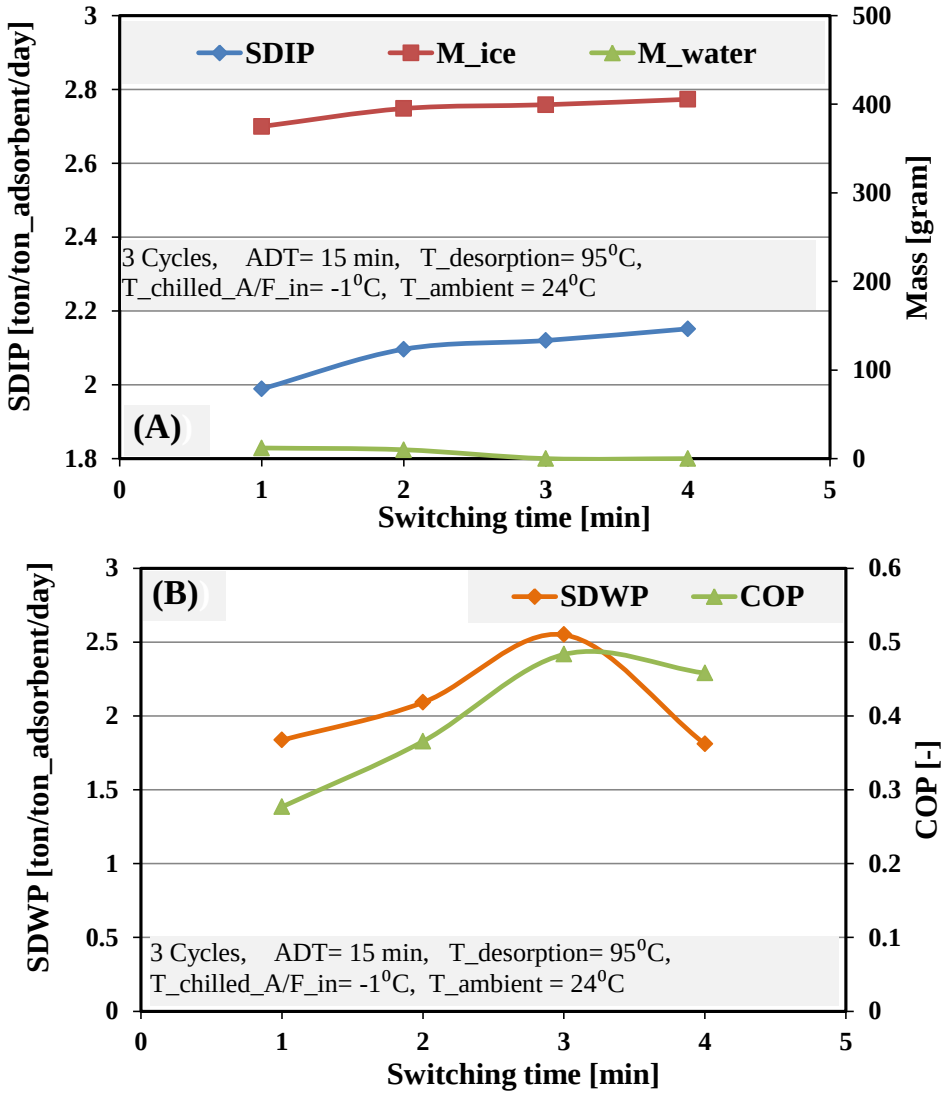

Figure 4-18 Effect of switching time on the performance of two bed adsorption ice making-desalination system based on the (A) SDIP, (B) SDWP and COP, and (C) SDSP.

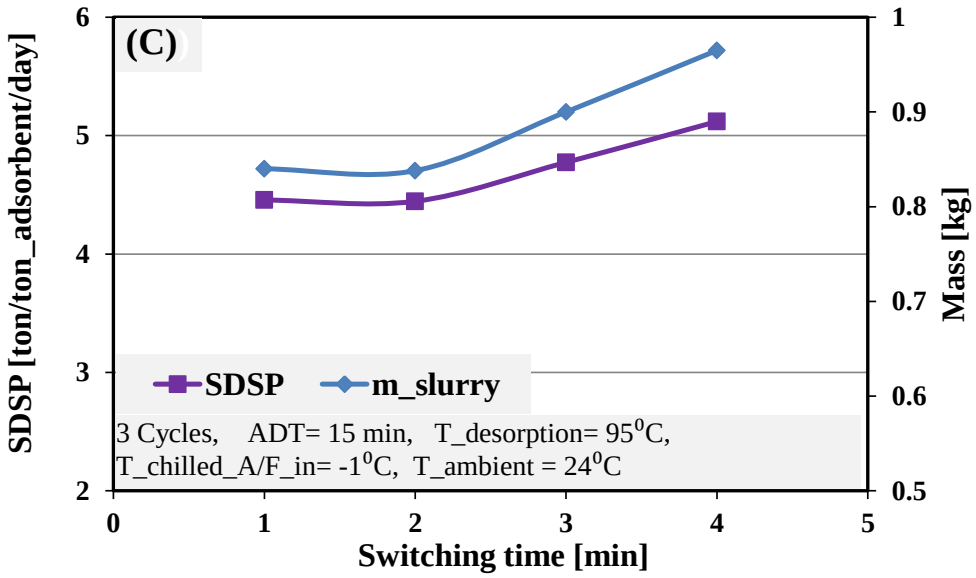

Figure 4-18 (Continued: effect of switching time on the performance on the SDSP and mass of ice slurry)

Based on the aforementioned study, the switching time of three minutes is chosen as an optimum value for any further parametric study using the current configuration of the two bed adsorption ice making- desalination system.

4.4.3 Adsorption/desorption time:

Figure 4-19 (A), (B) and (C) show the variation of the SDIP, SDWP, COP and SDSP with adsorption time. The initial conditions in table 1 were applied while five values of adsorption/desorption time varying from nine minutes up to 17 minutes to investigate the performance of the two bed adsorption ice making-desalination system. Figure 4-19 (A) shows that the SDIP increased by 3%, 8% and 19 % for each two minute increase in the adsorption/desorption time from nine to 15 minutes. This increase in the SDIP is produced by increasing the time available for adsorbent material to adsorb and desorb more refrigerant during the evaporation-adsorption and desorption-condensation processes. It could be seen also that the mass of ice is increased while the mass of non-frozen water in

the stainless steel cups decreased. There was a small decrease in the SDIP of 10% by increasing the adsorption/desorption time from 15 to 17 minutes. This decrease could be due to the fact that the ability of adsorbent material to adsorb or desorb the refrigerant starts to decrease by increasing the adsorption/desorption time based on the characterisation of CPO-27(Ni).

Figure 4-19 (B) shows an increase in the SDWP with percentage of 6.6%, 16% and 36% per two minutes by increasing the adsorption/desorption time from nine to 15 minutes. This significant increase is due to the high affinity of the adsorbent material to adsorb or desorb higher amount of the refrigerant with longer adsorption/desorption time. It could be noticed that there was a significant drop in the SDWP of 16.7% by increasing the adsorption/desorption time from 15 to 17 minutes. This increase and decrease in the SDWP due to the kinetics (as shown in Figure 2-4) of the adsorbent material to adsorb or release the refrigerant, where at the beginning of the adsorption process, the rate of adsorption is high and then it decreases when the equilibrium is approached. The figure also shows a gradual increase in the COP of the system of 20%, 14.3%, 5.3% and 2.7 % per two minutes by increasing the adsorption/ desorption time from nine to 17 minutes. This increase in the COP is because the cooling effect in the evaporator increases by increasing the adsorption time. However, it could be noticed that the rate of increase in the COP decreases by increasing the adsorption/desorption time.

Figure 4-19 (C) shows a small increase in the SDSP of 5.2%, 5.5% and 9% per two minutes by increasing he adsorption/desorption time from nine to 15 minutes. The increase in the SDSP is consistent with the increase in the mass of ice slurry as shown in the figure. The main reason of this increase in the SDSP is due to the improvement in the cooling effect

inside the evaporator by increasing the adsorption/desorption time. The SDSP reaches a steady condition with a negligible decrease of 0.3%.

Based on the above described results, the optimum adsorption/desorption time is selected as15 minutes to investigate other parameters.

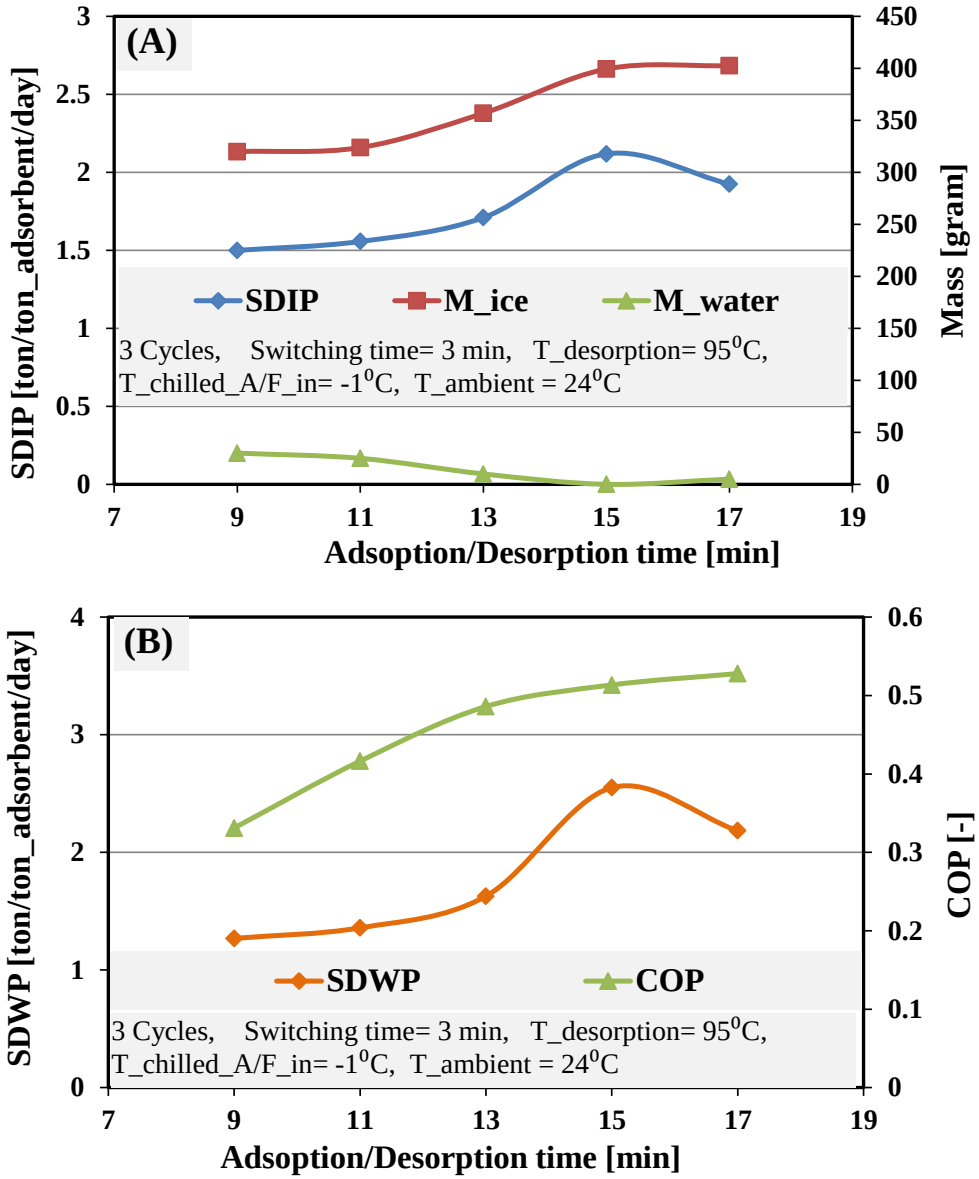

Figure 4-19 Effect of adsorption/desorption time on the performance of two bed adsorption ice making-desalination system based on the(A) SDIP, (B) COP and SDWP, (C) SDSP

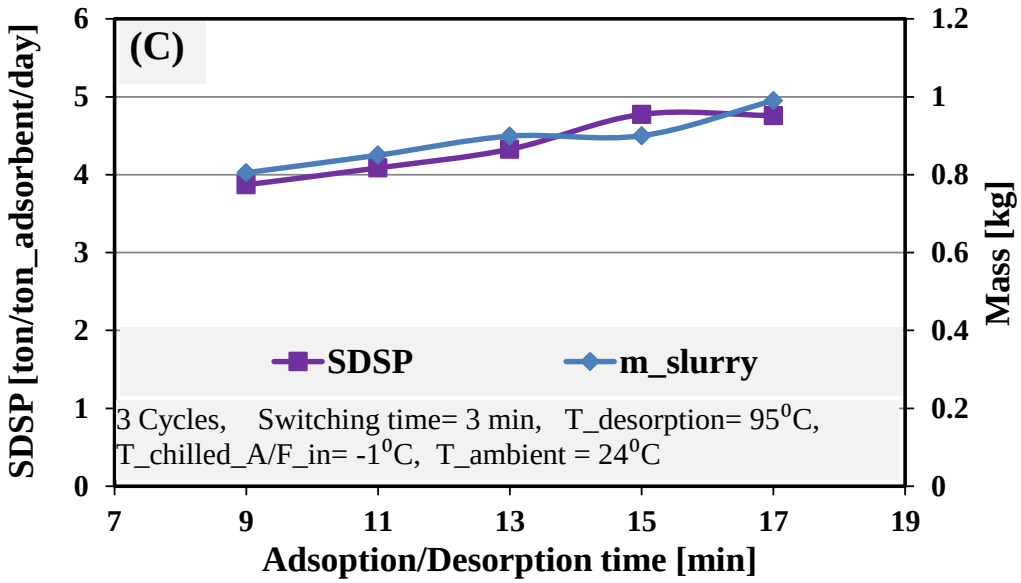

Figure 4-19 (Continued: effect of adsorption/desorption time on the SDSP).

4.4.4 Mass flow rate of heating & cooling water

Figure 4-20 (A), (B) and (C) show the effect of the heating and cooling water mass flow rate through the heat exchangers inside the adsorber beds on the performance of the two bed adsorption ice making system in term of SDIP, SDWP, COP and SDSP. The mass flow rate of circulated water is an important parameter which affects the performance of the system and needs to be optimised.

Figure 4-20 (A) shows that there is an increase in the SDIP of 8% and 17% per 4 L/min by increasing the mass flow rate of heating and cooling water from 4 to 12 L/min. This increase in the SDIP is due to the fact that the higher mass flow rate of heating and cooling water leads to increasing the heat transfer with the heat exchanger of the adsorber beds which in turn increases the adsorbed and desorbed refrigerant from the adsorbent material. This also resulted in increasing the mass ice while decreasing the mass of non-frozen water in the potable water.

Figure 4-20 (B) shows that there is an increase in the SDWP of 14.2% and 36.3% per 4 L/min by increasing the mass transfer of water from 4 to 12 L/min. The main cause of this increase is the increase in the heat transfer rate between the circulated water and the adsorbent material, which in turn allowed the adsorbent material to reach its desired conditions at shorter time. It could be also seen in Figure 4-20 (B) that there is a significant increase in the COP by 15.6% by increasing the mass flow rate from 4 to 8 L/min. This increase is due to improvement in the heat transfer which leads to physically produce high cooling effect despite the increase in a consumed heat of the current system. However, there was a considerable drop in the COP of 50% by increasing the mass flow rate from 8 to 12 L/min. This drop in the COP is due to the increases in the consumed heat in the beds is relatively higher than the increase in the cooling effect in the evaporator.

Figure 4-20 (C) shows an insignificant decrease in the SDSP and the mass of slurry ice with a maximum proportion of ±3% per 4 L/min increase in the mass flow rate from 4 to 12 L/min. The optimum mass flow rate is selected as 8 L/min based on the above described study.

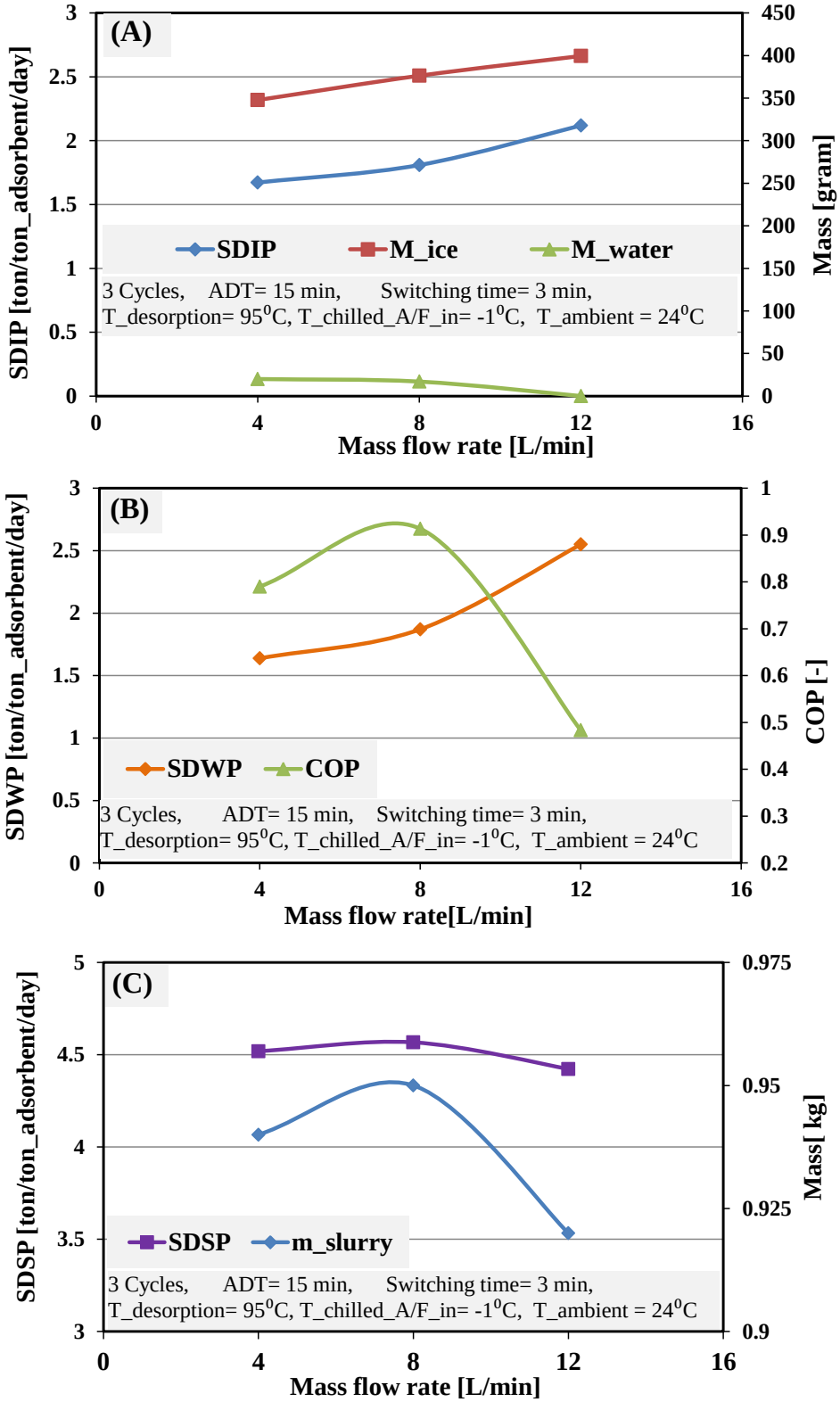

Figure 4-20 The effect of heating & cooling water mass flow rate on the performance of two bed adsorption ice making-desalination system based on the(A) SDIP, (B) SDWP and COP and (C) SDSP

4.4.5 Evaporator temperature

The evaporator temperature affects the freezing of pure water in the stainless steel cups and the ice formation in the saline water. Figure 4-21(A), (B) and (C) show the effect of evaporator temperature on SDIP, SDWP, COP and SDSP of the two bed adsorption ice making-desalination system.

Figure 4-21(A) shows that there is a drop in the SDIP of 2.3%, 24% and 9.6% per one degree increase in the evaporator temperature from -2°C to 1°C. It could be noticed that a significant drop in the SDIP occurred above -1°C which corresponds with the decrease in the mass of ice and increase in the mass of non-frozen water in the stainless steel cups. This drop in SDIP is due to the increase in the evaporator temperature which decreases the crystallization of the potable water in the stainless steel based on the freezing point of zero degree Celsius.

Figure 4-21(B) shows an increase in the SDWP of 6%, 34 % and 10% per one degree increase in the evaporator temperature from -2°C to 1°C. This increase is due to the fact that increasing the evaporator temperature increases the potential of evaporation of refrigerant in the evaporator, in turn, the adsorbent material adsorbs more refrigerant at high evaporation temperature. Therefore, the condensed refrigerant in the condenser will be higher during the desorption-condensation process at high evaporation temperature. A higher SDWP of 4 ton/day/ton of adsorbent was experimentally achieved by Alsaman et al (2016) [104] using the same desorption temperature of 95°C, however, at evaporator temperature of 30°C, compared to 2.5 ton/day/ton of adsorbent obtained using the current system at significantly lower evaporation temperature of 1°C. Figure 4-21 (B) shows also an increase in the COP of the system by 10.7%, 28.3% and 16% per one degree increase in

the evaporator temperature from -2°C to 1°C. This increase is due to the fact that the temperature drop between the inlet and outlet of water/antifreeze increases with increasing of the evaporation temperature, this in turn increases the cooling effect. The same trend was experimentally achieved by Chakaborty et al (2011) [120] with lower COP of 0.58 at desorption and evaporation temperature of 92°C and 7°C, respectively, compared to the achieved COP of 1.33 from the current system at 95°C and 1°C, respectively.

Figure 4-21(C) shows a significant decrease in the SDSP with 22.8%, 37.2% and 7% per one degree by increasing the evaporator temperature from -2°C to 1°C. This drop in the SDSP is because the operating temperature in the evaporator is higher than the freezing point of the seawater. It could be noticed that the drop in the SDSP corresponds to a significant increase in the COP (Figure 4-21(B)). This can be explained to be due to the increase in the evaporation process in the evaporator at high evaporation temperature; however, the potential to produce slurry ice decreases by increasing the evaporator temperature.

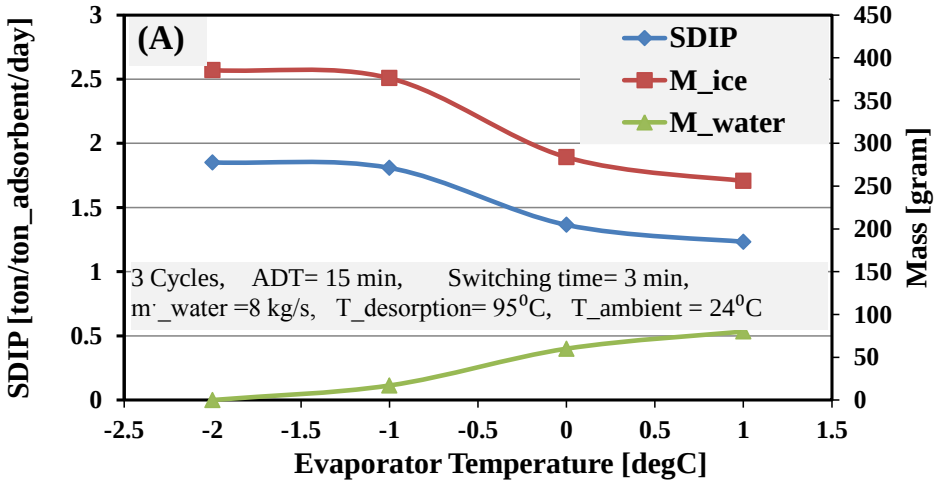

Figure 4-21 Effect of evaporator temperature on the performance of two-bed adsorption ice making-desalination system based on the (A) SDIP, (B) SDWP and COP, and (C) SDSP

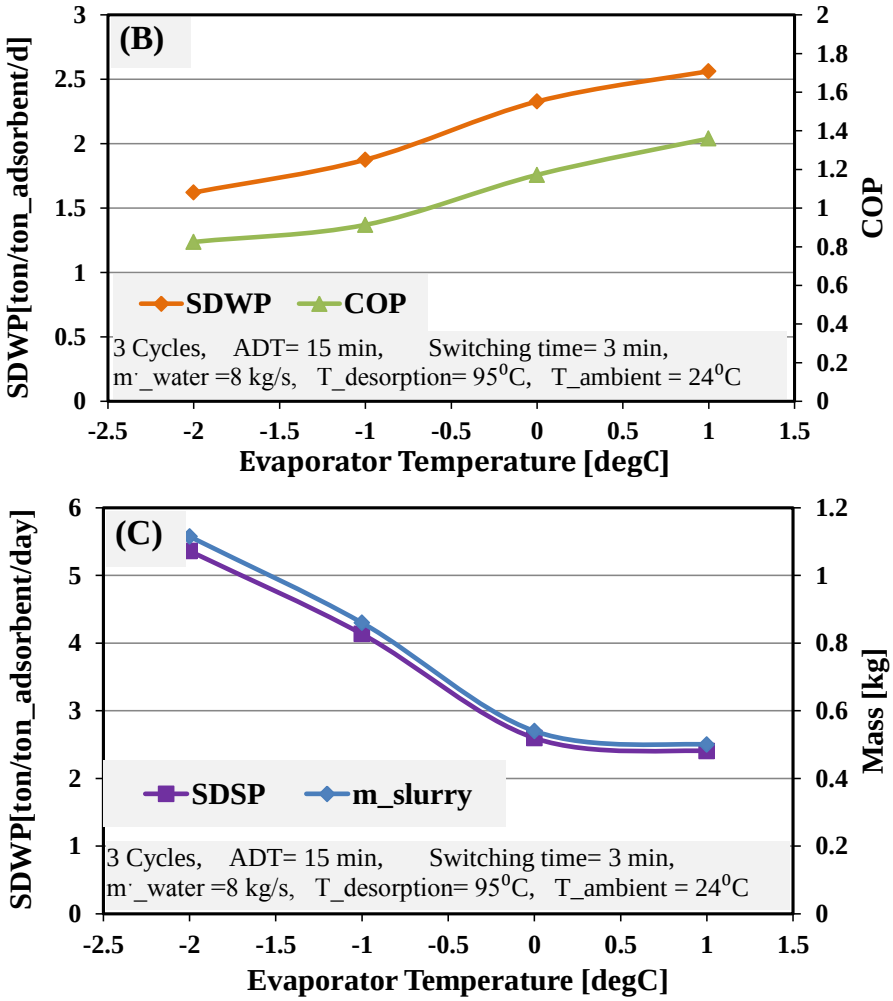

Figure 4-21 (Continued: effect of evaporator temperature on the (B) SDWP and COP, and (C) SDSP)

4.5 Results comparison with the single bed adsorption system

In order to investigate the advantage of two bed adsorption ice making system compared to the single one with multi outputs using CPO27Ni and potable-saline water as a working pair, a comparison of the various outputs for both systems in terms of producing ice, ice slurry, cooling and fresh water have been carried out in this section. The investigation was done at same conditions in terms of volume of potable water in the evaporator, desorption temperature, condensing temperature, salinity of sea water in the evaporator, ambient temperature, adsorption-desorption time and switching time.

Figure 4-22 shows that the single bed system produced a higher amount of SDIP compared to the SDIP of double bed system with an average rate of 77.4% per one degree of the water/antifreeze temperature ranging from -2°C to 1°C. This could be attributed to use the same configuration of evaporator using the same amount of potable water in the cups for the both test facilities taking in to account the design condition. However, the reductions in the SDIP between the maximum and minimum values of SDIP of the single bed adsorption system was 2.8 ton/day/ton of adsorbent by increasing the water/antifreeze temperature from -1°C to 1°C, however, it was just 0.57 ton/day/ton of adsorbent in the double bed systems. This means that the reduction in the increase of SDIP per 2°C of water/antifreeze temperature of the single bed system is about five times higher than its reduction of the double bed system. This could be explained by the fact that the cooling effect is more stable in the double bed system by increasing the water/antifreeze temperature from -2°C to 1°C despite the high SDIP of the single bed system.

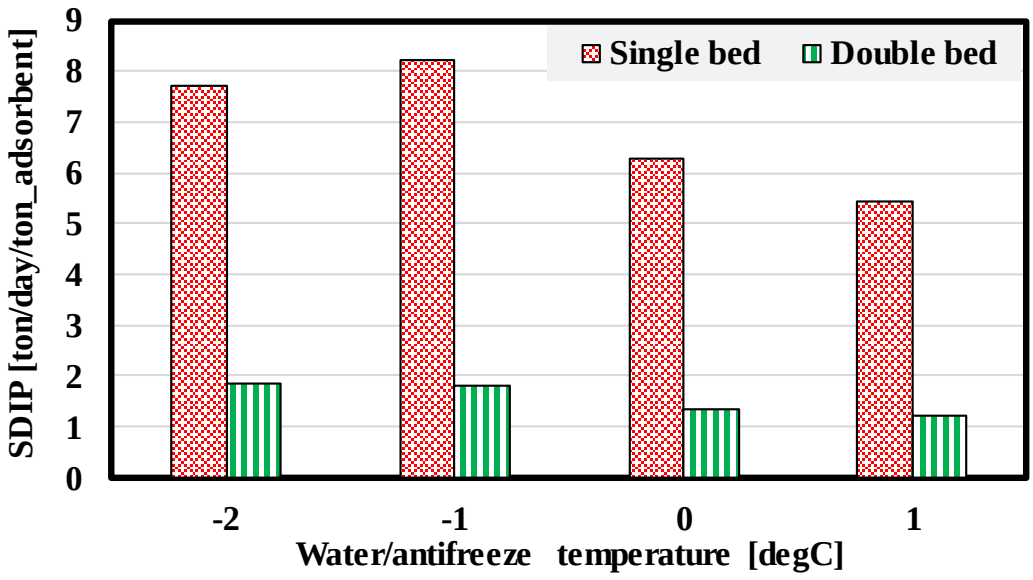

Figure 4-22 Comparison of the SDIP of the single and double bed adsorption ice making system based on multi outputs applications

Figure 4-23 shows a significant increase in the SDSP of the single bed system compared to the two bed system with an average rate of 80.4% per one degree of the water/freezing temperature from -2°C to -1°C and 0°C. This could be attributed to use the same configuration of evaporator using the same amount of potable water in the cups for the both test facilities taking in to account the design condition. However, the increase in SDSP was suddenly dropped to average rate of 46 % at water/antifreeze temperature of 1°C. This could be explained by highlighting the drop in the SDSP values, as by increasing water/antifreeze temperature from -2°C to -1°C, 0°C 1°C, the difference between the SDSP of the single and double bed systems reached to 22, 16.8, 12.6 and 2 ton/day per ton of adsorbent, respectively. In other words, the increase in SDSP of single bed system decreased about 11 times by increasing the evaporator temperature from -2°C to 1 °C. This confirms the reason of reduction in the increase of SDIP in Figure 4-22 with relatively high values.

The main reason behind the low values of the ice and slurry ice (see Figure 4-22 and Figure 4-23) of the double bed system compared to those of the single bed system is the exposed surface area of the seawater in the evaporator. As by using the same configuration of the evaporator, which is the shell and coil heat exchanger, the formed ice slurry leads to restricting and deteriorating the evaporation process in the evaporator with higher effect in case of the double bed system. Regarding the double bed system, the produced slurry ice is up to 0.9 kg per a single batch (3 cycle times) at evaporation temperature of -1°C, which is about twice the value in case of the single bed system at the same conditions. However, by using higher amount of adsorbent material in the two-bed system and using the same exposed surface area of seawater in the evaporator leading to decreasing the daily ice slurry production per a ton of adsorbent.

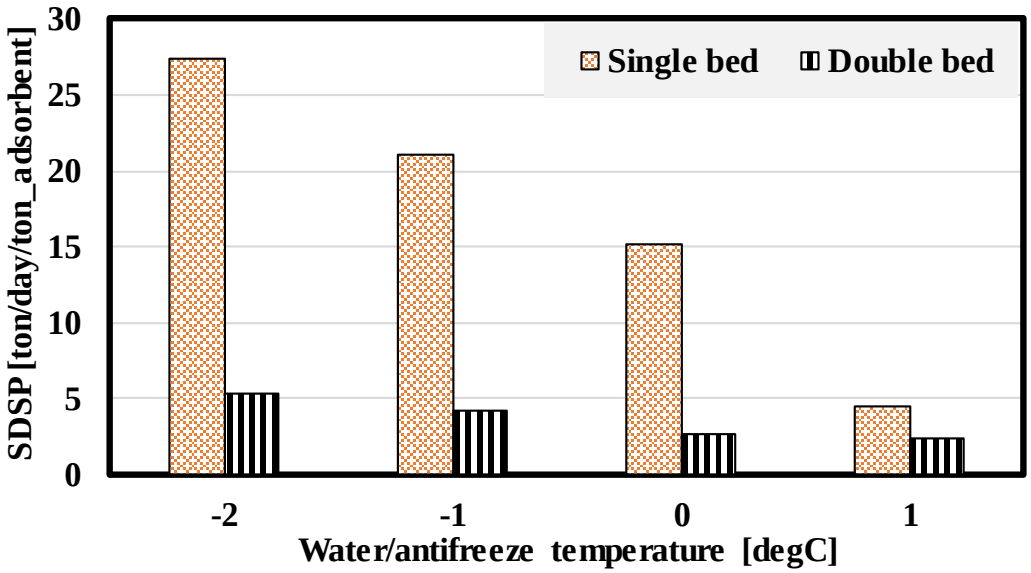

Figure 4-23 Comparison of the SDSP of the single and double bed adsorption ice making system based on multi outputs applications

Figure 4-24 shows a significant increase in the COP of the double bed system compared to the single bed system by an average rate of 45% per one degree of the water/antifreeze temperature from -2°C to 1°C. The difference between the COP of the double and single bed system are up to 0.374, 0.53 and 0.62 which are directly proportional to the increase in water/antifreeze temperature. The reason of this increase in the difference of COP between the double and single bed systems is due to the higher refrigeration effect of the double bed system compared to the single one by increasing the water/antifreeze temperature.

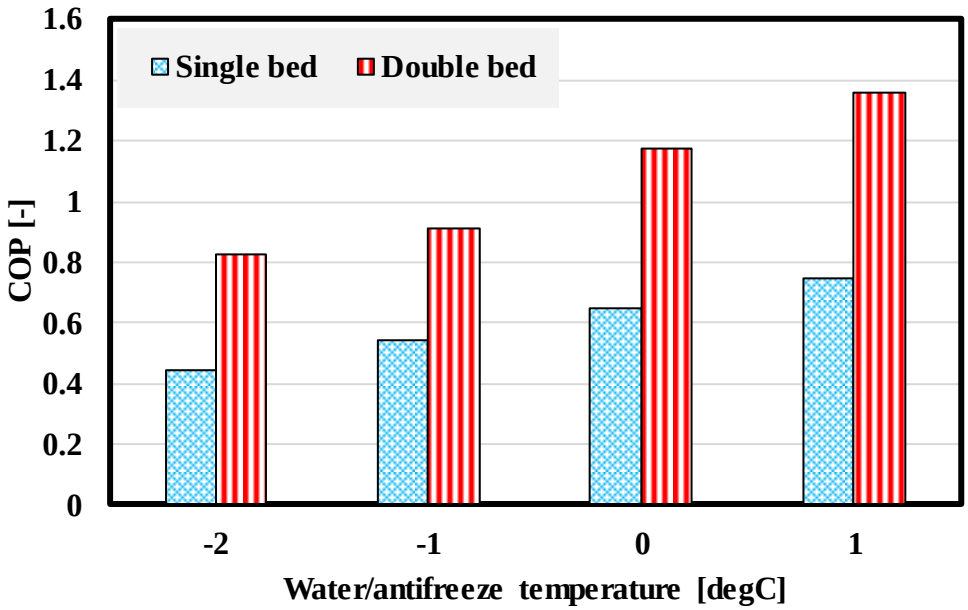

Figure 4-24 Comparison of the COP of the single and double bed adsorption ice making system based on multi outputs applications

Figure 4-25 shows a notable increase in the SDWP of the double bed system with average rate of 22% compared to the single bed system by increasing the water/antifreeze temperature from -2°C to -1°C, 0°C and 1°C. The rate of increase in the SDWP increased based on the differences between the SDWP of the double and single bed systems up to 0.22, 0.349, 0.68 and 0.69 by increasing water/antifreeze temperature from -2°C to -1°C, 0°C and 1 °C, respectively. This increase in the SDWP is due to adsorbing high amount of refrigerant by the adsorbent material in case of the double bed system which leads to increasing the condensation of fresh water in the condenser.

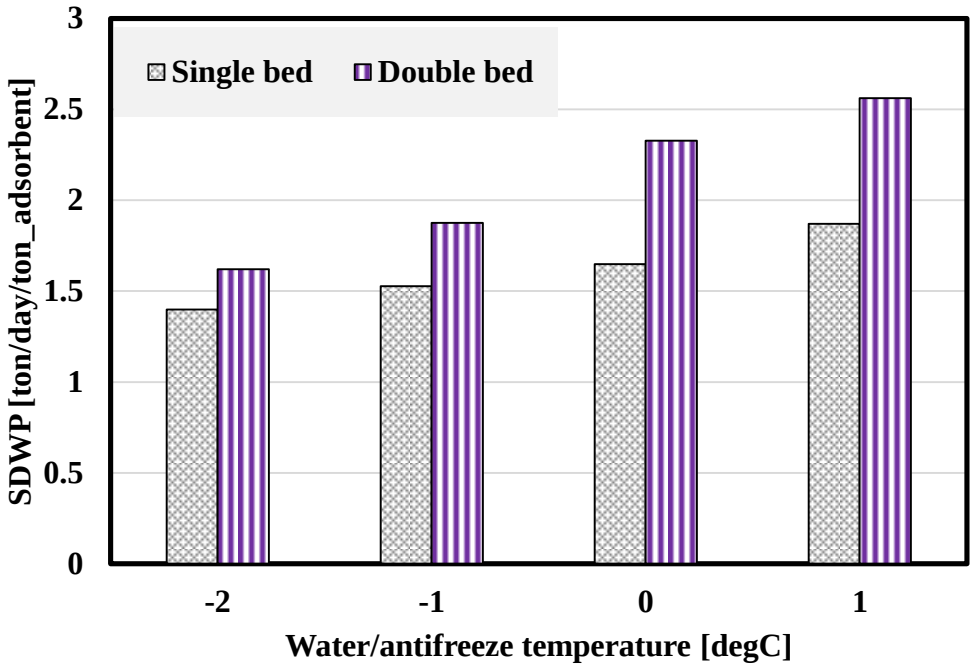

Figure 4-25 Comparison of the SDWP of the single and double bed adsorption ice making system based on multi outputs applications

4.6 Summary

The CPO 27(Ni) MOF two bed adsorption system was investigated for multi-output applications by evaluating its performance in terms of SDIP, SDWP, SDSP and COP. The test facility was built and all its components were described in this chapter including adsorber beds, evaporator, condenser, control and measuring devices. The test facility was operated for batch production of ice, ice slurry and distilled water based on the current configuration of the test facility. Based on batch production, the required time between the runs for preparing and collecting the output from the test facility was considered in the calculation of performance. Similar findings to those the single bed adsorption system were achieved by the two bed system in terms of cycles numbers (3 cycles), switching time (3min) and adsorption/desorption time (15min). The optimum mass flow rate of the heating

and cooling water in the adsorber beds is 8 L/min. The performance of the two bed adsorption system was compared with the single bed system in term of the SDIP, SDSP, SDWP and COP at various water/antifreeze temperatures. The SDIP and SDSP of the single bed system are higher than those the two bed adsorption system. However, the COP and SDWP of the two bed systems are higher than those of the single bed system.

CHAPTER 5

Conclusions and Recommendations

5.1 Introduction

Adsorption refrigeration and desalination systems have been increasingly investigated through the last decades to be used for producing ice, cooling and fresh water due to being environment friendly with no ozone depletion and low global warming potential. A number of industries require the simultaneous production of ice, cooling and distilled water like the fishing industry and the food chain. Therefore, in order to deliver all these outputs from one system, this thesis experimentally investigates the performance of single and double bed adsorption ice making system for multi outputs using CPO 27(Ni) MOF as an adsorbent material and potable/saline water as refrigerant. A novel technique (vacuum-direct freezing) is also developed to increase the outputs of the adsorption ice making system and enhancing the system performance. Moreover, the effects of various operating parameters on the performance of single and double bed system were experimentally investigated to determine the optimum operating conditions.

5.2 Conclusions

The current PhD project aimed to increase the outputs of adsorption ice making system which leads to enhance its performance for various applications. Also the project aimed to utilize the high thermo-physical properties of water to be used as refrigerant for ice making application. This could be achieved by lowering the freezing point of water using sea salt to take advantage of; (1) exploiting the sea water which is available at no cost to be used as a

refrigerant for cooling application <0℃ in the evaporator of adsorption ice making system, (2) delaying the formation of ice on the upper surface of refrigerant, which deteriorates the evaporation-adsorption process in the evaporator, (3) developing a novel technique (vacuum-direct freezing) by amalgamating two conventional techniques, namely; vacuum freezing process and direct freezing process (see sections 2.4.1.2 and 2.4.1.3, respectively) to be integrated with the adsorption ice making system to increase the production of ice, ice slurry, and cooling. The vacuum is achieved by the adsorbent material during the evaporation-adsorption process instead of the electrical vacuum pump of the conventional vacuum freezing process.

The CPO 27(Ni) MOF is used in the adsorption refrigeration system for ice making applications as it has a high affinity with water as presented in the literature review (section 2.2.4.1.2 (iv)) but it has not been used for cooling application <0℃ like ice making. The evaporator in this novel system could achieve three outputs; (1) Ice slurry: it is produced from the saline water during the evaporation- adsorption process, (2) Cooling: it is produced by circulating the fluid to be cooled in a coil submerged within the saline water (refrigerant) to be cooled during the evaporation-adsorption process, (3) Ice: it is produced by using potable water (as a second refrigerant) in separate cups which are immersed in the saline water refrigerant, where the ice firstly forms in the cups during the evaporation-adsorption process before the formation of ice slurry.

Saline water have been used as refrigerant in the adsorption desalination systems to produce fresh water in the condenser and cooling at evaporation temperature <0℃ for air conditioning application. However the daily water production rate of such system is limited. Therefore the production of fresh water from the condensation process as an

additional output (fourth) of the ice making adsorption system leads to further increasing the number of outputs.

In order to achieve the aims of this thesis, a test facility of one bed adsorption refrigeration system was modified to investigate the proposed novel technique for producing ice, ice slurry, cooling and desalinated water. A parametric study was experimentally investigated using the one bed adsorption ice making system to enhance the performance of the system in terms of SDIP, SDSP, COP and SDWP. Also a two bed adsorption system was constructed to investigate continuous production of ice, ice slurry, cooling and fresh water. A detailed comparison of the two bed and one bed systems was carried out to highlight the enhancement of the performance. Parametric studies were also experimentally investigated using the two bed adsorption system to evaluate the performance of the system in terms of the four outputs mentioned above. The contributions of this project are concluded as follows:

5.2.1 One bed adsorption system

- CPO-27 (Ni) MOF-water working pair shows the potential to be used for ice making application.
- The fresh and sea water can be used as refrigerant in adsorption systems to achieve low evaporation temperature <0 ℃ thus reducing dependence on CFCs and HFCs refrigerants for ice making applications.
- Based on 2000 ml of sea water as the main refrigerant in evaporator, the optimum volume of fresh water (as a secondary refrigerant) is 480 ml to provide a maximum ice production and COP of 10.2 ton/day/ton_adsorbent and 0.205 respectively.
- There is no major effect of increasing the fresh water in evaporator on the SDWP.

- Based on ice production of the single bed adsorption system, the optimum number of cycles is three cycles per batch.
- The optimum switching time and adsorption/desorption time are 3 and 15 min respectively for producing all outputs.
- There is an enhancement in SDIP up to 3.15 times with a maximum value of 8.2 ton/day/ton_ads using fresh and sea water as refrigerant compared to the maximum value reported in the literature using adsorption technique with methanol as refrigerant [13].
- With this technique, the optimum salinity is 35,000 ppm for maximum production of ice up to 8.3 ton/day/ton_ads with COP for cooling up to 0.9 and water desalination up to 1.8 ton/day/ton_ads.
- Increasing the desorption temperature from 88˚C to 93˚C produced significant enhancement in the SDWP and COP of the single bed adsorption system of 26% and 39%, respectively and with slightly lower enhancement in the SDIP and SDSP of 10%.
- The optimum water/anti freezing temperature is -1˚C to produce a maximum SDIP. By increasing the water/antifreeze temperature, the COP and SDWP significantly increased, however the SDIP and SDSP sharply decreased.
- Increasing the condensation temperature form 20˚C to 22.5˚C resulted in significant reduction in the SDWP and COP of 44.4% and 62% and slightly decreased in the SDIP and SDSP of 5% and 3%, respectively.

5.2.2 Two bed adsorption system

- Based on ice production of two bed adsorption system, the optimum number of cycles is three cycles per batch. Increasing the cycle numbers after the third cycle results in deteriorating the evaporation-adsorption due to ice formation on the top surface of the saline water.
- The optimum switching and adsorption/desorption time are the same as those of the single bed adsorption system (3 and 15 min, respectively).
- The optimum mass flow rate of the heating & cooling water through the adsorber beds is 8 L/min as the COP significantly decreased by 50% when increasing the mass flow rate from 8L/min to 12 L/min.
- The optimum water/antifreeze temperature in the evaporator of the two bed adsorption system is -1˚C. By increasing the water/antifreeze temperature, the SDWP and COP significantly increase, however the SDIP and SDSP sharply decrease.

5.2.3 General comparison with existed ice making system

This developed novel technology (vacuum-direct freezing) in the evaporator of adsorption ice making system offers the following advantages:

- Three times SDIP higher than the maximum value reported in the literature at the same desorption temperature about 100 ^{0}C.
- Produce four outputs from the adsorption ice making system compared to a maximum of two outputs as reported in the literature using other technologies like

integrating the ice making system with other systems, using developed adsorbent material, using developed bed design or using developed solar collector.

- Using sea and pure water as refrigerants compared to the commonly used refrigerants in the adsorption ice making systems like methanol and ammonia. Very limited work was found to use just water as refrigerant in the adsorption ice making system but with lower SDIP of 0.312 ton/day/ton of adsorbent compared to 7.8 ton/day/ton of adsorbent using this technology.
- CPO-27(Ni) MOF material has not been investigated before for application below 0 ^{0}C for adsorption ice making system compared to existing applications of desalination, thermal energy storage and air-conditioning.

5.3 Future work

In order to develop the performance of the two bed adsorption ice making system for multi outputs applications, many suggestions are recommended for future work:

- The evaporator of the adsorption ice making system integrated with the vacuum-direct freezing technique needs to be modified to enable a continuous operation instead of the batch operation as in this project. The evaporator needs to be integrated with means for moving the ice and ice slurry and means for draining the brine at specific times.
- The exposed surface area of the saline water in the evaporator of the current system need to be increased by using multi layers with the same arrangement (the combinations of saline water, potable water in cups and heat exchanger coil) to increase the potential of evaporation and reduce the crystallization impact of ice over the top layer of saline water.

- The condenser need to be equipped with means to drain the fresh water once reaching a specific level to enable the continuous operation of the system.
- The potential of lowering the freezing point of water using other additives with the sea salt need to be investigated.
- The effect of the salinity of water on the heat transfer coefficient need to be investigated.
- The effect of pressure inside the condenser on the performance of the cycle need to be investigated.

References

[1] R. Critoph, "Towards a one tonne per day solar ice maker," *Renewable Energy,* vol. 9, no. 1-4, pp. 626-631, 1996.

[2] S. M. Ali, and A. Chakraborty, "Adsorption assisted double stage cooling and desalination employing silica gel + water and AQSOA-Z02 + water systems," *Energy Conversion and Management,* vol. 117, pp. 193-205, 2016.

[3] R. HR, A. MO, T. IAW, and L. SL, "Comparative study of three different adsorbent-adsorbate working pairs for a waste heat driven adsorption air conditioning system based on simulation," *IJRRAS,* vol. 18, no. 2, pp. 109-121, 2014.

[4] W. Livingston. "New Liquid Cooled Servers with Adsorption Chillers Improve Efficiency, Reduce Footprint," http://www.ppiway.com/new-liquid-cooled-servers-with-adsorption-chillersimprove-efficiency-reduce-footprint/.

[5] SOLAIR. http://www.solair-project.eu/.

[6] T. F. Reichardt, "Technical and Economic Assessment of Medium Sized Solar-Assisted Air-Conditioning in Brazil," Departamento de Engenharia Civil, PUC-Rio, 2010.

[7] M. Hamdy, A. A. Askalany, K. Harby, and N. Kora, "An overview on adsorption cooling systems powered by waste heat from internal combustion engine," *Renewable and Sustainable Energy Reviews,* vol. 51, pp. 1223-1234, 2015.

[8] C. Li, R. Z. Wang, L. W. Wang, T. X. Li, and Y. Chen, "Experimental study on an adsorption icemaker driven by parabolic trough solar collector," *Renewable Energy,* vol. 57, pp. 223-233, 2013.

[9] S. J. Metcalf, Z. Tamainot-Telto, and R. E. Critoph, "Application of a compact sorption generator to solar refrigeration: Case study of Dakar (Senegal)," *Applied Thermal Engineering,* vol. 31, no. 14, pp. 2197-2204, 2011.

[10] E. Elsayed, A.-D. Raya, S. Mahmoud, P. A. Anderson, A. Elsayed, and P. G. Youssef, "CPO-27 (Ni), aluminium fumarate and MIL-101 (Cr) MOF materials for adsorption water desalination," *Desalination*, vol. 406, pp. 25-36, 2017.
[11] Z. Lu, R. Wang, and L. Wang, "Dynamic characteristics of a novel adsorption refrigerator with compound mass‐heat recovery," *International Journal of Energy Research*, vol. 37, no. 1, pp. 59-68, 2013.
[12] G. Lychnos, and Z. Tamainot-Telto, "Performance of hybrid refrigeration system using ammonia," *Applied Thermal Engineering*, vol. 62, no. 2, pp. 560-565, 2014.
[13] R. Wang, J. Wu, Y. Xu, and W. Wang, "Performance researches and improvements on heat regenerative adsorption refrigerator and heat pump," *Energy conversion and management*, vol. 42, no. 2, pp. 233-249, 2001.
[14] R. Wang, L. Wang, and J. Wu, *Adsorption refrigeration technology: theory and application*: John Wiley & Sons, 2014.
[15] B. Choudhury, P. K. Chatterjee, and J. P. Sarkar, "Review paper on solar-powered air-conditioning through adsorption route," *Renewable and Sustainable Energy Reviews*, vol. 14, no. 8, pp. 2189-2195, 2010.
[16] R. E. Critoph, and Y. Zhong, "Review of trends in solid sorption refrigeration and heat pumping technology," *Proceedings of the Institution of Mechanical Engineers, Part E: Journal of Process Mechanical Engineering*, vol. 219, no. 3, pp. 285-300, 2016.
[17] M. Z. I. Khan, K. C. A. Alam, B. B. Saha, Y. Hamamoto, A. Akisawa, and T. Kashiwagi, "Parametric study of a two-stage adsorption chiller using re-heat—The effect of overall thermal conductance and adsorbent mass on system performance," *International Journal of Thermal Sciences*, vol. 45, no. 5, pp. 511-519, 2006.
[18] M. O. a. K. t. E. P. f. W. Heat. https://think-left.org/2011/09/25/microwave-ovens-a-key-to-energy-production-from-wasted-heat/.
[19] Y. Hirota, Y. Sugiyama, M. Kubota, F. Watanabe, N. Kobayashi, M. Hasatani, and M. Kanamori, "Development of a suction-pump-assisted thermal and electrical hybrid adsorption heat pump," *Applied Thermal Engineering*, vol. 28, no. 13, pp. 1687-1693, 2008.
[20] D. V. C. Ltd. "Rotary Heat Engine (RHE)," http://www.davinci-mode.co.jp/e/rhe.html.
[21] A. Rezk, R. Al-Dadah, S. Mahmoud, and A. Elsayed, "Investigation of Ethanol/metal organic frameworks for low temperature adsorption cooling applications," *Applied Energy*, vol. 112, pp. 1025-1031, 2013.
[22] N. I. Ibrahim, M. M. A. Khan, I. M. Mahbubul, R. Saidur, and F. A. Al-Sulaiman, "Experimental testing of the performance of a solar absorption cooling system assisted with ice-storage for an office space," *Energy Conversion and Management*, vol. 148, pp. 1399-1408, 2017.
[23] Z. Qi, "Study on hybrid system of solar powered water heater and adsorption ice maker," *Int J Archit Sci*, vol. 6, no. 4, pp. 168-172, 2005.
[24] S. Garimella, A. M. Brown, and A. K. Nagavarapu, "Waste heat driven absorption/vapor-compression cascade refrigeration system for megawatt scale, high-flux, low-temperature cooling," *International Journal of Refrigeration*, vol. 34, no. 8, pp. 1776-1785, 2011.
[25] D. Wang, J. Zhang, X. Tian, D. Liu, and K. Sumathy, "Progress in silica gel–water adsorption refrigeration technology," *Renewable and Sustainable Energy Reviews*, vol. 30, pp. 85-104, 2014.

[26] M. Z. I. Khan, K. C. A. Alam, B. B. Saha, A. Akisawa, and T. Kashiwagi, "Study on a re-heat two-stage adsorption chiller – The influence of thermal capacitance ratio, overall thermal conductance ratio and adsorbent mass on system performance," *Applied Thermal Engineering,* vol. 27, no. 10, pp. 1677-1685, 2007.
[27] Z. S. Lu, R. Z. Wang, L. W. Wang, and C. J. Chen, "Performance analysis of an adsorption refrigerator using activated carbon in a compound adsorbent," *Carbon,* vol. 44, no. 4, pp. 747-752, 2006.
[28] Z. Tamainot-Telto, S. J. Metcalf, and R. E. Critoph, "Novel compact sorption generators for car air conditioning," *International Journal of Refrigeration,* vol. 32, no. 4, pp. 727-733, 2009.
[29] A. Allouhi, T. Kousksou, A. Jamil, Y. Agrouaz, T. Bouhal, R. Saidur, and A. Benbassou, "Performance evaluation of solar adsorption cooling systems for vaccine preservation in Sub-Saharan Africa," *Applied Energy,* vol. 170, pp. 232-241, 2016.
[30] X. Ji, X. Song, M. Li, J. Liu, and Y. Wang, "Performance investigation of a solar hot water driven adsorption ice-making system," *Energy Conversion and Management,* vol. 106, pp. 759-765, 2015.
[31] L. Jiang, L. Wang, R. Wang, P. Gao, and F. Song, "Investigation on cascading cogeneration system of ORC (Organic Rankine Cycle) and CaCl2/BaCl2 two-stage adsorption freezer," *Energy,* vol. 71, pp. 377-387, 2014.
[32] M. Gwadera, and K. Kupiec, "Adsorption refrigeration systems," *Inż. Ap. Chem,* vol. 50, no. 5, pp. 38-39, 2011.
[33] F. P. Song, L. X. Gong, L. W. Wang, and R. Z. Wang, "Study on gradient thermal driven adsorption cycle with freezing and cooling output for food storage," *Applied Thermal Engineering,* vol. 70, no. 1, pp. 231-239, 2014.
[34] R. Critoph, "An ammonia carbon solar refrigerator for vaccine cooling," *Renewable Energy,* vol. 5, no. 1-4, pp. 502-508, 1994.
[35] D. C. Wang, and J. Y. Wu, "Influence of intermittent heat source on adsorption ice maker using waste heat," *Energy Conversion and Management,* vol. 46, no. 6, pp. 985-998, 2005.
[36] H. Zhang, J. Quon, A. J. Alvarez, J. Evans, A. S. Myerson, and B. Trout, "Development of Continuous Anti-Solvent/Cooling Crystallization Process using Cascaded Mixed Suspension, Mixed Product Removal Crystallizers," *Organic Process Research & Development,* vol. 16, no. 5, pp. 915-924, 2012.
[37] M. Pons, and J. J. Guilleminot, "Design of an Experimental Solar-Powered, Solid-Adsorption Ice Maker," *Journal of Solar Energy Engineering,* vol. 108, no. 4, pp. 332, 1986.
[38] N. A. A. Qasem, and M. A. I. El-Shaarawi, "Improving ice productivity and performance for an activated carbon/methanol solar adsorption ice-maker," *Solar Energy,* vol. 98, pp. 523-542, 2013.
[39] A. P. F. Leite, and M. Daguenet, "Performance of a new solid adsorption ice maker with solar energy regeneration," *Energy Conversion and Management,* vol. 41, no. 15, pp. 1625-1647, 2000.
[40] A. P. F. Leite, M. B. Grilo, R. R. D. Andrade, F. A. Belo, and F. Meunier, "Experimental evaluation of a multi-tubular adsorber operating with activated carbon-methanol," *Adsorption,* vol. 11, pp. 543-548, 2005.

[41] Z. Li, and K. Sumathy, "A solar‐powered ice‐maker with the solid adsorption pair of activated carbon and methanol," *International Journal of Energy Research,* vol. 23, no. 6, pp. 517-527, 1999.
[42] A. Boubakri, J. Guilleminot, and F. Meunier, "Adsorptive solar powered ice maker: experiments and model," *Solar Energy,* vol. 69, no. 3, pp. 249-263, 2000.
[43] M. Li, C. J. Sun, R. Z. Wang, and W. D. Cai, "Development of no valve solar ice maker," *Applied Thermal Engineering,* vol. 24, no. 5-6, pp. 865-872, 2004.
[44] S. Kreussler, and D. Bolz, "Experiments on solar adsorption refrigeration using zeolite and water," *Laboratory for Solar Energy, University of Applied Sciences Lubeck,* 2000.
[45] M. Ramos, R. L. Espinoza, M. J. Horn, and A. P. F. Leite, "Evaluation of a zeolite-water solar adsorption refrigerator." pp. 14-19.
[46] X. Ji, M. Li, J. Fan, P. Zhang, B. Luo, and L. Wang, "Structure optimization and performance experiments of a solar-powered finned-tube adsorption refrigeration system," *Applied Energy,* vol. 113, pp. 1293-1300, 2014.
[47] H. Z. Hassan, A. A. Mohamad, and H. A. Al-Ansary, "Development of a continuously operating solar-driven adsorption cooling system: Thermodynamic analysis and parametric study," *Applied Thermal Engineering,* vol. 48, pp. 332-341, 2012.
[48] E. Anyanwu, "Review of solid adsorption solar refrigerator I: an overview of the refrigeration cycle," *Energy conversion and Management,* vol. 44, no. 2, pp. 301-312, 2003.
[49] T. TCHERNEV, "Solar air conditioning and refrigeration systems utilizing zeolites." pp. 209-215.
[50] Z. Tamainot-Telto, S. J. Metcalf, R. E. Critoph, Y. Zhong, and R. Thorpe, "Carbon–ammonia pairs for adsorption refrigeration applications: ice making, air conditioning and heat pumping," *International Journal of Refrigeration,* vol. 32, no. 6, pp. 1212-1229, 2009.
[51] M. I. González, and L. R. Rodríguez, "Solar powered adsorption refrigerator with CPC collection system: Collector design and experimental test," *Energy Conversion and Management,* vol. 48, no. 9, pp. 2587-2594, 2007.
[52] Z. Tamainot-Telto, and R. Critoph, "Adsorption refrigerator using monolithic carbon-ammonia pair," *International Journal of Refrigeration,* vol. 20, no. 2, pp. 146-155, 1997.
[53] M. Li, H. B. Huang, R. Z. Wang, L. L. Wang, W. D. Cai, and W. M. Yang, "Experimental study on adsorbent of activated carbon with refrigerant of methanol and ethanol for solar ice maker," *Renewable Energy,* vol. 29, no. 15, pp. 2235-2244, 2004.
[54] M. Pons, F. Meunier, G. Cacciola, R. Critoph, M. Groll, L. Puigjaner, B. Spinner, and F. Ziegler, "Thermodynamic based comparison of sorption systems for cooling and heat pumping: Comparaison des performances thermodynamique des systèmes de pompes à chaleur à sorption dans des applications de refroidissement et de chauffage," *International Journal of Refrigeration,* vol. 22, no. 1, pp. 5-17, 1999.
[55] R. G. Oliveira, V. Silveira, and R. Z. Wang, "Experimental study of mass recovery adsorption cycles for ice making at low generation temperature," *Applied Thermal Engineering,* vol. 26, no. 2-3, pp. 303-311, 2006.

[56] K. Wang, J. Y. Wu, R. Z. Wang, and L. W. Wang, "Composite adsorbent of CaCl2 and expanded graphite for adsorption ice maker on fishing boats," *International Journal of Refrigeration,* vol. 29, no. 2, pp. 199-210, 2006.
[57] L. W. Wang, R. Z. Wang, Z. S. Lu, C. J. Chen, K. Wang, and J. Y. Wu, "The performance of two adsorption ice making test units using activated carbon and a carbon composite as adsorbents," *Carbon,* vol. 44, no. 13, pp. 2671-2680, 2006.
[58] K. Sumathy, and L. Zhongfu, "Experiments with solar-powered adsorption ice-maker," *Renewable Energy,* vol. 16, no. 1-4, pp. 704-707, 1999.
[59] M. Li, and R. Wang, "A study of the effects of collector and environment parameters on the performance of a solar powered solid adsorption refrigerator," *Renewable Energy,* vol. 27, no. 3, pp. 369-382, 2002.
[60] A. D. Grekova, J. V. Veselovskaya, M. M. Tokarev, and L. G. Gordeeva, "Novel ammonia sorbents "porous matrix modified by active salt" for adsorptive heat transformation: 5. Designing the composite adsorbent for ice makers," *Applied Thermal Engineering,* vol. 37, pp. 80-86, 2012.
[61] G. Maggio, L. G. Gordeeva, A. Freni, Y. I. Aristov, G. Santori, F. Polonara, and G. Restuccia, "Simulation of a solid sorption ice-maker based on the novel composite sorbent "lithium chloride in silica gel pores"," *Applied Thermal Engineering,* vol. 29, no. 8-9, pp. 1714-1720, 2009.
[62] Z. S. Lu, R. Z. Wang, Z. Z. Xia, Q. B. Wu, Y. M. Sun, and Z. Y. Chen, "An analysis of the performance of a novel solar silica gel–water adsorption air conditioning," *Applied Thermal Engineering,* vol. 31, no. 17-18, pp. 3636-3642, 2011.
[63] K. Oertel, and M. Fischer, "Adsorption cooling system for cold storage using methanol/silicagel," *Applied Thermal Engineering,* vol. 18, no. 9, pp. 773-786, 1998.
[64] H. J. Dakkama, A. Elsayed, R. K. Al-Dadah, S. M. Mahmoud, and P. Youssef, "Integrated evaporator–condenser cascaded adsorption system for low temperature cooling using different working pairs," *Applied Energy,* vol. 185, pp. 2117-2126, 2017.
[65] F. Meunier, "Theoretical performances of solid adsorbent cascading cycles using the zeolite-water and active carbon-methanol pairs: four case studies," *Journal of heat recovery systems,* vol. 6, no. 6, pp. 491-498, 1986.
[66] R. Wang, M. Li, Y. Xu, and J. Wu, "An energy efficient hybrid system of solar powered water heater and adsorption ice maker," *Solar Energy,* vol. 68, no. 2, pp. 189-195, 2000.
[67] M. A. Alghoul, M. Y. Sulaiman, K. Sopian, and B. Z. Azmi, "Performance of a dual-purpose solar continuous adsorption system," *Renewable Energy,* vol. 34, no. 3, pp. 920-927, 2009.
[68] M. Li, R. Wang, H. Luo, L. Wang, and H. Huang, "Experiments of a solar flat plate hybrid system with heating and cooling," *Applied thermal engineering,* vol. 22, no. 13, pp. 1445-1454, 2002.
[69] E. Willers, and M. Groll, "Evaluation of metal hydride machines for heat pumping and cooling applications: Evaluation des machines à hydrure métallique dans les applications de pompes à chaleur et de refroidissement," *International Journal of Refrigeration,* vol. 22, no. 1, pp. 47-58, 1999.
[70] A. Dieng, and R. Wang, "Literature review on solar adsorption technologies for ice-making and air-conditioning purposes and recent developments in solar

technology," *Renewable and sustainable energy reviews,* vol. 5, no. 4, pp. 313-342, 2001.
[71] J.-Y. San, and W.-M. Lin, "Comparison among three adsorption pairs for using as the working substances in a multi-bed adsorption heat pump," *Applied Thermal Engineering,* vol. 28, no. 8-9, pp. 988-997, 2008.
[72] A. M. Elsayed, A. A. Askalany, A. D. Shea, H. J. Dakkama, S. Mahmoud, R. Al-Dadah, and W. Kaialy, "A state of the art of required techniques for employing activated carbon in renewable energy powered adsorption applications," *Renewable and Sustainable Energy Reviews,* vol. 79, pp. 503-519, 2017.
[73] R. Critoph, and Y. Zhong, "Review of trends in solid sorption refrigeration and heat pumping technology," *Proceedings of the Institution of Mechanical Engineers, Part E: Journal of Process Mechanical Engineering,* vol. 219, no. 3, pp. 285-300, 2005.
[74] R. Lartey, F. Acquah, and K. Nketia, "Developing national capability for manufacture of activated carbon from agricultural wastes," *Ghana Eng,* vol. 19, no. 1, pp. 1-2, 1999.
[75] Bansal RC, " Goyal M. Activated carbon adsorption," 2005.
[76] N. Spahis, A. Addoun, and H. Mahmoudi, "Study on solar adsorption refrigeration cycle utilizing activated carbon prepared from olive stones," *Revue des Energies renouvelables,* vol. 10, no. 3, pp. 415-420, 2007.
[77] M. O. Abdullah, I. A. W. Tan, and L. S. Lim, "Automobile adsorption air-conditioning system using oil palm biomass-based activated carbon: a review," *Renewable and Sustainable Energy Reviews,* vol. 15, no. 4, pp. 2061-2072, 2011.
[78] R. T. Yang, *Adsorbents: fundamentals and applications*: John Wiley & Sons, 2003.
[79] M. Li, R. Wang, Y. Xu, J. Wu, and A. Dieng, "Experimental study on dynamic performance analysis of a flat-plate solar solid-adsorption refrigeration for ice maker," *Renewable energy,* vol. 27, no. 2, pp. 211-221, 2002.
[80] N. Ghaffour, S. Lattemann, T. Missimer, K. C. Ng, S. Sinha, and G. Amy, "Renewable energy-driven innovative energy-efficient desalination technologies," *Applied Energy,* vol. 136, pp. 1155-1165, 2014.
[81] Q. M. Wang, D. Shen, M. Bülow, M. L. Lau, S. Deng, F. R. Fitch, N. O. Lemcoff, and J. Semanscin, "Metallo-organic molecular sieve for gas separation and purification," *Microporous and mesoporous materials,* vol. 55, no. 2, pp. 217-230, 2002.
[82] S. Qiu, and G. Zhu, "Molecular engineering for synthesizing novel structures of metal–organic frameworks with multifunctional properties," *Coordination Chemistry Reviews,* vol. 253, no. 23, pp. 2891-2911, 2009.
[83] A. Rezk, R. Al-Dadah, S. Mahmoud, and A. Elsayed, "Experimental investigation of metal organic frameworks characteristics for water adsorption chillers," *Proceedings of the Institution of Mechanical Engineers, Part C: Journal of Mechanical Engineering Science,* vol. 227, no. 5, pp. 992-1005, 2013.
[84] A. Elsayed, E. Elsayed, A.-D. Raya, S. Mahmoud, A. Elshaer, and W. Kaialy, "Thermal energy storage using metal–organic framework materials," *Applied Energy,* vol. 186, pp. 509-519, 2017.
[85] P. G. Youssef, H. Dakkama, S. M. Mahmoud, and R. K. AL-Dadah, "Experimental investigation of adsorption water desalination/cooling system using CPO-27Ni MOF," *Desalination,* vol. 404, pp. 192-199, 2017.

[86] B. Shi, A.-D. Raya, S. Mahmoud, A. Elsayed, and E. Elsayed, "CPO-27 (Ni) metal–organic framework based adsorption system for automotive air conditioning," *Applied Thermal Engineering,* vol. 106, pp. 325-333, 2016.
[87] S. Henninger, F. Schmidt, and H.-M. Henning, "Water adsorption characteristics of novel materials for heat transformation applications," *Applied thermal engineering,* vol. 30, no. 13, pp. 1692-1702, 2010.
[88] J. Ehrenmann, S. K. Henninger, and C. Janiak, "Water Adsorption Characteristics of MIL‐101 for Heat‐Transformation Applications of MOFs," *European Journal of Inorganic Chemistry,* vol. 2011, no. 4, pp. 471-474, 2011.
[89] F. Jeremias, D. Fröhlich, C. Janiak, and S. K. Henninger, "Advancement of sorption-based heat transformation by a metal coating of highly-stable, hydrophilic aluminium fumarate MOF," *RSC Advances,* vol. 4, no. 46, pp. 24073-24082, 2014.
[90] E. Elsayed, A.-D. Raya, S. Mahmoud, A. Elsayed, and P. A. Anderson, "Aluminium fumarate and CPO-27 (Ni) MOFs: characterization and thermodynamic analysis for adsorption heat pump applications," *Applied Thermal Engineering,* vol. 99, pp. 802-812, 2016.
[91] X. Song, X. Ji, M. Li, Q. Wang, Y. Dai, and J. Liu, "Effect of desorption parameters on performance of solar water-bath solid adsorption ice-making system," *Applied Thermal Engineering,* vol. 89, pp. 316-322, 2015.
[92] I. I. El-Sharkawy, M. Hassan, B. B. Saha, S. Koyama, and M. M. Nasr, "Study on adsorption of methanol onto carbon based adsorbents," *International Journal of Refrigeration,* vol. 32, no. 7, pp. 1579-1586, 2009.
[93] S. Gladis, "Ice slurry thermal energy storage for cheese process cooling," *ASHRAE Trans,* vol. 103, pp. 725-729, 1997.
[94] A. Subramani, and J. G. Jacangelo, "Emerging desalination technologies for water treatment: a critical review," *Water research,* vol. 75, pp. 164-187, 2015.
[95] H. Ettouney, "Conventional thermal processes," *Seawater Desalination,* pp. 17-40: Springer, 2009.
[96] P. Byrne, L. Fournaison, A. Delahaye, Y. A. Oumériane, L. Serres, P. Loulergue, A. Szymczyk, D. Mugnier, J.-L. Malaval, and R. Bourdais, "A review on the coupling of cooling, desalination and solar photovoltaic systems," *Renewable and Sustainable Energy Reviews,* vol. 47, pp. 703-717, 2015.
[97] K. C. Ng, K. Thu, Y. Kim, A. Chakraborty, and G. Amy, "Adsorption desalination: an emerging low-cost thermal desalination method," *Desalination,* vol. 308, pp. 161-179, 2013.
[98] K. Thu, A. Chakraborty, Y.-D. Kim, A. Myat, B. B. Saha, and K. C. Ng, "Numerical simulation and performance investigation of an advanced adsorption desalination cycle," *Desalination,* vol. 308, pp. 209-218, 2013.
[99] K. C. Ng, B. B. Saha, A. Chakraborty, and S. Koyama, "Adsorption desalination quenches global thirst," *Heat Transfer Engineering,* vol. 29, no. 10, pp. 845-848, 2008.
[100] R. Shone, "The freeze desalination of mine waters," *Journal of the Southern African Institute of Mining and Metallurgy,* vol. 87, no. 4, pp. 107-112, 1987.
[101] K. C. Kang, P. Linga, K.-n. Park, S.-J. Choi, and J. D. Lee, "Seawater desalination by gas hydrate process and removal characteristics of dissolved ions (Na+, K+, Mg 2+, Ca 2+, B 3+, Cl−, SO 4 2−)," *Desalination,* vol. 353, pp. 84-90, 2014.

[102] P. M. Williams, M. Ahmad, B. S. Connolly, and D. L. Oatley-Radcliffe, "Technology for freeze concentration in the desalination industry," *Desalination,* vol. 356, pp. 314-327, 2015.
[103] K. Thu, K. C. Ng, B. B. Saha, A. Chakraborty, and S. Koyama, "Operational strategy of adsorption desalination systems," *International Journal of Heat and Mass Transfer,* vol. 52, no. 7, pp. 1811-1816, 2009.
[104] A. S. Alsaman, E. S. Ali, K. Harby, A. A. Askalany, and M. S. Ahmed, "PERFORMANCE IMPROVEMENT OF A SOLAR DRIVEN ADSORPTION DESALINATION SYSTEM BY HEAT RECOVERY OPERATION."
[105] S. Mitra, P. Kumar, K. Srinivasan, and P. Dutta, "Performance evaluation of a two-stage silica gel+ water adsorption based cooling-cum-desalination system," *international journal of refrigeration,* vol. 58, pp. 186-198, 2015.
[106] S. M. Ali, P. Haider, D. S. Sidhu, and A. Chakraborty, "Thermally driven adsorption cooling and desalination employing multi-bed dual-evaporator system," *Applied Thermal Engineering,* vol. 106, pp. 1136-1147, 2016.
[107] X. Wang, K. C. Ng, A. Chakarborty, and B. B. Saha, "How heat and mass recovery strategies impact the performance of adsorption desalination plant: theory and experiments," *Heat transfer engineering,* vol. 28, no. 2, pp. 147-153, 2007.
[108] K. Thu, "Adsorption desalination: theory & experiments," 2010.
[109] X. Wang, and K. C. Ng, "Experimental investigation of an adsorption desalination plant using low-temperature waste heat," *Applied Thermal Engineering,* vol. 25, no. 17, pp. 2780-2789, 2005.
[110] P. G. Youssef, S. M. Mahmoud, and R. K. Al-Dadah, "Effect of evaporator temperature on the performance of water desalination/refrigeration adsorption system using AQSOA-ZO2," *World Academy of Science, Engineering and Technology, International Journal of Environmental, Chemical, Ecological, Geological and Geophysical Engineering,* vol. 9, no. 6, pp. 701-705, 2015.
[111] P. G. Youssef, S. M. Mahmoud, and R. K. Al-Dadah, "Numerical simulation of combined adsorption desalination and cooling cycles with integrated evaporator/condenser," *Desalination,* vol. 392, pp. 14-24, 2016.
[112] M. W. Shahzad, K. C. Ng, K. Thu, B. B. Saha, and W. G. Chun, "Multi effect desalination and adsorption desalination (MEDAD): A hybrid desalination method," *Applied Thermal Engineering,* vol. 72, no. 2, pp. 289-297, 2014.
[113] D. Zejli, R. Benchrifa, A. Bennouna, and O. Bouhelal, "A solar adsorption desalination device: first simulation results," *Desalination,* vol. 168, pp. 127-135, 2004.
[114] A. A. Askalany, "Innovative mechanical vapor compression adsorption desalination (MVC-AD) system," *Applied Thermal Engineering,* vol. 106, pp. 286-292, 2016.
[115] K. Thu, H. Yanagi, B. B. Saha, and K. C. Ng, "Performance investigation on a 4-bed adsorption desalination cycle with internal heat recovery scheme," *Desalination,* vol. 402, pp. 88-96, 2017.
[116] A. S. Kim, H.-S. Lee, D.-S. Moon, and H.-J. Kim, "Performance control on adsorption desalination using initial time lag (ITL) of individual beds," *Desalination,* vol. 396, pp. 1-16, 2016.
[117] K. Thu, B. B. Saha, K. J. Chua, and K. C. Ng, "Performance investigation of a waste heat-driven 3-bed 2-evaporator adsorption cycle for cooling and desalination," *International Journal of Heat and Mass Transfer,* vol. 101, pp. 1111-1122, 2016.

[118] B. B. Saha, I. I. El-Sharkawy, M. W. Shahzad, K. Thu, L. Ang, and K. C. Ng, "Fundamental and application aspects of adsorption cooling and desalination," *Applied Thermal Engineering,* vol. 97, pp. 68-76, 2016.
[119] A. Al-Ansari, H. Ettouney, and H. El-Dessouky, "Water–zeolite adsorption heat pump combined with single effect evaporation desalination process," *Renewable Energy,* vol. 24, no. 1, pp. 91-111, 2001.
[120] A. Chakraborty, K. Thu, and K. C. Ng, "Advanced adsorption cooling cum desalination cycle-a thermodynamic framework."
[121] S. Mitra, K. Srinivasan, P. Kumar, S. Murthy, and P. Dutta, "Solar driven adsorption desalination system," *Energy Procedia,* vol. 49, pp. 2261-2269, 2014.
[122] K. Thu, H. Yanagi, B. B. Saha, and K. C. Ng, "Performance analysis of a low-temperature waste heat-driven adsorption desalination prototype," *International Journal of Heat and Mass Transfer,* vol. 65, pp. 662-669, 2013.
[123] K. C. Ng, K. Thu, B. B. Saha, and A. Chakraborty, "Study on a waste heat-driven adsorption cooling cum desalination cycle," *International Journal of refrigeration,* vol. 35, no. 3, pp. 685-693, 2012.
[124] B. Shi, "Development of an MOF based adsorption air conditioning system for automotive application," University of Birmingham, 2015.
[125] E. Haque, and S. H. Jhung, "Synthesis of isostructural metal–organic frameworks, CPO-27s, with ultrasound, microwave, and conventional heating: Effect of synthesis methods and metal ions," *Chemical engineering journal,* vol. 173, no. 3, pp. 866-872, 2011.
[126] A. S. Alsaman, A. A. Askalany, K. Harby, and M. S. Ahmed, "A state of the art of hybrid adsorption desalination–cooling systems," *Renewable and Sustainable Energy Reviews,* vol. 58, pp. 692-703, 2016.
[127] K. Habib, B. B. Saha, A. Chakraborty, S. Koyama, and K. Srinivasan, "Performance evaluation of combined adsorption refrigeration cycles," *international journal of refrigeration,* vol. 34, no. 1, pp. 129-137, 2011.
[128] R. Best, J. Islas, and M. Martinez, "Exergy efficiency of an ammonia-water absorption system for ice production," *Applied energy,* vol. 45, no. 3, pp. 241-256, 1993.
[129] K. Cheatle, *Fundamentals of test measurement instrumentation*: ISA--Instrumentation, Systems, and Automation Society, 2006.
[130] A. M. Elsayed, "Heat transfer in helically coiled small diameter tubes for miniature cooling systems," University of Birmingham, 2011.

Appendix A

Uncertainties of measuring instrument

1 Thermocouples

Overall uncertainty of the all listed thermocouples in the Table 3.1 and Table 4.1 was calculated using Root Square Sum (RSS) [129, 130] as follows,

$$U_{thermo} = \pm\sqrt{(U_{st})^2 + (U_{curve\ fit})^2} \quad (1)$$

Where $U_{overall}$, U_{st} and $U_{curve-fit}$ are the uncertainties of the overall, standard and curve fit, respectively.

The curve fit uncertainty could be statically calculated as follows,

$$U_{curve-fit} = t_{n-1,95\%} \times S_x \quad (2)$$

Where $t_{n-1,95\%}$, n and S_x are the student distribution factor, the number of collected data and the standard deviation of the mean, respectively.

The S_x could be calculated using the equation as follows,

$$S_x = \frac{\sigma}{\sqrt{n}} \quad (3)$$

Where σ is the standard deviation which could be calculated as follows,

$$\sigma = \sqrt{\frac{1}{n-1}\sum_{i=1}^{n}(x_i - \bar{x})^2} \quad (4)$$

Where x_i and $\bar{x}$ are the reading of alcohol thermometer and the curve fit value. Table A.1 shows the method to calculate the overall uncertainty of one T type thermocouple.

Table A.1 T-type thermocouple overall uncertainty calculation

Data point	**Measurement of alcohol thermometer [˚C]**	**Measurement of thermocouple [˚C]**	**Curve fit equation y = 0.9992x + 0.0756**	**Deviation $(x_i - \bar{x})^2$**
1	18.9	18.848629	18.9091501	8.37243E-05
2	25.9	26.22317	26.27779146	0.14272639
3	41.8	41.511132	41.55352309	0.060750865
4	59.3	59.41535	59.44341772	0.020568642
5	77.1	77.22033	77.23415374	0.017997225
6	94.6	94.911	94.9106712	0.096516595
7	101.5	101.15315	101.1478275	0.124025484
Summation of deviation points ($\sum_{i=1}^{n}(x_i - \bar{x})^2$) = 0.463				
Degree of freedom (n-1) = 6				
Standard deviation (σ) = 0.27768				
Standard deviation of mean (S_x) = 0.10495				
Student distribution factor = 2.447				
Uncertainty curve fit = 0.256829254				
Overall uncertainty of thermocouple (T-type) = ± 0.258575 K				

2 Pressure transducer

The overall uncertainty of the all used pressure transducers in the single and double beds systems were calculated using the same equations (1) to (4) as shown in Table A. 2

Table A. 2 pressure transducer uncertainty calculations

Data point	**Measurement of gauge pressure [mbar]**	**Measurement of pressure transducer [mbar]**	**Curve fit equation y = 0.9902x + 1.714**	**Deviation** $(x_i - \bar{x})^2$
1	0	1.12	2.823024	7.969465
2	100	101.95	102.6649	7.101639
3	200	199.1	198.8628	1.293178
4	300	268.8	297.5858	5.828555
Summation of deviation points ($\sum_{i=1}^{n}(x_i - \bar{x})^2$) = 22.19284				
Degree of freedom (n-1) = 3				
Standard deviation (σ) = 2.719855				
Standard deviation of mean (S_x) = 1.359928				
Student distribution factor = 2.7764				
Uncertainty curve fit = 3.776				
Overall uncertainty of pressure transducer (T-type) = ± 3.77 mbar (± 0.377 kpas)				

Appendix B

Preliminary design of two bed adsorption system

Adsorbent type: CPO-27(Ni) MOF

Adsorbent mass: 585 * 2 gram

Specific heat of CPO-27(Ni): 0.93000 @ 20.0 ˚C

0.99000 @ 71.1 ˚C

Thermal conductivity of CPO-27(Ni) : 0.067 @ 21.2 ˚C

0.193 @ 149.4 ˚C

1 Bed Design

For the already manufactured bed which is made by Weatherite, the bed is a finned tube type with the following dimensions:

Fin width = 190 mm

Fin height = 34 mm

Fin thickness = 0.105 mm

Fin pitch = 1.016 mm

Tube outer diameter=15.875 mm

Tube thickness = 0.8 mm

Tube length = 350 mm

Number of tubes per fin area = 6

Number of passes =2

Fins are made of Aluminium and tubes are made of copper.

Rectangular tube width = 47 mm

Rectangular tube height = 18 mm

Rectangular tube length = 180+121 mm

Rectangular tube thickness =0.8 mm

No of holes = 15

1.1 Mass calculations:

1.1.1 Fins

No of fins per tube length= 350 / 1.016 ≅ 344 fin

Fin side area = (190 x 34) – (6 x 0.25 x π x 15.8752) = 5272.404 mm^2

Fins volume = 5272.404 x 0.105 x 344 = 190709.5 mm^3 = 0.000191 m^3

Fins mass/pass = volume x aluminium density (2720 kg/m^3)

= 0.000191 x 2720 = 0.51873 kg

Total fins mass = 0.51873 x 2= 1.03746 kg

1.1.2 Circular tubes

Tube volume = 0.25 x π x (15.875^2 – 14.275^2) x 425

= 16102.23 mm^3 = 1.61022E-05 m^3

Tubes mass/pass = no of tubes per pass x volume x copper density (8940 kg/m^3)

= 6 x 1.61022E-05 x 8940 = 0.8637 kg

Total tubes mass = 0.8637 x 2= 1.727448 kg

1.1.3 Circular tubes (headers)

Tube volume = 0.25 x π x (18^2 – 16^2) x 630

= 23968.15283mm^3 = 2.39682E-05 m^3

Total tubes mass (header) = volume x copper density (8940 kg/m^3)

= 2.39682E-05 x 8940 = 0.21 kg

1.1.4 Rectangular tube

Tube volume= ((47 x 18) – (45 – 16)) x (180+121) – (π/4) x 18^2 x 17

= 26716.4 mm^3 = 2.67164E-05 m^3

Total tubes mass (rectangular) = volume x copper density (8940 kg/m^3)

= 0.238 kg

1.2 Heat of adsorbent:

$$Q_{ads} = M_{ads} \times C_{ads} \times (T_3 - T_1)$$

$$Q_{ads} = 1.17 \times 0.97 \times (70 - 30) = 45.39\ kJ$$

1.3 Heat of Metals:

$$Q_{Metal} = M_{fin} \times C_{Al}\,(T_3 - T_1) + (M_{cir.\ tube} + M_{cir.\ tube\ header} + M_{rectangular\ tube}) \times C_{Copper}\,(T_3 - T_1)$$

$$Q_{Metal} = 1.03746 \times 0.91\,(70 - 30) + (1.72 + 0.21 + 0.238) \times 0.39\,(70 - 30)$$

$$= 71.58\ kJ$$

1.4 Heat of adsorption:

Isosteric heat of adsorption for CPO-27(Ni) is 3236 kJ/kg of water vapor.

$$Q_{reaction} = M_{ads} \times \Delta w \times h_{ads}$$

$$Q_{reaction} = 1.17 \times 0.05 \times 2621 = 153.32\ kJ$$

1.5 Heat of Refrigerant:

$$Q_{Ref} = M_{Ads} \times w_{max}\, C_{ref}\,(T_2 - T_1) + M_{ads}\,(0.5 \times (w_{max} + w_{min}))C_{ref}\,(T_3 - T_2)$$

$$Q_{Ref} = 1.17 \times 0.45 \times 4.18\,(58 - 30) + 0.5 \times (0.45 + 0.41) \times 4.18\,(70 - 58)$$

$$= 83\ kJ$$

1.6 Total Heat supplied:

Total heat needed = $45.39 + 71.58 + 153.32 + 83$ = 353.29kJ

For 640 second half cycle time,

$$Q_{Heating} = 353.29\ kJ/640\ \text{sec} = 0.552\ kW = 552\ W$$

2 Condenser Design

For these operating conditions, amount of water produced per second is:

$\dot{m}$ produced water = 0.05 *1.17 (kg adsorbent per bed)/640 (sec. cycle time)

= 9.4E-05 kg/s

= 8.15 kg- water /day, for the 1 kg adsorbent.

Heat of condensation is:

$Q_{cond}=m_{water}$ x h_{fg}

Where h_{fg} =2446.5 kJ/kg at T_{cond} = 23 ^{o}C, then

Q_{cond}=2446.5 x 8.15 = 19944.5 kJ/day = 0.23 kW = Q_{cond}

Cooling coil calculations:

$$Q_{cond} = UA\Delta T_{cw}$$

Where Q =230 W, U =500 W/(m^{2}K), ΔT_{cw} =3°C, then A=0.1538 m^2

Coil length is calculated by:

$$A = (\pi \times d_{coil}) \times l$$

Then the length of coils is l =6.12 m

3 Evaporator Design

$\dot{m}$ water vapour to be vaporized = 0.05 *1.17 (kg adsorbent per bed)/640 (sec. cycle time)

= 9.14E-05 kg/s

$Q_{evap} = m_{water} \times h_{fg}$

Where h_{fg} = 2489.1 kJ/kg at T_{evap} = 5 ^{o}C, then

Q_{evap}=2465.4 x 1.4835 x 10^{-4} = 0.227 kW = Q_{evap}

Chilled water coil calculations:

$$Q_{evap} = UA\Delta T_{chilled\_w}$$

Where Q =227W, U =300 W/(m^{2}K), $\Delta T_{chilled\_w}$=4°C, then

Coil length is calculated by:

$A = (\pi \times d_{coil}) \times l$

Then the length of coils is l =7.5439 m